rijksuniversiteit
groningen

A thesis submitted in partial fulfillment for the degree of Master of Science

Optimality Control and Social Behavior of Electric Vehicles with Vehicle-to-Grid Options

Author:
Piter de Graaf

Supervisors:
prof. dr. ir. J.M.A. Scherpen
dr. G.K.H. Larsen
dr. A. Silani

Discrete Technology and Production Automation
Faculty of Science and Engineering

May 2020

RIJKSUNIVERSITEIT GRONINGEN

Abstract

Faculty of Science and Engineering
Discrete Technology and Production Automation

Master of Science

by Piter de Graaf

Due to the electrification of the transport sector, electric travel appears to become dominant. Alongside this, the penetration of renewable energy sources (RESs) increases. Smart charging addresses challenges resulting from both these trends. It reduces the peak load demand of EVs and brings flexible stabilizing capacity to the grid. For smart charging to be successful the participation of EV owners is required. However, the behavior of EV owners related to smart charging is neither well analyzed nor effectively quantified. This work's contributions include: (1) an analysis of survey results regarding EV owners' social behavior related to smart charging, (2) a proposal of a novice hierarchic and dynamic smart charging framework in which social behavior is embedded, (3) an expansion of this framework with wind power generation, and, (4) the simulation results of the proposed model. The simulation results confirm that smart charging is beneficial to the stability of the power grid. Furthermore, it shows that the willingness of EV owners to follow a smart charging contract should be increased, in order to increase the stabilizing capacity of EVs. Moreover, the survey results show that a financial incentive is not necessarily a strong motivator to convince EV owners to participate in smart charging. However, there is a correlation between the willingness of EV owners to smart charge and their environmental self-identity. With this in mind it is proposed that putting emphasis on the environmental benefits of smart charging will increase their willingness to smart charge.

Contents

References 80

List of Figures

List of Tables

Abbreviations

B2G	Building-to-grid
BLD	Building
DSO	Distribution Network Operator
EV	Electric Vehicle
G2V	Grid-to-vehicle
HVAC	Heating, Ventilation and Air Conditioning
ICEV	Internal Combustion Engine Vehicle
MPC	Model Predictive Control
PV	Photovoltaic
RES	Renewabble Energy Sources
SoC	State of Charge
TSO	Transmission System Operator
V2G	Vehicle-to-grid

Chapter 1

Introduction

In this chapter the optimality control and social behavior of electric vehicles with vehicle-to-grid options is introduced. Furthermore, previous work on smart charging and behavioral aspects of EV owners are reviewed. It will be shown that social factors for smart charging are neglected. Moreover, the problem is analyzed in detail, where the smart charging system and its stakeholders are determined.

This chapter consists out of 8 sections. First, the background of the problem is introduced. Secondly, the problem context is given. Thirdly, the system containing the problem is provided. In section 4 the stakeholders and their stakes in the system and problem are discussed. Next, the problem is defined. In section 6 the research goal is given. In section 7 the research questions are provided. Finally, the further outline of the thesis is given.

1.1 Background

Worldwide governments aim at reducing greenhouse gas (GHG) emissions in order to slow down the global climate change. The Paris Agreement signed by 196 countries in 2016 is evidence for this. This agreement aims at controlling the global temperature increase below 2°C. Each country must plan a long term program to lessen the global warming.

As a result, governments plan to increase the penetration of renewable energy production, such as wind power, solar power and hydropower. These Renewable Energy Sources (RES) produce energy from sources that consistently replenish, without carbon dioxide emission. The major drawback for most of these energy sources, in particular wind and solar power, is their uncontrolled energy production. The power production of RES are dependent on weather conditions, such as wind and solar radiation. Which create a surplus or shortage of power at different times. In contrast, energy generation from nuclear plants or fossil fuel can be adjusted to provide the demand of the energy consumers. Furthermore, the current power system is demand driven, *i.e.* energy is produced to provide for the demand of consumers. The increasing penetration of RES challenges the stability of the current energy grid. Thus, new control strategies are required to address the problem of uncertain RES in power networks.

In Europe the transportation system is accounted for 28% of the total greenhouse gas emissions. A solution for reducing these emissions is electrifying transportation system. Thus, governments aim at increasing the number of plug-in electric vehicles (EVs) on the road. These cars are fully electric powered and produce no CO2 emissions and are future alternatives for internal combustion engine vehicles (ICEVs). Governments encourage people to buy EVs via paying subsidies. For example the German government plans to have 10 million EVs on the road by 2030 (The Local, 2020). Also, the Dutch government plans to have 200,000 EVs on the road by 2020 and 1 million by 2025, where the first target already has been met (Netherlands Enterprise Agency, 2020). Consequently, such a fleet of EVs will have to be powered by the power grid. Electrifying the transportation system will increase the power demand dramatically. Thus, the current uncontrolled charging of EVs is untenable, as it would require the power capacity of the grid to dramatically increase.

1.2 Problem context

The increase of the energy production from RES and the electrification of road transport are methods that reduce greenhouse gas emissions. However, they bring some challenges with them. RESs disrupt the stability of the power grid. Additionally, the increase of EVs results in an increase in power demand. Consequently, this requires an increase in power generation, which requires an increase of the capacity of the power grid. A potential solution to these challenges is the smart charging of EVs. In contrast to the regular uncontrolled charging, smart charging is a controlled way of charging an EV. The power is not only provided to the vehicle, grid-to-vehicle (G2V), but also provided back to the grid, vehicle-to-grid (V2G). This creates a demand-side flexibility. Ideally, the EV's battery is charged when load demand is low, while power generation is high and the EV's battery is discharged when load demand is high, while power generation is low. Therefore, the smart charging of EVs can aid in stabilizing the system and lessen the need for an increase of the maximum capacity of the power grid.

Although smart charging can bring many benefits to the energy grid, EV owners should give permission that their EV is used for smart charging. Smart charging has some disadvantages for EV owners, such as a reduction of flexibility and degradation of the EV's battery. The participation of EV owners is crucial to the success of smart charging. Thus, it is required to motivate the EV owners to participate in smart charging. EV owners will be more willing to lend their car for smart charging if there is compensation for their costs and incentives to participate. It can be expected that the more EVs are available for smart charging, the more the grid can benefit and the less individual EVs are burdened. So the availability of many EV's for smart charging will be an important factor for the success of smart charging.

As smart charging gained interested from 2002 onward quite some papers have done research on smart charging (Mwasilu, Justo, Kim, Do, & Jung, 2014). The relevance of deploying this technology started to appear from 2012, when the market of renewables and EV batteries started to accelerate (Waldron, Rodrigues, Gillott, Naylor, & Shipman, 2019). Most of these works focus on the technical feasibility and the profitability of smart charging (Sovacool & Hirsh, 2009). What has not been taken into account is the willingness of EV owners to participate in smart charging, a determining factor for the success of the smart charging contract.

Although this problem is global and relevant for many energy markets, this thesis considers the Dutch power grid, since different countries have different electricity systems, where stakeholders and dynamics between them, regulations and loads are different. However, the results from this thesis can be generalized to other energy markets.

1.3 Literature Review

In this section the body of work related to smart charging and social factors of EV owners is reviewed. Firstly, the EV penetration and it's implications are discussed. Then, a literature review of smart charging or V2G is introduced. Next, recent works on the behavior of EV owners are introduced. Finally, the contributions of this work is explained.

1.3.1 EV penetration and its implications

An EV is defined by the US department of energy as a vehicle that draws electricity from a battery with a capacity of at least four kilowatt-hours and is capable of being charged from an external source (U.S. Department of Energy, n.d.). The review of

EVs components and technological challenges associated with its energy storage system and power electronic devices are discussed in (Amjad, Neelakrishnan, & Rudramoorthy, 2010). Many challenges emerge when EVs plug into the electric power system since EV charging imposes a significant load to the grid. A conceptual framework to successfully integrate EVs into electric power systems is proposed by (Lopes, Soares, & Almeida, 2010). EV driving data is used to investigate the integration into the Danish power network in (Wu et al., 2010). (Garcia-Valle & Lopes, 2012) investigates the EV integration into modern power network extensively. Grid, economic and environmental impacts of EV penetration are reviewed in (Richardson, 2013). A survey on grid impact and charging strategies is presented in (Green II, Wang, & Alam, 2011). A detailed review of the Dutch electricity grid and its market is provided by (Van Tilborgh, 2018) and (Verbong & Geels, 2007).

With an increasing penetration of EVs in the transport sector, a charging integration strategy should be implemented. Keeping the current uncontrolled or passive charging strategies can be detrimental to the electricity grid, since it the peak load is not controlled. In order to control a large fleet of EVs, an intermediate organisation might be needed. An aggregator can perform this function such that economical, and technological aspect of the EVs are taken into account. An investigation of the profitably of vehicle-to-grid charging for an aggregator in the Dutch electricity market is performed by (Van Tilborgh, 2018). A literature review on aggregators is presented in (Bessa & Matos, 2012). In (Peng, Liu, & Jiang, 2012), economic dispatch strategies and risk management of EVs are discussed. An analysis of pilot projects on smart grids and aggregators is performed by (Niesten & Alkemade, 2016). Different approaches for integration of EVs in the power systems and smart grids are given in (Galus, Vayá, Krause, & Andersson, 2013).

In (García-Villalobos et al., 2014) a comparison between different smart charging approaches is presented. Four different EV integration approaches or charging strategies are given and their advantages and drawbacks are discussed. Firstly, Figure 1.1 shows that the current uncontrolled approach would result in a peak power increase, associated with the penetration of EVs. Secondly, off-peak charging does not increase the peak load and is easy to implement. However, we observe from Figure 1.1 that peak charging may result in supply-demand imbalance because of the rapid power demand increased by EV charging. Finally, Figure 1.1 gives two smart charging approaches; valley filling and peak shaving. Peak shaving is considered more complex as it requires bi-directional charging. For both approaches implementation is considered complex. The willingness of EV owners is required in order to integrate the charging strategy. In Figure 1.1, the peak shaving graph shows a reduction in peak load by using bi-directional charging for EVs. Indeed, this could be achieved by charging EVs during off peak hours, at

		Advantages	Drawbacks
Uncontrolled Charging	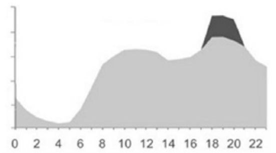	✓ Easy implementation ✓ User friendly	× Overload of transformers and lines × Voltage deviations × Peak power increase × Increase of electricity CO_2 intensity × Electricity cost increase × Needs to reinforce the grid
Off-peak Charging	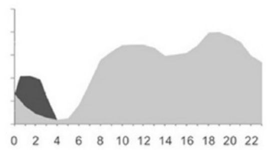	✓ Easy implementation ✓ Demand profile flattened ✓ Better integration of wind energy at off-peak hours ✓ Delay in grid investments	× Imbalances due to rapid increase of power consumed by PEVs × Possible overload of transformers and lines × Possible voltage deviations × Willingness of the customer required
Smart Charging (Valley filling)	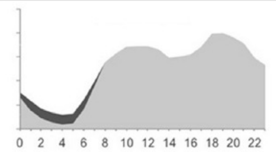	✓ Ancillary services provision ✓ Demand profile flattened ✓ Better integration of wind energy at off-peak hours ✓ Delay in grid investments	× Complex implementation × ICT technologies required × Willingness of the customer required
Smart Charging (Peak saving)	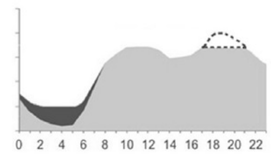	✓ Ancillary services provision ✓ Peak power reduction ✓ Optimal integration of intermittent RES ✓ Reduction of electricity CO_2 intensity ✓ Less investments in network reinforcements	× Very complex implementation × ICT technologies required × Willingness of the customer required × Premature degradation of batteries resulting of using V2G × Energy losses in grid-battery-grid transmissions

FIGURE 1.1: Advantages and drawbacks of the different EV integration approaches. Adopted from (García-Villalobos et al., 2014)

night, providing electricity back to the grid and minimizing charging during peak hours, when the electricity demand is high. Relating to this, RESs can charge the EVs when uncontrolled electricity production is high and the demand is low.

1.3.2 Vehicle-to-grid

EVs can be plugged into the grid where the power flow can be bidirectional, *i.e.*, the EV's battery can be charged and discharged. Indeed, the vehicle-to-grid (V2G) concept can be a possibility, to provide power back to the grid. Also, V2G can be used for the control and management of EV loads by the power system coordinator or the power aggregators via the communication between the vehicles and power grid (Tan et al., 2016). In contrast, in the literature unidirectional smart charging refers to smart charging without V2G. Which already provides benefits compared to uncontrolled charging and is less complex than bidirectional smart charging (Sortomme & El-Sharkawi, 2010). However, we use the smart charging as the controlled bi-directional (V2G and G2V) charging of an EV. In (Kempton & Tomić, 2005a) and (Kempton & Tomić, 2005b) the V2G concept was introduced with its main objectives, stabilizing the grid and exploiting the large-scale RESs. Further research on V2G relates to the following: the power system (Ma, Houghton, Cruden, & Infield, 2012), emissions (Sioshansi & Denholm, 2009) and related social issues (Sovacool & Hirsh, 2009). In (Sovacool & Hirsh, 2009), the benefits

Benefits	Drawbacks
Reducing power grid losses	Battery degradation
Preventing power grid overloading	Complex hardware infrastructure
Improving load profile	High investment cost
Maintaining voltage level	Social barriers
Renewable energy intermittent	
Failure recovery	
Maximization profit	
Minimization emission	

TABLE 1.1: The benefits and drawbacks of bidirectional V2G (Tan et al., 2016), (Yilmaz & Krein, 2012), (Mullan et al., 2012)

and barriers for V2G transition are presented. The latter disputes the idea that the only important challenges for the greater use of EVs and V2G systems are technical. The paper assesses the social barriers facing this transition. Moreover, (Sioshansi & Denholm, 2009) shows the potential of V2G for a significant reduction in GHG emissions in comparison with internal combustion engine vehicles (ICEV). Moreover, (Ma et al., 2012) shows the benefits of vehicle to grid for load balancing the energy and cost savings through a model for an EV storage system integrated with a standardized power system. The case study shows the vehicle owner's cost is halved in the latter approach.

The benefits and drawbacks of the bidirectional smart charging concept are shown in table 1.1. A drawback to V2G methods is battery degradation, which occurs due to the frequent charging and discharging cycles (Dogger, Roossien, & Nieuwenhout, 2010). A study conducted by (Peterson, Apt, & Whitacre, 2010) concluded that several thousand days of driving and bi-directional charging causes less than 10% capacity loss regardless of the amount of V2G support used. However, intermittent modes of V2G could lead to rapid capacity fade. Also, for smart charging, certain technologies and hardware are required. The complexity of V2G requires additional hardware, which needs extra investments (Tan et al., 2016). For example, a bidirectional EV charger typically consists of a AC/DC and DC/DC converter (Verma, Singh, & Shahani, 2011). Furthermore, smart charging is often coupled with dynamic energy pricing, this requires technologies that enable customers to react to price signals quickly and without much effort. In (Hildermeier et al., 2019), among others, a review of existing practises and policies regarding such technologies is presented. Moreover, the significance of solutions that seek to track user behaviors and routines is underlined in (Waldron et al., 2019). A main challenge for tracking software is safeguarding the privacy of users. Additionally, the profitability of V2G for aggregators and EV owners and the influence of governmental subsidy policies are discussed in (Mullan et al., 2012), (Yilmaz & Krein, 2012), (Van Tilborgh, 2018) , (Bhandari, Sun, & Homans, 2018), (Hong, Koo, Jeong, & Lee,

2012) and (White & Zhang, 2011).

A summary of the main optimization techniques to achieve different vehicle to grid objectives while satisfying multiple constraints is presented in (Tan et al., 2016). According to (Tan et al., 2016) there are five main optimization methods for smart charging EVs with different possible objectives and their associated constraints, shown in Table 1.2.

1.3.3 Social factors

In the literature there exists few works about the behavior of EV owners. For many V2G studies only the technical challenges are addressed. According to (Sovacool, Noel, Axsen, & Kempton, 2018) only 2.1% in the field of V2G addressed user behaviors and routines, with 1.1% addressing range anxiety adoption issues. In 2010 the unpredictability brought by users' behavior to V2G was identified . Furthermore, (Waldron et al., 2019) identified some user-centered challenges in V2G that can be divided in social (attitudes, socioeconomic) and practical issues (vehicle availability, user predictability, behavioural incentives). According to Waldron et al. to implement smart charging successfully some social challenges must be overcome. Amongst these are: user anxiety related to implementation, the integrating of behavior analysis algorithms and acquiring real world data regarding economic, social and environmental benefits. For instance, range anxiety results in EV owners acquiring a high battery state-of-charge (SOC) in order to keep their flexibility high (Fasugba & Krein, 2011). This might prevent EV owners from actively participating in smart charging. Furthermore, it has been shown by (Kuang, Chen, Hu, & Yang, 2017) that patterns of vehicle use, SOC on arrival and desired SOC on departure can significantly affect the impact that V2G services could have on load management in different building types.

In (X. Wang, Nie, & Cheng, 2019), a cost analysis to obtain an optimal planning scheme for V2G is performed, in which EV penetration is varied according to charging preference and customer damage cost. It indicates that the stochastic behavior of EV users poses a challenge to policy makers. It uses an optimization method for real-world travel records and cost statistics to show the efficiency of the optimization algorithm. According to (X. Wang et al., 2019), there are two ways to mitigate the impact of EV penetration on power systems: controlling the users' charging behavior directly and upgrading the power system ahead. Charging behavior is considered in (Shen, Fang, Ye, & Kadoch, 2020) for V2G in a smart grid . It is determined how to identify EVs which can be scheduled for V2G charging. They found that grouping EVs on the basis of charging behavior is an effective method for the purpose of EVs for V2G.

Optimization method	Objective
a. Particle swarm optimization	a. Minimize operation cost
b. Genetic algorithm	b. Maximize renewable energy generation
c. Linear programming	c. Minimize error of load curve
d. Quadratic programming	—-from target load curve
e. Ant colony optimization	d. Minimize power losses
	e. Minimize emission
	f. Maximize profit

Constraint
a. Power Balance
b. Voltage limit
c. Generation limit
d. Line thermal limit
e. Forecast load
f. Upstream supplier limit
System loading limit

Table 1.2: The optimization methods, objectives and constraints for V2G optimization adopted from (Tan et al., 2016)

Moreover, there are many EV related subjects for which user behavior is studied. Such as electric vehicle penetration in transportation. In (Energy Element, 2013), among others, market barriers to EV adoption are discussed. Some of its findings are, firstly, the five attitudinal factors which differentiate the EV purchase segments most strongly are: identity, anxiety, parking difficulty, willingness to pay and symbolic motives. Secondly, key factors affecting purchase of EVs are: vehicle price and running cost, brand and segment supply, access to charging, driving range and charging time, and the consumers' receptiveness to EVs. Thirdly, countries with the highest rates of EV penetration have taken significant cost measures. Smart charging can aid in reducing the total cost of ownership of an EV, thus help with addressing cost barriers for EV adoption (Waldron et al., 2019). Furthermore, non-cost barriers are also strongly addressed by these countries, such as vehicle supply, consumer receptiveness to EVs and extending access to public charging infrastructure. Fourthly, EV owners prefer overnight charging at home or workplace. Lastly, recharging time is consistently reported as a barrier. All though smart charging will mostly take place during long idle times of EVs, smart charging influences the recharging time.

Additionally, in (Ashkrof, de Almeida Correia, & van Arem, 2020) the route choice behavior of EV drivers in the Netherlands was investigated where the classic route measures (travel time and travel cost), vehicle-related variables (SOC at the origin and destination) and charging characteristics (availability of a fast charging point at the destination, fast charging duration, waiting time in the queue of a fast-charging station) can significantly influence the EV drivers route choice and charging behavior. Other papers discuss the behavior and demographics of EV adoption (Wee, Coffman, & Allen, 2020), (Mukherjee & Ryan, 2020) and (Shalender & Sharma, 2020).

The greenhouse gas emissions of EVs depends on the electricity mix of the electricity source and the driving behavior, discussed in (Faria et al., 2013) and (Karabasoglu & Michalek, 2013). An EV driving model with a data driven approach was introduced by (Lee & Wu, 2016). (G. Wang, Makino, Harmandayan, & Wu, 2020) investigates EV drivers' eco-driving behaviors and motivations through a questionnaire and statistical analysis of those results. Firstly, the paper shows that EV drivers possess significantly calmer driving maneuvers and more fuel-efficient driving habits. Secondly, EV drivers have much more more willingness to save energy in compensation of travel time. Thirdly, they have more willingness to adopt eco-friendly in-vehicle display technologies. These results underlines the unique behavior found in EV drivers in comparison with internal combustion engine vehicle drivers. A review of EV penetration rate studies and their methods is presented in (Al-Alawi & Bradley, 2013). They found that the market penetration of EVs is a key factor in predicting the effects of EVs on the grid, the environment and transportation.

Increasing EV penetration can be beneficial for governments, willing to reduce CO2 emissions. Countries with high EV penetration put significant measures in place to tackle cost and non-cost barriers (Energy Element, 2013). Furthermore, research on EV adoption and the behavior associated with it is presented in (Wee et al., 2020), (Mukherjee & Ryan, 2020), (Shalender & Sharma, 2020). (Wee et al., 2020) analyzed EV registration numbers in Hawaii through demographic and transportation behavior. They found that a higher income and higher education result in more registered EVs. All public charging has a significant impact on EV registration, with a larger magnitude for fast charging. However, trip distance is not linearly related to EV adoption. A commute shorter than 20 min or longer than 45 minutes is associated with fewer EV registration. This can possibly be explained by range anxiety for longer drivers and the upfront investment might not be merited for shorter drivers. In (Mukherjee & Ryan, 2020), different factors influencing the early EV adoption in Ireland are investigated. It was found that a university degree, a charge point near and long-distance commuters (at least one hour) are positive determinants for EV adoption. Rented accommodation and a younger age are negative determinants. (Shalender & Sharma, 2020) uses an extended theory of planned behavior model to predict EV adoption intention in India. It was found that attitude, subjective norm, perceived behavior control, moral norm, and environmental concern have a positive relation with adoption intention of EV buyers. An analysis on consumer's attitudes and perceptions on EVs is shown in (Egbue & Long, 2012). A comparison of attitude towards EVs between consumers who experienced EVs and consumers without EV experience was performed in (Jensen, Cherchi, & Mabit,

2013) and (Bühler, Cocron, Neumann, Franke, & Krems, 2014). It was shown that attitudes towards EVs already were mainly positive. The high acquisition cost might be the major barrier for EV adoption.

Some other concepts, such as the behavior of EV owners, are investigated in (Zhao, Zhang, Yang, Chai, & Li, 2020), where the pricing of private charging pile sharing is considered. Furthermore, the charging behavior is relevant to car sharing concepts in order to find an optimal charging and re-positioning model (Folkestad, Hansen, Fagerholt, Andersson, & Pantuso, 2020). Route choice and waiting time are of determining factors for the optimal location and capacity of charging stations (Chen, Qian, Miao, & Ukkusuri, 2020). In (Schmidt, Staudt, & Weinhardt, 2020), the importance of the user's behavior is highlighted by showing its impact on the economic evaluation of public destination charging stations.

In current literature, there is still a focus on the technical aspects of smart charging (Sovacool & Hirsh, 2009) (Hildermeier et al., 2019), while social issues can be a major barrier against successful implementation of smart charging. Moreover, an important factor in EV owners behavior is their willingness to lend their car for smart charging. V2G deteriorates the car's battery and reduces the flexibility of users. Thus, potential methods to increase the willingness of EV owners to smart charge should be determined. The effect of financial participation should be investigated, as it is a factor that can influence this willingness and can aid in lowering the total cost of ownership (Bühler et al., 2014). Furthermore, certain policies can influence EV owners to lend their car to an aggregator.

1.3.4 Contributions

Smart charging can be very beneficial for the power grid, renewable energy penetration and different stakeholders. However, there exist some barriers which have to be addressed, of which many are of a social nature. The simulating of smart charging is often accomplished through designing an optimization problem with different constraints, such that an objective has to be minimized. Previous works on creating optimization models have neglected the behavior of EV owners and their willingness to lend their car for smart charging. While social barriers are a significant challenge for the implementation of V2G (Tan et al., 2016). This paper will address the social factors of EV owners' behavior and their willingness to follow smart charging. These social factors will be included in simulations of a smart charging optimization problem in the Dutch power grid.

1.4 Problem analysis

1.4.1 System description

Figure 1.2 depicts the Dutch electricity system with smart charging where the RES and non-RES are the sources of power. The Transmission System Operator (TSO) transports the electricity through the country at high voltage to minimize energy loss from transportation. Then the energy is converted and the Distribution System Operator (DSO) distributes the energy to the consumer. Currently, the energy consumption is demand driven. However, in the future new control strategies are required for not only EV charging, but other energy consumption as well. A building or home will consume the energy for its needs and EVs are smartly charged for transport. Also, an aggregator will control the charging and discharging of the EVs. Indeed, an aggregator will have smart charging contracts with EV owners that makes their EV available. An aggregator can use the EV fleet as a stabilizing factor to the grid. In this thesis, smart charging in smart parking lots at office buildings is considered. Smart charging should provide benefits during the day as there is more energy consumption, more RES generation and a big supply-demand mismatch between them. From this starting point the system is expanded to include a smart building, a DSO grid, a TSO grid and energy generation. It can be expanded further to include the EVs smart charging at home, smart homes with photovoltaic (PV) systems, renewable energy generation and an aggregator.

For success of smart charging, the cooperation of EV owners is required. Therefor we need to understand the behavior of EV owners. In Figure 1.3 a flow chart is given for when an EV arrives at a smart parking lot. These are the factors that are directly relevant for the charging of an EV in a smart parking lot. An EV arrives at a certain time, with a certain state-of-charge (SOC), with or without a smart charging contract. The EV owner gives his departure time and its desired SOC. The EV is charged and then leaves with a certain SOC at a certain time. In order to model the smart charging of EVs these behavioral factors should be considered unknown.

1.4.2 Stakeholder Analyses

In this section, different units involved in smart charging are introduced. Firstly consider the Electricity suppliers which can also be the energy generators, for instance in the Netherlands these are Nuon and Essent. They want to supply energy at a minimum cost and sell it in order to make a profit, where the energy price is regulated by the government.

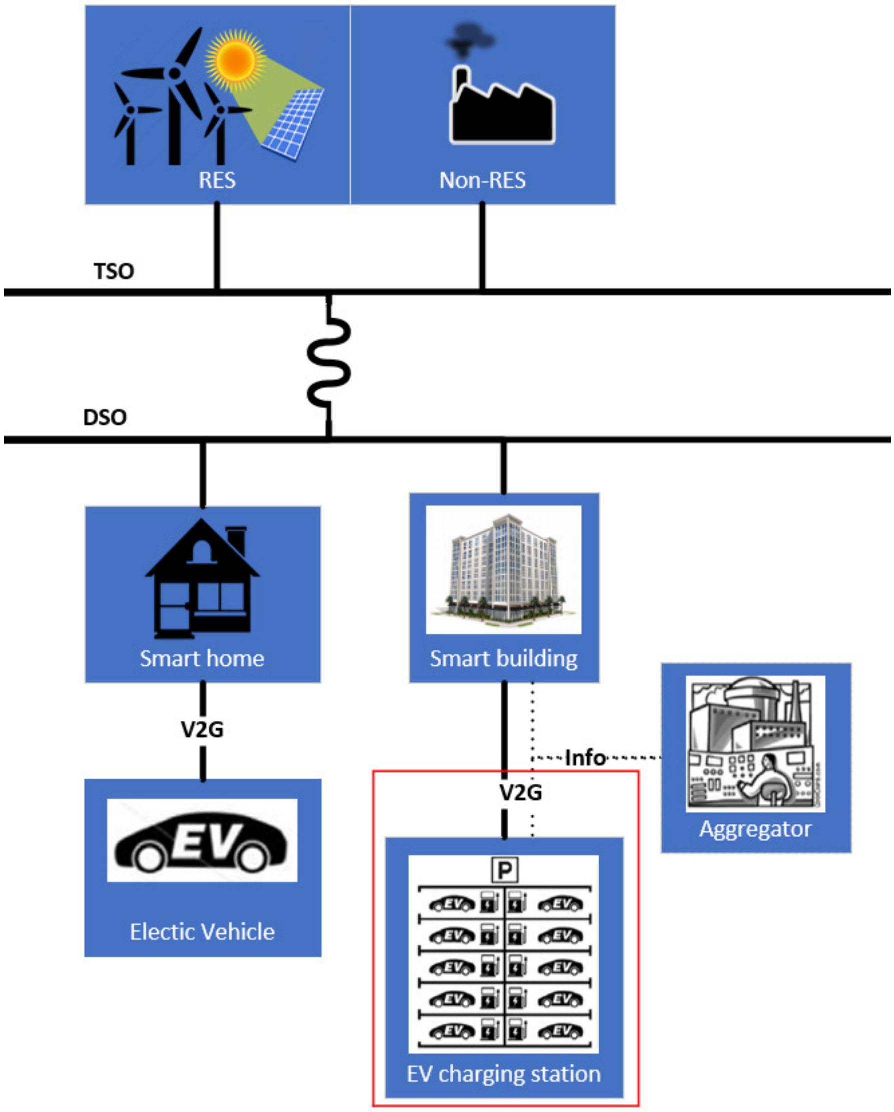

FIGURE 1.2: The system shown with power and communication lines between the relevant aspect. The initial system is indicated with red

The TSO is responsible for stabilizing the energy grid and controlling the supply and demand, for instance, in the Netherlands this is TenneT. The TSO transports energy over the low-voltage transmission grid. When in microgrids the load demand is less than its supply, the excess of energy is sold to other microgrids and for a shortage of electricity the microgrid buys energy from other microgrids. A high penetration of RESs will make the control of the supply-demand mismatch more difficult. Smart charging is a concept that aids in stabilizing the grid.

There are multiple DSOs in the Netherlands responsible for the construction, development, maintenance and management of the electricity grids associated with their geographical area. A DSO should provide electricity for consumers through the high voltage distribution grid.

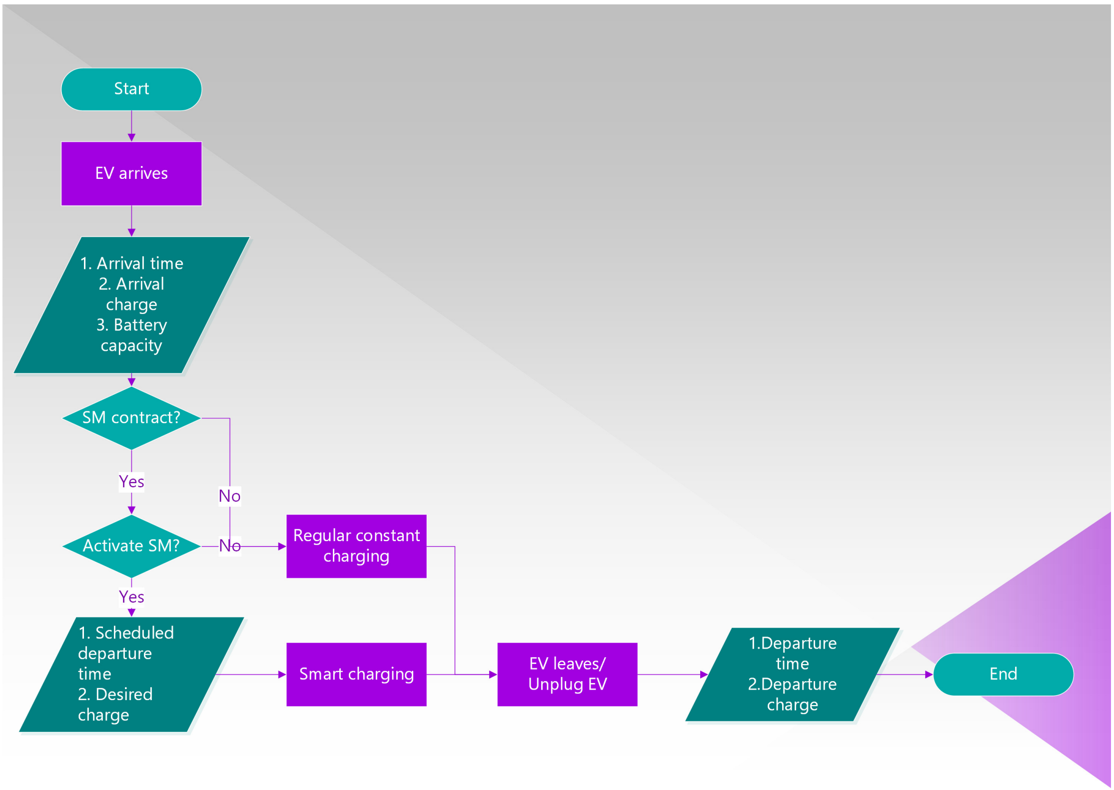

Figure 1.3: The relevant behavior of EV owners presented as a flow chart

An aggregator provides regulating services in order to make a profit. It combines the EVs information with a smart charging contract to provide stabilization to the grid, in return an aggregator will receive payment. An aggregator is required to meet the desired charge at the desired departure time for its EV owners. Furthermore, they should provide EV owners with some profits for lending their EV's battery for smart charging.

EV owners might be the most important stakeholder for smart charging. When an EV owner agrees to follow the smart charging contract, he gives an aggregator control over the (dis)charging of the battery of his EV. Smart charging degrades the battery life of EVs and reduces the EV owner's flexibility and autonomy. However, they could be convinced to participate in smart charging with a (financial) incentive outweighing the disadvantages. Many EV owners acquired EVs in order to reduce their carbon footprint (Shalender & Sharma, 2020); therefore, their environmental concerns can be an important factor for them to participate in a smart charging contract.

The load demand of electricity consumers must be provided. They have a contract with an energy supplier and they want to receive energy whenever they desire. Indeed, they see the energy grid as a black box. Some electricity consumers are also generating energy via PV or solar panels, who are often called a prosumer.

Stakeholder	**Goal**
Electricity suppliers	Provide electricity
TSO	Stable grid and controlled supple and demand
DSO	Reliable distribution of electricity
Aggregator	Profitable smart charging
EV owner	Transportation and incentives for smart charging
Consumer	Reliable power supply
Companies with a - smart parking lot	Extra revenue stream, extra services for employees
Government	Electricity for its citizens and meet emission goals

Table 1.3: The stakeholders and their main goals

Companies that might adopt a smart parking lot are a stakeholder, as in this thesis parking lots at offices are considered. They can benefit from smart buildings and smart charging of EVs as they provide value to the power grid, which can provide the company with a financial compensation in return. Smart charging at their facility would provide a company with an extra revenue source. While charging facilities and electric transportation can be offered to employees. The companies owning EVs become more attractive if they can compensate for their costs via smart charging.

The Dutch government plan to provide people with electricity for an affordable price. In addition, they plan to reduce the greenhouse gas emissions by using RES instead of conventional generation resources and by electrifying the transportation system.

1.4.3 Problem Definition

As described in extend in previous sections, smart charging is a concept with great potential. It should be determined whether smart charging will truly be beneficial, and more specifically beneficial in the Dutch electricity system. There exists no research on the willingness of EV owners to participate in smart charging, while smart charging depends mainly on the willingness of EV owners to lend their EV. Thus, this lack of knowledge is problematic. In order to guarantee that smart charging is a feasible concept, the public's willingness should be known. Additionally, the behavior of EV owners relating to this subject should be determined such that the effect of smart charging on the grid can truly be determined. For an EV owner there will be several disadvantages and advantages to follow smart charging. Thus, there is a lack of knowledge on, firstly, the willingness of EV owners to follow smart charging. Secondly, the barriers of smart charging for EV owners. Thirdly, how the willingness will influence the success of smart charging.

1.5 Research Goal

The main goal of smart charging is preserving the stability of the power network by controlling the supply-demand mismatch in power grids and minimizing the peak load. The supply-demand mismatch will become a bigger issue as the RES penetration increases. The peak load will increase as power demand from uncontrolled EV charging increases. In order to address the smart charging for EVs, the behavior of the EV owners should be considered. Since the behavior can greatly influence the potential benefits and the feasibility of smart charging and it can create some practical issues for smart charging of EVs. The main objectives of this study are summarized in the following research goal:

To propose a V2G-MPC frequency control model in which social behavior is embedded and to determine the effects of these social aspects on the system.

1.6 Research Questions

In this section research questions are determined with the purpose of achieving the research goal in a structured manner. Research questions can either be a knowledge question or a design question (Wieringa, 2010). The research questions that will be answered in this thesis are given as follows:

1. Are EV owners willing to smart charge?
2. What obstructs and aids the EV owner's willingness to follow smart charging?
3. How should a V2G-MPC model be designed, such that simulations can be done?
4. How does the willingness to follow smart charging affect the stability of the power grid?
5. What other factors influence the success of smart charging?
6. Can the smart charging of EVs aid in reducing a supply-demand mismatch resulting from uncontrolled renewable energy production?

1.7 Thesis outline

The research questions outlined in the previous section will be answered in the rest of the thesis. In Chapter 2 the results of a survey performed by the EV charging company NewMotion is provided. The results will be analyzed and answer research questions

1 and 2. In chapter 3 background information on model predictive control (MPC) is discussed. Then, in chapter 4 the V2G-MPC model is provided, with it research question 3 will be answered. In chapter 5 the simulation setup and the simulation results are presented and discussed. In this chapter research questions 4 and 5 will be answered. In chapter 6 research question 6 is answered, as the framework for integrating wind power generation into the system is proposed and the simulation results of the W-V2G-MPC model are presented. Finally, in chapter 7 the findings will be shortly discussed in the conclusion. Additionally, limitations to this work and opportunities for future research will be discussed.

Chapter 2

Survey Results

In this chapter relevant results of a survey are discussed and analyzed. The survey was distributed to its customers by New Motion, which is a company which provides EV charging solutions. These survey results aid in answering research questions 1 and 2. It will be determined that most EV owners are very willing to follow a smart charging contract. Furthermore, the survey results will show that EV owners are barely motivated by financial incentives in order to smart charge. The environmental contribution that smart charging provides seems to be an important motivator.

The outline of this chapter is as follows: First, in section 1 the participants and procedures are discussed. Second, in section 2 the relevant measures and results are discussed. Finally, in section 3 the most important results in the chapter are shortly discussed in the chapter's conclusion.

2.1 Participants and procedures

The customers of New Motion received an invitation email to participate in an online questionnaire on electric driving. The link to the questionnaire was included in the newsletter of New Motion. In total 5493 participants started to fill out the questionnaire of which 4492 met the criterion and filled out of at least 80% of the questionnaire, which is a response rate of 82%. Additionally, for the simulations we only selected participants from the Netherlands, those who own a full EV and those who are employed. This left us with a sample of 1201 participants. In Figure 2.1 the percentage of participants from different countries is shown. The choice of including only participants from the Netherlands was mad for the reason that the model is based on the Dutch energy system and charging stations are geographically fixed. The smart charging of a full EV, in contrast to plug-in hybrid cars, is very beneficial, due to its relative large

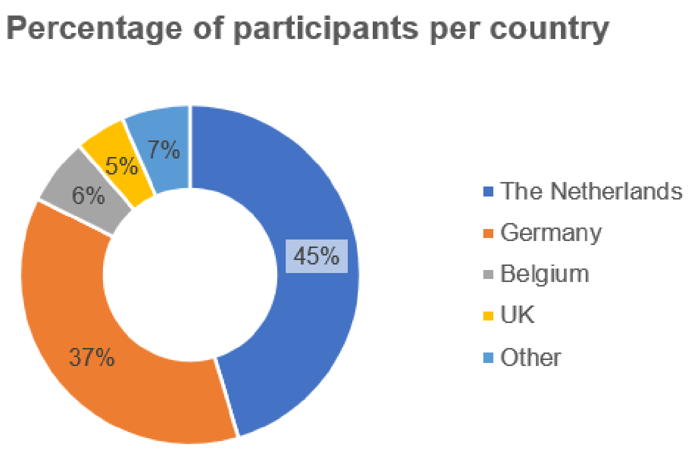

FIGURE 2.1: The percentage of participants from different countries

battery capacity. In (Van Tilborgh, 2018) it was found that plug in hybrid cars are not suitable for V2G. Furthermore, people who work have more motivation to participate in smart charging contract since our optimization will focus on EV owners that arrive and leave charging stations at smart parking lots at an office space at predictable hours. Of the sample 91% was male, 8% was female and 1% other or preferred not to say. Most participants had an age range of 51-60 years, namely 47%. The average high age of participants could be explained by the high acquisition cost of EVs, as (Mukherjee & Ryan, 2020) found that young age was a negative determinant for EV adoption. Most participants adopted their car through their employer or through their own company. Most participants drive 25,000 - 50,000 km per year (42%) or 15,000 - 25,000 km per year (41%). Most participants have a charge point available at work (81%) and at home (75%). The majority of the participants own a Tesla EV (43%), 13% own a Hyundai, 10% own a Nissan. Tesla's cars have more capacity than other EVs on the market. A more detailed overview of the surveys statistics can be found in Appendix B.

2.2 Measures

The survey consisted out of approximately 50 questions. As this thesis considers smart charging of EVs the following measures from the survey are relevant;

- range anxiety,
- environmental self-identity (ESI),
- battery charge when arriving at work,
- minimal battery charge when leaving work,
- willingness to smart charge,

- willingness to have their battery used to power offices.

User-centered challenges regarding smart charging are divided into social and practical issues by (Waldron et al., 2019). Indeed, range anxiety, ESI and willingness measures are of a social nature, the battery charge is of a practical nature. The questions from this survey related to these measures are given in Appendix A. All questions, except the measures on battery charge, could be answered on a scale from 1 strongly disagree to 5 strongly agree. For the results in this chapter only the participants from the Netherlands, with a full electric EV are considered, unless indicated differently.

The range anxiety was measured with one item, *i.e.*, the range of my electric vehicle is sufficient for my everyday use. Most of the participants indicated that the range of their electric vehicle is sufficient for their everyday use, with a mean of M = 4.41 and a standard deviation of SD = 0.99. This is promising, as (Fasugba & Krein, 2011) found that range anxiety hinders smart charging participation. Furthermore,the ESI was measured via two items (I see myself as a pro-environmental person; acting environmentally-friendly is an important part of who I am). The items formed a reliable scale, $\alpha = .87$. On average, participants scored relatively high (M = 4.26, SD = .82). This should be no surprise as multiple studies found that EV owners have a unique behavior, for example, EV owners drive very eco-friendly (G. Wang et al., 2020).

Participants were asked about how full their battery usually is when they arrive at work and what the charge should at least be when they leave work. Participants could answer from 0-100% with steps of 10%. The results are given in Figure 2.2. On average the battery is 64% (SD = 18.79%) full on arrival and 49% (SD = 28.03%) full on departure. Thus as averages, the departure charge is lower than the arrival charge. These results show that when an EV follows the smart charging contract, it can potentially provide more V2G power than G2V power.

In order to determine the willingness of participants to use smart charging they were asked if they are willing to use smart charging on a scale of 1 to 5. Overall participants

Method of car adoption	**Frequency**	**Average smart charging willingness**	**SD**
Private	165	4.11	1.15
Own company	446	3.95	1.33
Lease through employer	481	3.87	1.15
Company vehicle	60	3.75	1.14
Private lease	30	3.63	1.18

TABLE 2.1: The average willingness of participants to smart charge dependent on car adoption method

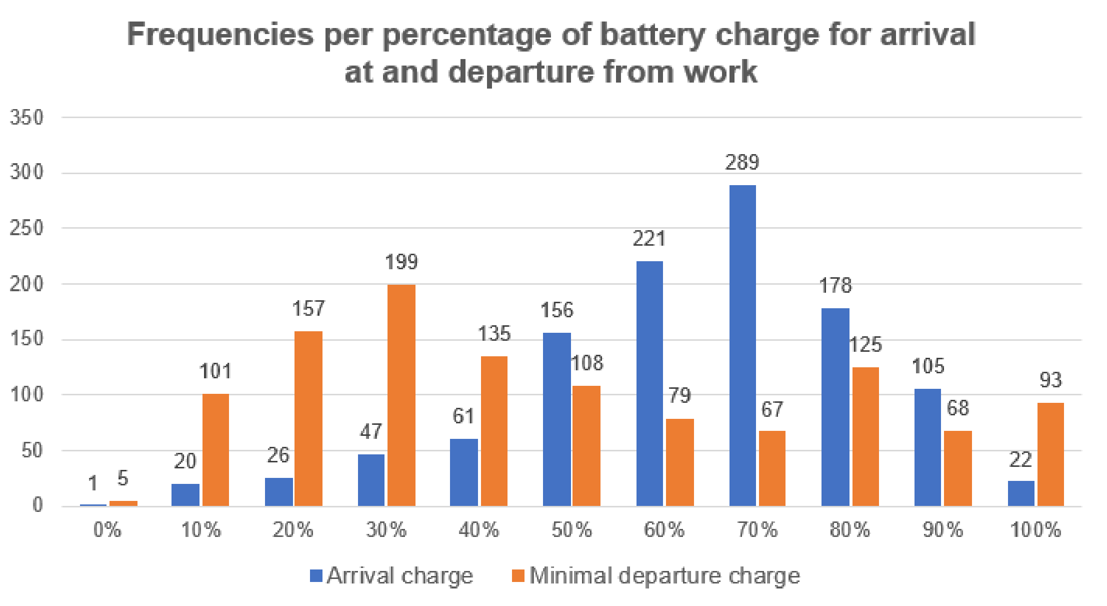

FIGURE 2.2: The amount of charge when arriving at work and the desired charge when leaving for survey participants

were willing to use smart charging with average of M = 3.92 and variance of SD = 1.16. Then they were asked whether they are willing to use smart charging when smart charging contract financially compensates for customers. Interestingly the participants have less willingness if they are financially compensated (M = 3.83, SD = 1.17). Both results are given in Figure 2.3 as a histogram. This shows that financial incentives are not necessarily the main motivator for EV owners.

Furthermore, the car adoption method has influence on the willingness of the EV owners to follow the smart charging contract, *i.e.*, participants who bought their car privately or via their own company have more willingness to follow a smart charging contract than participants who lease their car or drive a company vehicle. Thus, when an EV is owned privately the owner is more likely willing to make their EV available for smart charging. Also, the willingness to smart charge differs between different countries. In Figure 2.2 it can be seen that participants from Germany and the UK have significantly more willingness to follow smart charging contracts than participants from the Netherlands and Belgium. In (Energy Element, 2013) it was shown that countries with high penetration of EVs had introduced measures to promote EV adoption, such as consumer receptiveness to EVs. It is possible that the UK and Germany put more effort in promoting receptiveness to concepts addressing environmental issues, and by doing so increased the willingness to smart charge. Further research is required to substantiate this idea.

Additionally, participants were asked how willing they are to share the power of the EV battery with the power grid of their office (M = 2.84, SD = 1.51), when they gain financially (M = 3.11, SD = 1.50), or when they have sufficient energy to commute

Country	**Percentage of total**	**Average smart charging willingness**	**SD**
Netherlands	45%	3.92	1.16
Germany	37%	4.20	1.11
Belgium	6%	3.88	1.22
UK	5%	4.18	1.20
Other	7%	3.84	1.39

TABLE 2.2: The average willingness of participants to smart charge dependent on their country

home (M = 3.53, SD = 1.51). The willingness to provide power to the office is lower than the willingness to smart charge. This can be explained by the framing of the questions. Participants have a high ESI as shown earlier, and are therefor motivated to have more environmentally-friendly contributions in society. Participants might have less willingness to share power of their EV with their office, as the benefits to the environment are not sufficiently clear. While the explanation on smart charging mentions the benefits to solar and wind energy, and to the public as well as to the private power grid. The only disadvantage mentioned in the question on providing power back to the office is the degeneration of the EV's battery, while the question on smart charging mentions as disadvantages that the car might not immediately charge after plugging into the charge point or that charging may take longer. Degeneration of an EV's battery might be considered a bigger disadvantage than longer charging times by the participants.

Generally for correlations with a value of $r \in [0.00, 0.20)$ the correlation is considered very weak and for $r \in [0.20, 0.40)$ the correlation is considered weak. In Table 2.3 the correlations between different question subjects and the ESI and range anxiety and

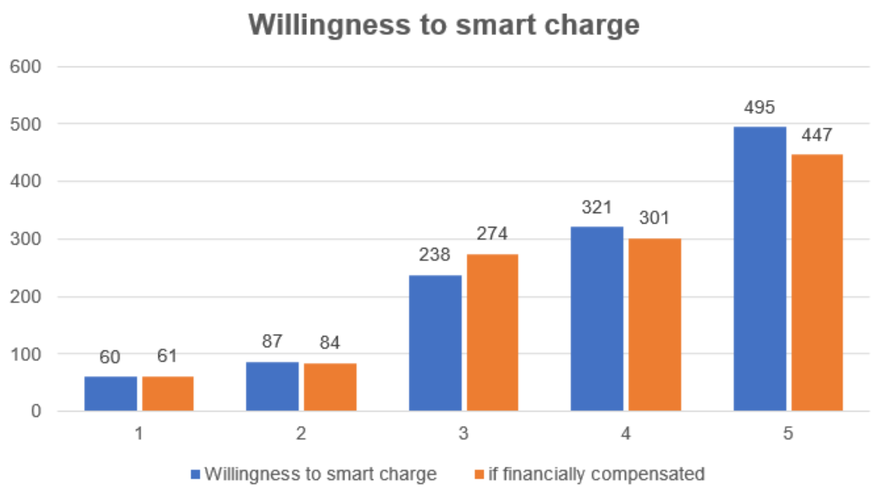

FIGURE 2.3: Frequencies of answers on willingness to use smart charging with and without financial compensation

Question subject	**Environmental self-identity (ESI)**	**Range Anxiety**
Willingness to smart charge	$r = 0.29$, $p < 0.001$)	$r = 0.15$, $p < 0.001$
W to SC with financial incentive	$r = 0.13$, $p < 0.001$	$r = 0.09$, $p < 0.01$
Willingness to power office	$r = 0.15$, $p < 0.001$	$r = 0.08$, $p < 0.01$
W to p o with financial incentive	$r = 0.11$, $p < 0.001$	$r = 0.09$, $p < 0.01$
W to p o with sufficient charge	$r = 0.13$, $p < 0.001$	$r = 0.01$, $p = 0.84$

Table 2.3: Correlation

its p-value are given. It was found that people have more willingness to follow smart charging contracts the stronger their ESI is. However, ESI is less strongly related to willingness to smart charge when financial compensation is received. This lower correlation with ESI could explain the reason for a lower willingness to follow the smart charging contract when financially compensated while participants with high ESI might find it more important to contribute to environmental issues than receiving financial compensation. Furthermore, the correlation between ESI and the question on participants having their EV's battery used to power offices has a weak correlation, also when they gain financially, and when they have enough energy to commute home.

Furthermore, the more people think their range is sufficient for their daily use, the more willingness they have to follow a smart charging contract. As range anxiety is correlated to willingness to the smart charging without financial compensation and with financial compensation. Also, people with low range anxiety have more willingness to provide the office with power without financial compensation, and with financial compensation, but it is not related to participants' willingness when they have enough energy to commute home.

2.3 Conclusion

From the survey results it can be inferred that most of the participants are willing to participate in smart charging. The mean value for whether participants are willing to participate in smart charging is 3.92 on a scale from 1 strongly disagree to 5 strongly agree, *i.e.*, answering research question 1 ('Are EV owners willing to smart charge?').

Also, there exists a positive correlation between ESI and the willingness to smart charge. EV owners with high environmental self-identity are more likely to lend their EVs for smart charging. However, range anxiety has a weak correlation with the willingness to smart charge, *i.e.*, EV owners are less likely to participate in smart charging if they have anxiety about the range of their EV. Moreover, if an EV is privately owned, EV owners have more willingness to follow the smart charging. Additionally, from the survey it can be inferred that the arrival charge is higher than the desired minimum departure charge, *i.e.*, EVs can therefor deliver power to smart parking lots. With this an answer to research question 2 is provided ('What obstructs and aids the EV owner's willingness to follow smart charging?'). Furthermore, the results from the survey will be used in the smart charging optimization model, which is presented in Chapter 4.

Chapter 3

Preliminaries

In this chapter a theoretical background of the main methodology of this thesis is introduced, *i.e.*, model predictive control (MPC). Also, its main benefits and drawbacks are discussed and the reasons for using MPC are elaborated.

3.1 Model Predictive Control

Model Predictive Control (MPC) is a control methodology that is an effective means of dealing with large multi-variable constrained control problems. It is widely used in different research areas, such as the process industry (Qin & Badgwell, 2003) (Jin, Kumar, & Elia, 2009), building heating, ventilation and air conditioning (HVAC) studies (Pavlak, Henze, & Cushing, 2014) and power systems (Ernst, Glavic, Capitanescu, & Wehenkel, 2008) (Taha et al., 2017). MPC based methods started to gain interest in the late 1970s. These preceding methods took advantage of the increasing potential of digital computers (Camacho & Alba, 2013).

All MPC approaches posses common elements, but different options for each element can be chosen. These elements are as follows; prediction model, objective function and control law. In MPC, an optimal control sequence is calculated by repeatedly optimizing a cost or objective function over a time horizon, while the model of the system is simulated. The model's behavior is determined over the time horizon. The results of the first time step in the time horizon of the model is applied to the controller of the system, the rest is discarded. Then, the state of the system is updated and the time horizon is shifted one step. This new state is used to calculate a new optimal control sequence and the process is repeated. This approach results in lower computational times and accurate results, as each time step a relative small finite horizon is simulated instead of calculating the results for all the time steps at once.

A MPC approach is utilized in power systems to control the frequency of the grid. In the optimization problem the operational objectives are taken into account, such as the frequency control, supply-demand balance, minimization of cost, maximization of utilities and satisfaction of operational constraints. In this thesis a model representing the Dutch power grid will be proposed. For the utilization of MPC we are primarily interested in finite-horizon MPC for discretized linear systems. A general formulation of this is as follows:

$$\text{minimize}X \sum_{k \in K} J(x,u) \tag{3.1}$$

$$\text{subject to } x(k_0) = x_0 \tag{3.2}$$

$$x(k+1) = Ax(k) + Bu(k) \tag{3.3}$$

$$x(k+1) \in Z,\ u(k) \in U, \tag{3.4}$$

$$\forall k \in K \tag{3.5}$$

where it assumed that the feasible sets Z and U are convex (Simon, 2017). The decision variables in X should be chosen over a horizon of time steps K such that the sum of the cost function $J(x,u)$ is minimized. The system state is bounded by the initial state 3.2, is subject to the dynamics 3.3, and both the state and input must belong to the feasible sets Z and U. Commonly, the cost function is formulated as

$$J(x,u) = x(k)^T Q x(k) + u(k)^T R u(k), \tag{3.6}$$

where the penalties of deviations in $x(k)$ and $u(k)$ are represented in the cost matrices Q and R. As the cost function steers the state and input to zero, the cost function can be modified when a different state and/or input is desired:

$$J(x,u) = (x(k) - \bar{x})^T Q (x(k) - \bar{x}) + (u(k) - \bar{u})^T R (u(k) - \bar{u}). \tag{3.7}$$

The linear equivalent of 3.6 is

$$J(x,u) = q^T x(k) + r^T u(k), \tag{3.8}$$

where q and r are cost vectors. Linear cost functions minimizes the corresponding elements, while quadratic cost functions steer the elements to a desired value.

The successful deployment of MPC requires "getting right" multiple aspects of the control problem. Thus MPC requires an accurate model of the system, which can be a large drawback, as it can be costly to generate (Darby & Nikolaou, 2012). However, if the mathematical model of the system is accurate, MPC has many advantages. Furthermore, centralized MPC with many constraints and control inputs can result in computational complexity and can become excessive (Ilic, Xie, & Joo, 2011). Nonetheless, MPC van be easily implemented and improved, thus the underlying optimization model can be modified if the accuracy of the systems mathematical description is improved or if the system is changed.

MPC is widely used for power systems and its open methodology results in accurate descriptions of the physical power network. Also, MPC provides the possibility to modify the system model and to simulate a largely different system. The aforementioned benefits outweigh this potential disadvantage. Furthermore, this thesis continuous on previous work, namely (Badings, Rostampour, & Scherpen, 2019b). In (Badings et al., 2019b) building-to-grid is integrated in power systems to create demand-side flexibility. However, we focus on the smart charging of EVs and behavioral factors of EV owners.

Chapter 4

MPC based Frequency Control Model with Social Behavior and Vehicle-to-Grid Options

In this chapter research questions 3 is addressed, as a dynamical framework of a power system with (bi-)directional charging of EVs is proposed, *i.e.*, the V2G MPC model. The hierarchical structure between TSO, DSO, Bld and EV are introduced, representing the interactions between different stakeholders in the power system. Indeed, multiple DSOs can be connected to a centralized TSO, multiple Blds to a DSO and multiple EVs to a Bld. Then, a centralized MPC based method is proposed to optimize the control variables simultaneously over a common time horizon.

The system model is proposed in the 4.1 in an hierarchical manner. Then, the TSO model is discussed in section 4.1.2, the DSO model in section 4.1.3. Next, the building model with its HVAC dynamics and the EV model are introduced in section 4.1.4. Finally, the optimization problem is given in section 4.2.

4.1 System Model

In this section, the system model is described. This model integrates the Transmission System Operator (TSO), Distribution System Operator (DSO), Building units (BLD) and Electric Vehicle (EV) models. These models are hierarchically connected. Then, their cost and utility functions are introduced for the formulation of an optimization problem.

4.1.1 System Description

Consider the system consists of the set of TSO and DSO buses. Let $\mathcal{T} = \{1, \dots, n_t\}$ denote the set of TSO buses, $\mathcal{D} = \{1, \dots, n_d\}$ denotes the set of DSO networks, $\mathcal{G} = \{1, \dots, n_g\}$ denotes the set of generators connected to TSO buses, $\mathcal{B} = \{1, \dots, n_b\}$ denotes the set of all building in the network. Let T_f be the prediction time horizon of the MPC and h be the time step of the simulation, then we define $\tau := \{t + h, t + 2h, \dots, t + T_f\}$ as the set of prediction time steps and $\Gamma := \{0, 1, \dots, \frac{T_f}{h} - 1\}$ the set of iteration time steps.

4.1.2 TSO model

In this subsection, we introduce the dynamic model of TSO buses. Let $\mathcal{T}_j^n$ be the set of neighboring buses of TSO bus j. Now we define the incidence matrix $\Pi \in \mathbb{R}^{n_t \times n_g}$, representing the connection of generators to TSO buses, as

$$\pi_{j,k} = \begin{cases} 1, & \text{if generator } k \quad \text{is connected to bus } j \\ 0, & \qquad\qquad\qquad\quad \text{else.} \end{cases} \tag{4.1}$$

The dynamics of TSO, called swing dynamics, for bus $j \in \mathcal{T}$ is given by

$$\begin{aligned} \dot{\delta}_j(t) =& f_j \\ M_j \dot{f}_j(t) =& -(d_j + \hat{d}_j)\omega_j(t) + \sum_{k=1}^{n_g} \pi_{j,k} P_{g_k}(t) \\ & - P_{bl_j}(t) - P_{ld_j}(t) \\ & - \sum_{i \in \mathcal{T}_j^n} b_{ji} \sin(\delta_j(t) - \delta_i(t)), \end{aligned} \tag{4.2}$$

where f_j is the frequency deviation from its nominal value, δ_j is the rotor angle, P_{bl_j} is uncontrollable load, P_{ld_j} is the controllable external load, M_j is the moment of inertia, d_j is the damping coefficients, $\hat{d}_j$ is the frequency-sensitive portion of the uncontrollable load at bus j, P_{g_k} is the generated power by generator k, and b_{ji} is the susceptance coefficient of the transmission line j and i. We can write (4.2) compactly as

$$\begin{aligned} F_{tso} \dot{x}_{tso}(t) =& A_{tso} x_{tso}(t) + B_g P_g(t) \\ & - B\big(P_{bl}(t) + P_{ld}(t) + \Phi(\delta(t))\big), \end{aligned} \tag{4.3}$$

where $x_{tso}(t) = [\delta_1, \ldots, \delta_{n_t}, f_1, \ldots, f_{n_t}]^T$, $\Phi(\delta(t)) = [\phi_1, \ldots, \phi_{n_t}]^T$ with $\phi_j = \sum_{i \in \mathcal{T}_j^n} b_{ji} \sin(\delta_j(t) - \delta_i(t))$, and

$$F_{tso} = \begin{bmatrix} \mathbb{I}_{n_t} & \mathbf{0}_{n_t \times n_t} \\ \mathbf{0}_{n_t \times n_t} & M \end{bmatrix}, \; A_{tso} = \begin{bmatrix} \mathbf{0}_{n_t \times n_t} & \mathbb{I}_{n_t} \\ \mathbf{0}_{n_t \times n_t} & -D \end{bmatrix},$$

$$B = \begin{bmatrix} \mathbf{0}_{n_t \times n_t} \\ \mathbb{I}_{n_t} \end{bmatrix}, \; B_g = \begin{bmatrix} \mathbf{0}_{n_t \times n_g} \\ \Gamma \end{bmatrix},$$

with M =diag$(m_1, \ldots, m_{n_t})$ and D =diag$(d_1 + \hat{d}_1, \ldots, d_{n_t} + \hat{d}_{n_t})$.

Then, we can discretize (4.3) by the virtue of first-order Gear's method as (Sincovec, Erisman, Yip, & Epton, 1981).

$$x_{tso}(t+h) = f_{tso}\big(x_{tso}(t), P_g(t), P_{ld}(t), P_{bl}(t)\big) \tag{4.4}$$

where h is the discretization time step. Now the following constraints can be considered as $\forall k \in \mathcal{G}$ and $\forall t \in \Gamma$

$$P_{g_k}^{min} \leq P_{g_k}(t+qh) \leq P_{g_k}^{max}, \tag{4.5}$$

$$P_{g_k}^{down} \leq P_{g_k}(t+qh+1) - P_{g_k}(t+qh) \leq P_{g_k}^{up}, \tag{4.6}$$

$$\mathbf{1}_{n_t}^T\big(\Pi P_g(t+qh) - P_{ld}(t+qh)\big) = 0, \tag{4.7}$$

4.1.3 DSO Model

In this subsection, we introduce the dynamic model of DSO. The set of DSO networks is given by $\mathcal{D} = \{1, \ldots, n_d\}$. Let $\mathcal{D}_i = \{1, \ldots, n_d^i\}$ denote the set of buses (nodes) of DSO i. Let each TSO network be connected to n_d DSO networks and let $\mathcal{D}_i^{n,m}$ denote the neighborhood set of bus i of DSO network m. Each TSO can be connected to one or multiple DSO networks which is modeled by the incidence matrix $\Lambda^m \in \mathbb{R}^{n_t \times n_d^m}$

$$\lambda_{j,i}^m = \begin{cases} 1, & \text{if bus } i \text{ of DSO } m \text{ is connected to TSO bus } j \\ 0, & \text{else.} \end{cases} \tag{4.8}$$

Now let $P_{j,i}^m$ denote the active power transmitted between DSO bus $i \in \mathcal{D}_i$ of DSO $m \in \mathcal{D}$ and TSO bus $j \in \mathcal{T}$. Then, the transmission matrix of DSO m can be given by P_{IMP}^m composed of $P_{j,i}^m$. This transmitted power can be considered as load for the TSO and generator for the DSO if the transmission matrix is positive. Since the DSO buses are not connected to generators, we can consider $M = 0$, $D = 0$; thus, the swing dynamics for the bus i of DSO $m \in \mathcal{D}$ can be given by

$$\begin{aligned} N_i^m \dot{\delta}_i^m(t) =& - P_{bd_i}^m(t) + \sum_{j=1}^{n_t} \lambda_{j,i}^m P_{j,i}^m(t) - \sum_{j \in \mathcal{D}_i^{n,m}} \Big(g_{ji}^m \cos(\delta_i^m(t) - \delta_j^m(t)) \\ & + b_{ij}^m \sin(\delta_i^m(t) - \delta_j^m(t)) \Big) \end{aligned} \tag{4.9}$$

where $P_{bd_i}^m(t)$ is the total load at bus i of DSO m and g is the line transmission conductance. Then, $P_{ld}(t)$ in (4.2) (TSO networks) can be given by

$$P_{ld}(t) = \sum_{m=1}^{n_d} \big(\Lambda^m \circ P_{IMP}^m(t)\big) \mathbf{1}_{n_d^m}. \tag{4.10}$$

and the transmitted power from TSO to DSO m in DSO network can be given by

$$P_{ld}^m = \big(\Lambda^m \circ P_{IMP}^m(t)\big)^T \mathbf{1}_{n_t} \tag{4.11}$$

Now we can rewrite (4.9) compactly for DSO $m \in \mathcal{D}$ as

$$F_{dso}^m \dot{x}_{dso}^m(t) = A_{dso}^m x_{dso}^m(t) + B_d^m \big(P_{ld}^m(t) - P_{bd}^m(t) - P_{bl}^m(t) - \Phi^m(\delta^m(t))\big), \tag{4.12}$$

where $x_{dso}^m(t) = [\delta_1^m, \ldots, \delta_{n_d^m}, f_1^m, \ldots, f_{n_d^m}^m]^T$, $P_{bl}^m(t)$ is the uncontrollable load, $P_{bd}^m(t)$ is the controllable load of DSO m buses, $\Phi^m = [\phi_1^m, \ldots, \phi_{n_d^m}^m]^T$ with
$\phi_i^m = \sum_{j \in \mathcal{D}_i^{n,m}} b_{ij}^m \sin(\delta_i^m(t) - \delta_j^m(t))$, and

$$F_{tso}^m = \begin{bmatrix} \mathbb{I}_{n_d^m} & \mathbf{0}_{n_d^m \times n_d^m} \\ \mathbf{0}_{n_d^m \times n_d^m} & \mathbf{0}_{n_d^m \times n_d^m} \end{bmatrix},$$

$$A_{tso} = \begin{bmatrix} \mathbf{0}_{n_d^m \times n_d^m} & \mathbb{I}_{n_d^m} \\ \mathbf{0}_{n_d^m \times n_d^m} & -N^m \end{bmatrix}, \; B_d^m = \begin{bmatrix} \mathbf{0}_{n_d^m \times n_d^m} \\ \mathbb{I}_{n_d^m} \end{bmatrix},$$

with $N^m = diag(N_1^m, \ldots, N_{n_t}^m)$.

Again we can discretize (4.12) by the virtue of first-order Gear's method as (Sincovec et al., 1981),

$$x_{dso}^m(t+h) = f_{dso}^m\big(x_{dso}^m(t), P_{IMP}^m(t), P_{bd}^m(t), P_{bl}^m(t)\big), \tag{4.13}$$

where h is the discretization time step. Now the following constraints can be considered for DSO $m \in \mathcal{D}$ in DSO network $\forall t \in \Gamma$

$$\mathbf{1}_{n_d^m}^T \big(P_{ld}(t+qh) - \Lambda^m P_{bd}(t+qh)\big) = 0. \tag{4.14}$$

4.1.4 Building Model

In this subsection, the model of the building thermal comfort level, the model of EVs per building model and the building's load model are introduced. The building units are connected to DSO buses through the incidence matrix $\Sigma^m \in \mathbb{R}^{n_d \times n_b}$ for DSO $m \in \mathcal{D}$ as given as

$$\sigma_{i,n}^m = \begin{cases} 1, & \text{if building } n \text{ is connected to bus } i \text{ of DSO } m \\ 0, & \text{else.} \end{cases} \tag{4.15}$$

4.1.4.1 Building thermal comfort model

Based on the models proposed in (Taha et al., 2017), (Pavlak et al., 2014) and (Badings et al., 2019b), consider the following first-order continuous-time equations as the building's thermal dynamics:

$$\dot{T}_{wall} = \frac{T_{amb} - T_{wall}}{C_{wall}R_2} + \frac{T_{zone} - T_{wall}}{C_{wall}R_1} + \frac{\dot{Q}_{sol}}{C_{wall}} \tag{4.16}$$

$$\dot{T}_{zone} = \frac{T_{wall} - T_{zone}}{C_{zone}R_1} + \frac{T_{amb} - T_{zone}}{C_{zone}R_{win}} + \frac{\dot{Q}_{int} - \dot{Q}_{hvac}}{C_{zone}} \tag{4.17}$$

where $T_{zone}(t)$ and $T_{wall}(t)$ are the building interior (zone) and wall temperatures. $T_{amb}(t)$ is the ambient temperature, and C_{zone} and C_{wall} are, respectively, the lumped thermal capacities of the zone and the walls plus roof. The parameters R_1, R_2 and R_{win} are, respectively, resistance parameters of the external wall, internal wall and windows. $\dot{Q}_{sol}$ is the sum of the absorbed solar radiation on the external wall. $\dot{Q}_{hvac}$ is the cooling and heating load, where HVAC stands for Heating, Ventilation and Air Conditioning. The consumed HVAC power is proportional to the load via $\dot{Q}_{hvac}(t) = \mu_{hvac}P_{hvac}(t)$. The building dynamics of (4.16) and (4.17) for the building n_b are described with the following state space model:

$$\dot{x}_b^{n_b}(t) = A_b^{n_b}x_b^{n_b}(t) + B_p^{n_b}P_{hvac}^{n_b}(t) + B_{w_b}^{n_b}w_b^{n_b}(t), \tag{4.18}$$

where $x_b^{n_b}(t) = \begin{bmatrix} T_{wall}^{n_b} & T_{zone}^{n_b} \end{bmatrix}^T$, $w_b^{n_b} = \begin{bmatrix} T_{amb}^{n_b} & \dot{Q}_{sol}^{n_b} & \dot{Q}_{int}^{n_b} \end{bmatrix}^T$, and the system matrices are defined as

$$A_b^{n_b} = \begin{bmatrix} -\frac{1}{C_{wall}}\frac{1}{R_1} + \frac{1}{R_2} & 1C_{wall}R_1 \\ \frac{1}{C_{zone}R_1} & -\frac{1}{C_{zone}}(\frac{1}{R_1} + \frac{1}{R_{win}} \end{bmatrix}^{n_b}, \tag{4.19}$$

$$B_p^{n_b} = \begin{bmatrix} 0 \\ -\frac{\mu_{hvac}}{C_{zone}} \end{bmatrix}^{n_b}, \; B_{W_b}^{n_b} = \begin{bmatrix} \frac{1}{C_{wall}R_2} & 1C_{wall} & 0 \\ \frac{1}{C_{wall}R_{win}} & 0 & 1C_{wall} \end{bmatrix}^{n_b} \tag{4.20}$$

The complete building dynamics for the full set $\mathcal{B}$ of buildings are described by the state space model

$$\dot{x}_b(t) = A_b x_b(t) + B_p P_{hvac}(t) + B_{w_b} w_b(t) \tag{4.21}$$

where block diagonal system matrices are defined as $A_b = \text{diag}(A_b^{n_b})_{n_b \in \mathcal{B}}$, $B_p = \text{diag}(B_p^{n_b})_{n_b \in \mathcal{B}}$ and $B_{w_b} = \text{diag}(B_{w_b}^{n_b})_{n_b \in \mathcal{B}}$. The state variable of the model are denoted as $x_b = \left[x_b^1, ..., x_b^{n_b}\right]^T \in \mathbb{R}^{2n_b}$ where x_b^l denotes the state variables of the building n_b. The input $P_{hvac} \in \mathbb{R}^{n_b}$ is the the cooling load set points of individual buildings. Additionally, we define $w_b = \begin{bmatrix} T_{amb} & \dot{Q}_{sol} & \dot{Q}_{int} \end{bmatrix}^T \in \mathbb{R}^{3n_b}$ where T_{amb}, Q_{sol} and Q_{int} denotes the ambient temperature, solar radiation and internal heat gain of buildings, respectively.

4.1.4.2 Electric Vehicle Model

We consider EVs in parking lots of a building waiting for charging. Let the active power of EV i be denoted by $p_{ev_i}(t)$ for all $i \in \mathcal{B}$.

The parameters for each EV are determined as follows. The survey results are used as inputs for each EV. It provides the model with the car type, the battery's capacity, the willingness to smart charge, the arrival charge and the desired departure charge. For each participant from the selected survey population an entry into a matrix is created with all the aforementioned parameters. For each EV a random row from the matrix is selected.

Now, we consider that there exist a smart charging contract and each EV can follow or unfollow the smart charging contract. In case the EV follows this contract, the charging of an EV is bi-directional. However, if the EV does not follow the contract, then an EV is only charged (G2V) and not discharged (V2G). There are three approaches for determining whether an EV has the smart charging mode either ON or OFF. First, the choice is based on the willingness of EV owners to smart charge, where for willingness $1-2$ smart charging is OFF, for $4-5$ it's ON and for 3 there is a 50% of smart charging being ON or OFF. Second, there is an alternative approach possible, as the survey question on the willingness to smart charge was answered on a 1 to 5 scale, not with a yes or a no. EVs with a smart charging contract will not always activate the smart charging mode. This creates a second question for EVs that follow the smart charging contract, whether they activate smart charging. This depends on how enthusiasm an EV owner has for smart charging. In this case it is first determined whether an EV has a smart charging contract in the same manner as the first approach. Then, based on their willingness there is a probability for EVs to actually activate smart charging. For a willingness of 3 this is $\rho_{act_i} = 60\%$, for a willingness of 4 this is $\rho_{act_i} = 80\%$ and for a willingness of 5 this is $\rho_{act_i} = 100\%$. Third, the mode smart charging mode can be determined with a general probability $\rho_{ev} \in [0, 1]$ for which smart charging is ON. Smart charging is OFF for $1 - \rho_{ev}$.

Now let EVs arrive at the parking lots at T_{arr} and departure from the parking lots at T_dep. Then, the state of charge of EV in the ON mode is given by $\forall i \in \mathcal{B}$ and $t \in [T_{dep}, T_{arr}]$

$$x_{ev_i}(t + qh + 1) = \delta_{ev_i} x_{ev_i}(t + qh) + b_{ev_i} P_{ev_i}(t + qh) \tag{4.22}$$

where P_{ev_i} is the (dis)charging input power, and x_{ev_i} depicts the energy stored in battery of EV i. Also, $\delta_{ev_i} \leq 1 and b_{ev_i}$ are the self-discharging energy loss, charging efficiency coefficient, respectively. The state of charge of an EV with smart charging mode OFF is given by $\forall i \in \mathcal{B}$, $t \in [T_{dep}, T_{arr}]$

$$x_{ev_i}(t + qh + 1) = \begin{cases} \delta_{ev_i} x_{ev_i}(t + qh) + b_{ev_i} P_{ev_i}(t + qh), & \text{if } x_{ev_i} \leq x^*_{ev_i} \\ \delta_{ev_i} x_{ev_i}(t + qh), & \text{else.} \end{cases} \tag{4.23}$$

where $u_{ev_i}(t) \geq 0$, and $x^*_{ev_i}$ is the desired the state of charge indicated by the EV owner.

Now we consider the associated constraints of Evs as $\forall i \in \mathcal{B}$ and $t \in [T_{dep}, T_{arr}]$

$$P^{min}_{ev_i} \leq P_{ev_i}(t + qh + 1) \leq P^{max}_{ev_i}, \tag{4.24}$$

$$x^{min}_{ev_i} \leq x_{ev_i}(t + qh) \leq x^{max}_{ev_i}, \tag{4.25}$$

where $u^{max}_{ev_i}$, $u^{min}_{ev_i}$ are the maximum and minimum active power ratings, $q^{max}_{ev_i}$, $q^{min}_{ev_i}$ are the maximum and minimum reactive power, and $x^{max}_{ev_i}$, $x^{min}_{ev_i}$ are maximum and minimum of the energy stored in battery of Ev i.

Now a cost function for battery degradation of EVs is considered as $\forall i \in \mathcal{B}$, $t \in [T_{dep}, T_{arr}]$

$$C^b_{ev_i}(t) = \frac{1}{2} \beta^0_{ev_i} \sum_{t \in \Gamma} \big(P_{ev_i}(t + 1) - p_{ev_i}(t)\big)^2, \tag{4.26}$$

where $\beta^0_{ev_i}$ is a positive constant. EV owners give the desired charging level at a specific time slot, the departure time, which is modelled as a cost function given by $\forall i \in \mathcal{B}$,

$t \in [T_{dep}, T_{arr}]$

$$C_{ev_i}^T(t) = \frac{1}{2}\beta_{ev_i}^1 \big(x_{ev_i}(T_{dep}) - x_{ev_i}^*\big)^2, \tag{4.27}$$

where $\beta_{ev_i}^1$ is a positive constant and $x_{ev_i}^*$ is the desired state of charge of EVs. Depending on whether an EV leaves with more or less charge than when it arrived, EV owners will pay for charge they received or receive payment for charge they provided. This is modelled as a cost function given by $\forall i \in \mathcal{B}$, $t \in [T_{dep}, T_{arr}]$

$$C_{ev_i}^P(t) = \frac{1}{2}\beta_{ev_i}^2 \big(x_{ev_i}(T_{dep}) - x_{ev_i}(T_{arr})\big) \tag{4.28}$$

Therefore, the cost of EVs can be given by $\forall i \in \mathcal{B}$ and $t \in [T_{dep}, T_{arr}]$

$$C_{ev_i}(t) = C_{ev_i}^b + C_{ev_i}^T + C_{ev_i}^P, \tag{4.29}$$

Now we can formulate the total active power of building at bus i of DSO m as

$$\begin{aligned} P_{bd}^m &= [P_{bd_1}^m, \dots, P_{bd_{n_d^m}}^m]^T \\ &= \Sigma^m \big(P_{hvac} + P_{ev} + P_{misc}\big), \end{aligned} \tag{4.30}$$

where P_{hvac}, P_{misc} and P_{ev} are the column vectors for the HVAC power demand, the uncontrollable miscellaneous power consumption and the EV power demand.

Now the following constraints can be considered as $\forall i \in \mathcal{B}$, $\forall t \in \Gamma$

$$\sum_{m=1}^{n_d} P_{bd}^m(t+qh) = P_{hvac}(t+qh) + P_{ev}(t+qh) + P_{misc}(t+qh). \tag{4.31}$$

4.2 MPC Based Optimal Frequency Control

In this section, we formulate the optimal frequency control problem as an optimization problem, MPC can be used to solve the problem. We consider the discretized model of TSO, DSO, BLD and EV. Let $x(t) = \big(P_g(t), P_{IMP}(t), P_{bd}(t), P_{hvac}(t), P_{ev}(t)\big)^T$ be the decision variable vector. Where $t \in \Gamma$ indicates the time steps. Then, the finite-horizon optimization problem can be given by

$$\begin{aligned} \min_x \quad & \sum_{t \in \mathcal{T}} \Big(\big(f_{tso}(t)\big)^T f_{tso}(t) + \sum_{m=1}^{n_d} \big(f_{dso}^m(t)\big)^T f_{dso}^m(t)\Big) \\ & + \sum_{i=1}^{n_b} C_{ev_i}(t) \\ s.t. \quad & (4.4) - (4.7), (4.13) - (4.14), (4.29) \end{aligned} \tag{4.32}$$

Subject to, $\forall t \in \Gamma$

1. TSO, DSO, BLD, EV Dynamics:

$$x_{tso}(t+1) = f_{tso}\big(x_{tso}(t+1), P_g(t+1), P_{ld}(t+1), P_{bl}(t+1)\big), \tag{4.33}$$

$$x^m_{dso}(t+1) = f^m_{dso}\big(x^m_{dso}(t+1), P^m_{IMP}(t+1), P^m_{bd}(t+1), P^m_{bl}(t+1)\big), \tag{4.34}$$

$$x_{bd}(t+1) = f_{bd}\big(x_{bd}(t+1), P_{hvac}(t+1), P_{ev}(t+1)\big), \tag{4.35}$$

For smart charging ON (4.36)

$$x_{ev_i}(t+1) = \delta_{ev_i} x_{ev_i}(t+1) + b_{ev_i} P_{ev_i}(t+1), \tag{4.37}$$

For smart charging OFF (4.38)

$$x_{ev_i}(t+1) = \tag{4.39}$$

$$\begin{cases} \delta_{ev_i} x_{ev_i}(t+1) + b_{ev_i} P_{ev_i}(t+1), & \text{if } x_{ev_i} \leq x^*_{ev_i} \\ \delta_{ev_i} x_{ev_i}(t+1), & \text{else.} \end{cases} \tag{4.40}$$

2. Generation power and ramp limits.

$$P^{min}_{g_t} \leq P_{g_t}(t+1) \leq P^{max}_{g_t} \tag{4.41}$$

3. TSO network balance

$$\mathbf{1}^T_{n_t}\big(\Pi P_g(t+1) - P_{ld}(t+1)\big) = 0 \tag{4.42}$$

4. DSO network balance

$$\mathbf{1}^T_{n^m_d}\big(P_{ld}(t+1) - \Lambda^m P_{bd}(t+1)\big) = 0 \tag{4.43}$$

5. Building power balance

$$\sum_{m=1}^{n_d} P^m_{bd}(t+1) = P_{hvac}(t+1) + P_{ev}(t+1) + P_{misc}(t+1) \tag{4.44}$$

6. Building comfort limits

$$x^{min}_{bd}(t+1) \leq x_b(t+1) \leq x^{max}_b(t+1) \tag{4.45}$$

7. HVAC power and ramp limits

$$P^{min}_{hvac} \leq P_{hvac}(t+1) \leq P^{max}_{hvac} \tag{4.46}$$

$$P^{down}_{hvac} \leq P_{hvac}(t+1) - P_{hvac}(t) \leq P^{up}_{hvac} \tag{4.47}$$

8. EV capacity limit and (dis)charge limits

$$x_{ev}^{min} \leq x_{ev}^{i}(t+1) \leq x_{ev}^{max} \tag{4.48}$$

For smart charging mode ON

$$0 \leq P_{ev}^{i} \leq P_{ev}^{max} \tag{4.49}$$

For smart charging mode OFF

$$P_{ev}^{min} \leq P_{ev}^{i}(t+1) \leq P_{ev}^{max} \tag{4.50}$$

Furthermore, let the optimal solution of the proposed V2G-MPC framework be the following:

$$x^{*}(t) = \left(P_{g}^{*}(t), P_{IMP}^{*}(t), P_{bd}^{*}(t), P_{hvac}(t), P_{ev}^{*}(t)\right) \tag{4.51}$$

At each time step $t \in \Gamma$ the solution is solved for a set prediction horizon T_p. Then the state variables are initialized for the next time step $t+1$.

Chapter 5

Simulation Setup and Results

In this chapter the simulation results from the V2G MPC model proposed in the previous chapter are discussed. Furthermore, in this chapter research question 3 and 4 are answered, as the effect of the EV owner's willingness to smart charge is determined and the effect of other parameters is discussed.

In section 5.1 the simulation setup is discussed. In section 5.2 the simulation results are presented, where different scenarios are compared.

5.1 Simulation setup

In Chapter 4 the V2G-MPC model is formulated in an iterative manner. However, to improve the computational performance of the code, a stacked formulation was implemented. The state of the system is not calculated attractively over time, but the trajectory is calculated over the complete prediction horizon. Stacked MPC is achieved by creating stacked dynamics. Where time steps are combined into the system's state. This approach was also used in (Badings et al., 2019b) for their BtG-MPC model.

The optimization is implemented in MATLAB, where Yalmip is used as interface and Gurobi is used as solver. The building parameters and the non-controlable loads (P_{misc}) were adopted from (Taha et al., 2017). Grid parameters were obtained from MatPower IEEE 5-bus power system (Zimmerman, Murillo-Sánchez, & Thomas, 2010). The network used for the simulations is given in Figure 5.1 where there are 13 buildings, 2 DSOs, 1 TSO and 3 non-renewable power generator sources in the network. In Appendix C all the simulation parameters are given. All simulations are simulated for 24 hours, with a prediction time horizon of 1 hour and a step width of 5 minutes.

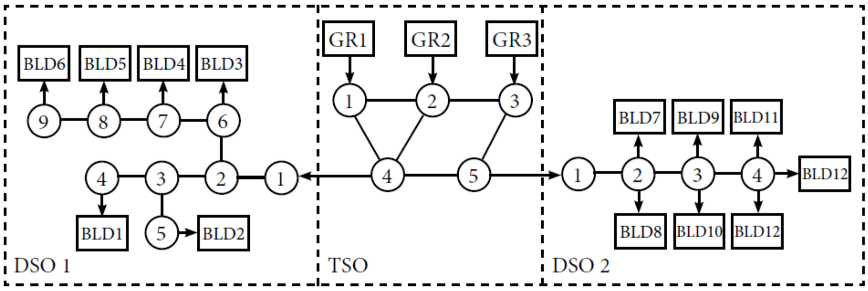

FIGURE 5.1: The network topology of the TSO, DSO, BLD system

In order to simulate the charging of EVs correctly, input parameters for each EV are required. In the flow chart in chapter 1 Figure 1.3 these parameters are shown. Specifically, an EV arrives at a certain time, with an initial SOC and a maximum and minimum capacity. The EV owner gives the departure time and the desired minimal SOC. Next, smart charging mode is either ON or OFF. Finally, when the EV leaves at the departure time, it has a certain SOC. However, the arrival and departure times are not given in the NewMotion survey. We consider the smart parking lots are part of office buildings. Thus, EV owners travel to the buildings to go to their jobs. Since the working hours are predictable, it is possible to use a normal distribution to determine the working hours of EV owners. The mean for arrival time used is 8:30 AM and the mean for departure time used is 5:00 PM, the standard deviation used is 45 minutes.

Furthermore, the NewMotion survey results give us the arrival charge, the minimal departure charge, the willingness to smart charge and the car type. The car type can be used to determine the car's capacity, which is shown in Appendix B in Table B.3. The arrival and departure charge are given in percentage of the car's capacity. The willingness to smart charge is given on a scale from 1 to 5. This is converted to ON or OFF by considering EV owners with a willingness of 1 or 2 to have smart charging OFF, and EV owners with a willingness of 4 and 5 to have smart charging ON. Moreover, for a willingness of 3, EV owners have a 50% change of following a smart charging contract. For every survey participant an entry with his determined EV parameters is created. All these entries are combined in a matrix. To determine the parameters for each EV, a row is selected via uniformly distributed randomization. This is a more accurate approach than determining every EV parameter separately, as EV owners with different EV types have different values for these parameters. Furthermore, there is also a possibility to determine the status of the smart charging mode based on a probability, $\rho_{ev} \in [0, 1]$. If this approach is used, from the survey results it can be determined that $\rho_{ev} = 78\%$. Additionally, in subsection 5.2.2 another alternative approach is discussed.

5.2 Simulation results

In this section the simulation results are presented. For every section two scenarios are compared. At the end of this section a general conclusion on these simulation results is provided.

For most simulations the computational time is considered 40 minutes which depends on the number of EVs used in the simulation, at least 5 EVs and at most 50 EVs. Each EV requires an "individual" cost function that changes each iteration, ensuring that the EVs meet their desired SOC at the departure time.

The stability of the grid is expressed in the frequency deviation of the TSO and DSO busses. For determining the total grid frequency deviation only the voltage angle is considered. Generally, deviations are caused by sudden changes in power loads and flows. In this V2G-MPC model the ramp up/down of the building grid load, VAC power or miscellaneous loads, is the main cause for frequency deviations. Additionally, the EVs power demand causes frequency deviations when EVs are required to meet the desired state of charge at the departure time. The EVs arrive around 8:30 AM and leave around 5:00 PM, thus the EVs only affect the grid within this time frame.

5.2.1 Willingness levels

The main objective of smart charging is stabilizing the grid. The V2G-MPC model can be used to show this beneficial effect. Therefore, the smart charging of EVs should result in a more stable grid. Scenario 1: 0% of the EVs are smart charging, thus every EV can only be charged G2V. Scenario 2: 100% of the EVs are smart charging. It is expected that the grid is more stable for scenario 2.

The resulting network frequency deviations of the TSO and DSO for scenario 1 and 2 over 24 hours are given in Figure 5.2 and Figure 5.3, respectively. The figures give the maximum and minimum value of the frequency deviation in order to provide a representation of the frequency deviation over time. Furthermore, the combined SOC of EVs per building and the combined power flow of EVs per building are given for both scenarios in Figure 5.5 and Figure 5.6, respectively. When comparing both scenarios it can be observed from the figures that there is a reduction in grid frequency deviation. In Scenario 2, when EVs are smart charging, the EVs smart charging results in a smoother building load to the grid. The EVs are used to compensate for variations in building-side loads and for variations in EV loads, *i.e.*, building loads power can often get this power from other EVs parked at the same building. Consequently, the total grid frequency deviation is reduced by 13% in the full network, and by 22% in the DSO network.

Furthermore, as EVs are only smart charging for on average 8 hours and 30 minutes, their stabilizing factor is limited to this time frame. Thus, when the total grid frequency over the time period of 7:45 AM to 17:45 PM (mean plus standard deviation) is considered, then the total grid frequency deviation is reduced by 33% and for the DSO network by 54%. It can be concluded that smart charging results in a more stable grid.

Moreover, in Figure 5.4 the power flow of all buildings combined is shown for both scenarios. It shows the total, the EV, the HVAC and the miscellaneous power flow over time. Additionally, in Figures 5.5 and 5.6 the SOC and the power flow over time of all EVs combined per building can be observed, respectively. Logically, the SOC of combined EVs only increases for scenario 1 and the combined EV's power flow is never negative, as V2G is not enabled. Thus, for scenario 2 it can be seen that the SOC decreases and the combined power flow per building is mostly negative. The survey provided results for the arrival and the minimum departure charge. In chapter 2 it was shown that the average departure charge was 15% lower than the average arrival charge. Thus EVs are able to provide power back to the grid. Which can be seen in Figure 5.6.

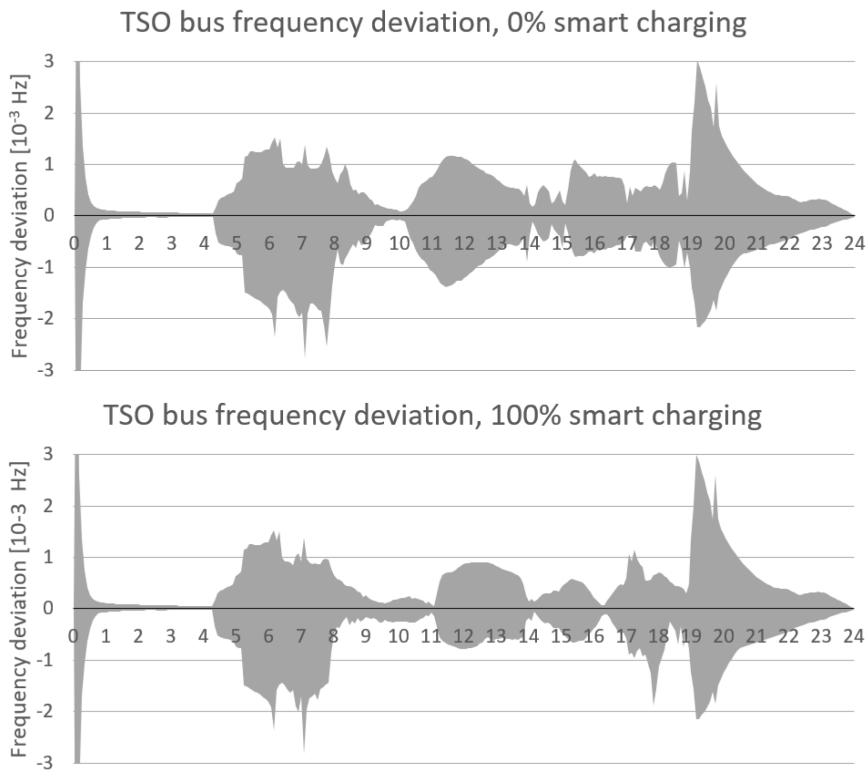

Figure 5.2: Scenario 1: the TSO bus frequency deviation for 0% and 100% of EVs smart charging

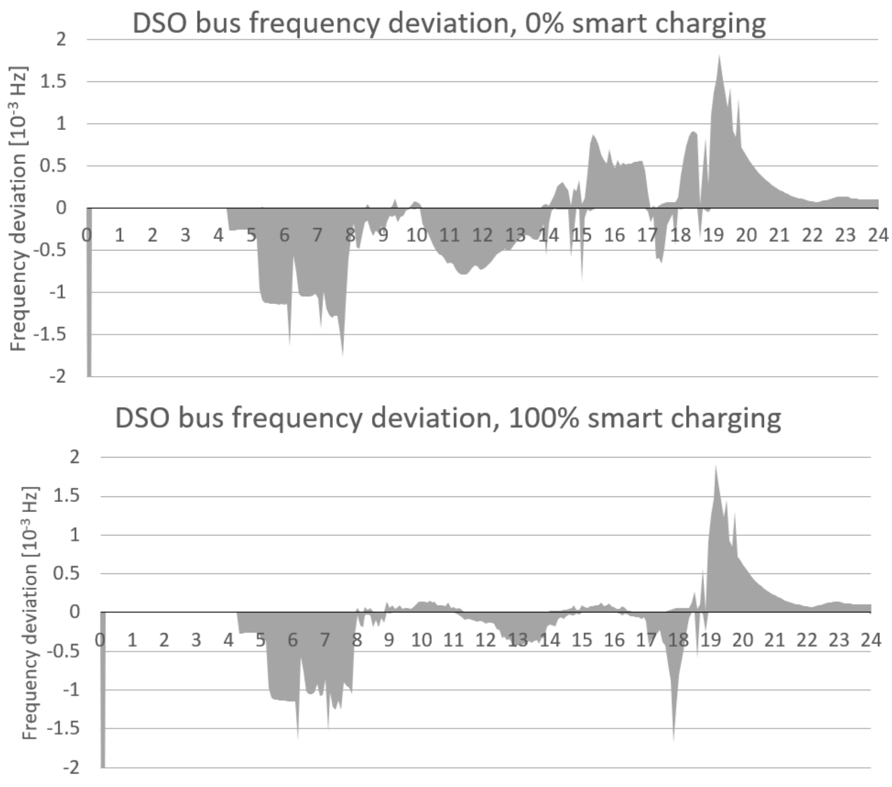

FIGURE 5.3: Scenario 1: the DSO bus frequency deviation for 0% and 100% of EVs smart charging

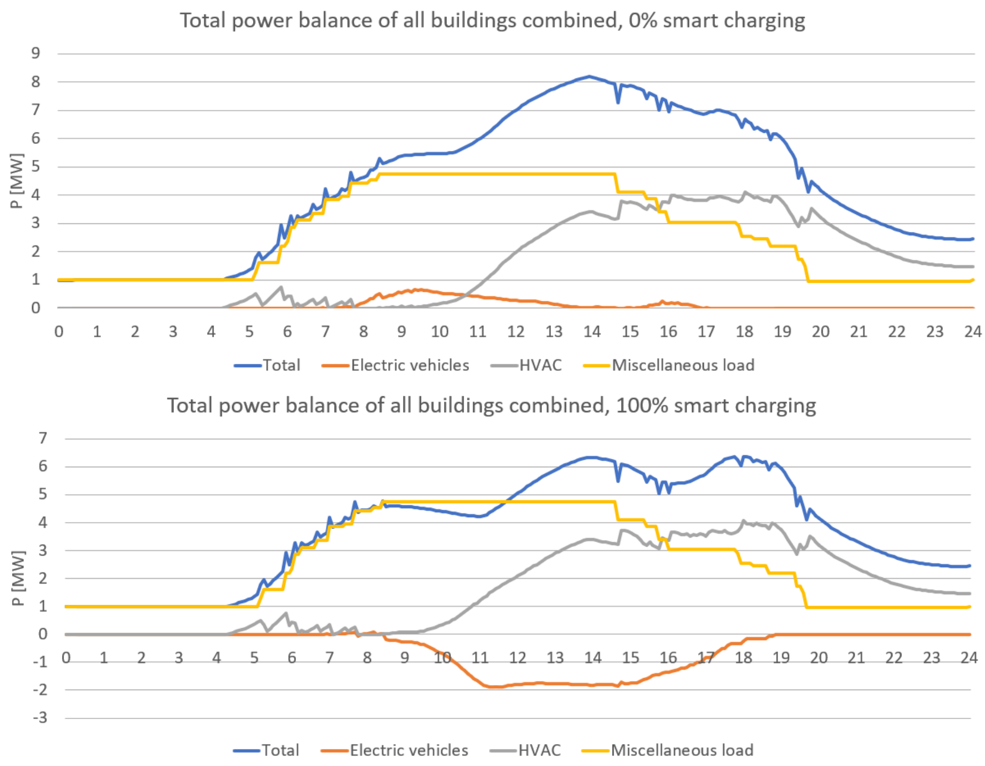

FIGURE 5.4: The total building, EV, miscellaneous and HVAC power flow over time for 0% and 100% of EVs smart charging

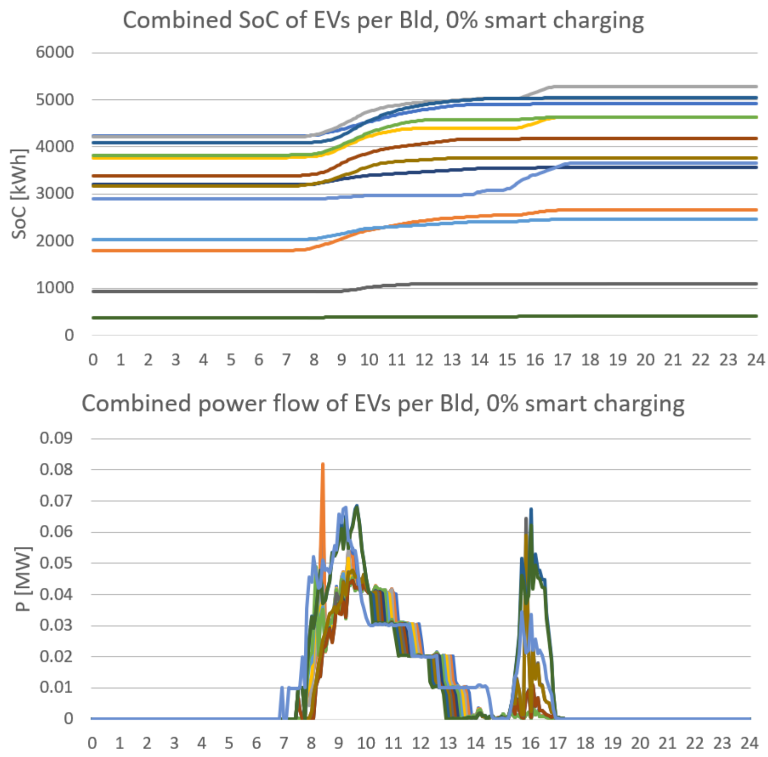

FIGURE 5.5: Scenario 2: the combined SOC and power flow of EVs per building for 0% of EVs smart charging

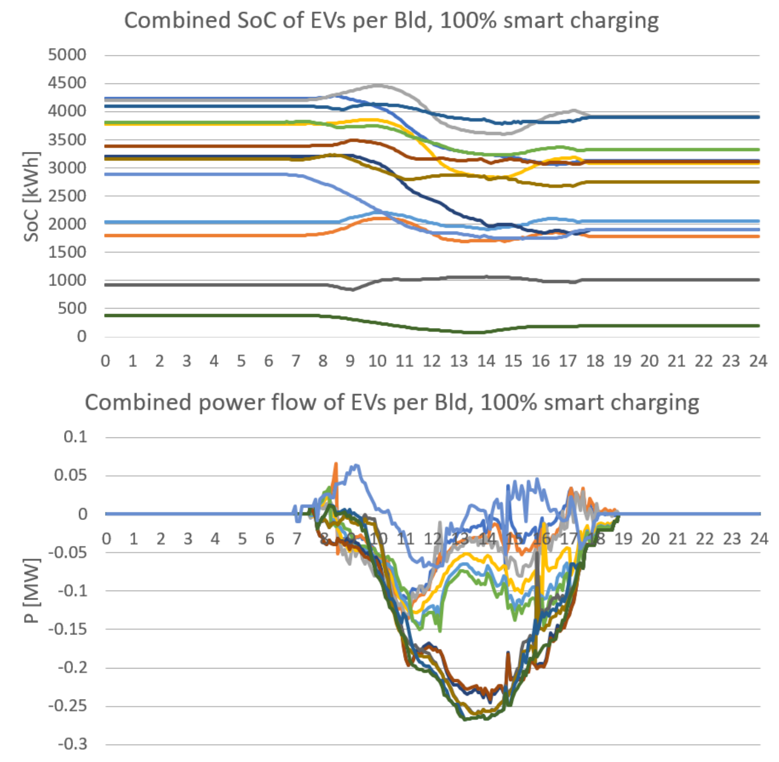

FIGURE 5.6: Scenario 2: the combined SOC and power flow of EVs per building for 100% of EVs smart charging

5.2.2 Asking participants if they activate smart charging

A two-step approach to determining whether an EV has smart charging ON or OFF was introduced in Chapter 4. More precisely, based on EV owners' willingness to smart charge it is determined whether they have a smart charging contract. Then, based on this willingness it will be determined whether they activate smart charging. For willingness 5, this activation probability is $\rho^2_{ev_i} = 100\%$, for willingness 4 $\rho^2_{ev_i} = 80\%$, and for willingness 3 $\rho^2_{ev_i} = 60\%$. Figure 5.7 shows the probabilities for each option based on the survey results. Figure 5.8 show the percentage of EVs will eventually smart charge with this approach.

The difference between the introduced two-step approach and the approach from the previous section, where $\rho_{ev_i} = 78\%$, is fewer EVs with smart charging mode ON. The higher the number of EVs that smart charge, the less frequency deviation is experienced in the grid. Consequently, the total grid frequency deviation increases by 5% in the full network, and by 2% in the DSO network.

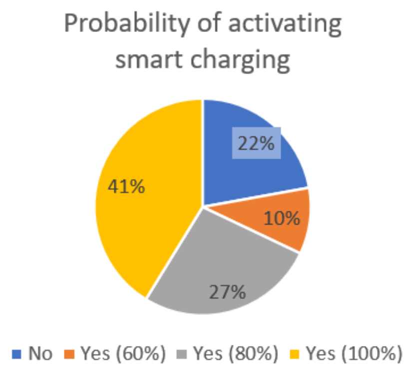

FIGURE 5.7: Based on the willingness to smart charge, the distribution in percentage for each different option of the two-step approach is given

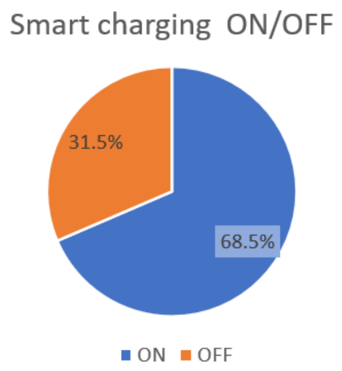

FIGURE 5.8: The percentages of EVs that have smart charging ON and OFF for the two-step approach

5.2.3 Number of Electric vehicles

In this section two scenarios are compared. Scenario 1: we have on average 5 EVs per building. Scenario 2: we have on average 50 EVs per building. Thus, a simulation with few and with many EVs are compared. It is expected that increasing the number of EVs per building results in: Firstly, a more stable grid, since more EVs are available to provide flexibility to anticipate power fluctuations. Secondly, the power load of each individual EV are reduced, since the load required for stabilizing can be spread among more EVs.

In Figure 5.9 the average power load of all the EVs is shown over time for both scenarios. It can be observed that the power load for scenario 2 is less than for scenario 1. Also, scenario 1 has more and bigger fluctuations. For scenario 1 the average G2V power load for an EV is 15.3 kWh and for V2G this is -14.2 kWh. For scenario 2 the average G2V power load is 11.3 kWh and the average V2G power load is -12.4 kWh. This is a reduction of 26% G2V power and 13% V2G power. Thus, as expected the power load of each individual EV are reduced if the number of EVs is increased. Additionally, EVs provide power to the system as on average their SOC decreases. So an increase of the number of EVs also results in decrease in power generation, in this case a decrease of 7%. This is not ideal, as it is not realistic for an EV to charge over night to then provide power to the office during the day. This issue is addressed in Section 5.2.5.

Furthermore, for scenario 2 the number of EVs is increased by ten fold. Thus, the the total power demand of the EVs is much larger for the second scenario. This increase can increase the frequency deviation as more power is required. However, there are also more EVs available to provide power V2G. Moreover, it was found that the total frequency deviation is reduced by only 1%, and for the DSO network only the reduction is 6%. The corresponding figures of the frequency deviation for TSO and DSO can be found in Appendix D. If instead of 24 hours, we look at the time frame from 7:45 to 17:45, then total frequency deviation is reduced by 8%, and for the DSO network the reduction is 26%. Hence, more EVs provide a more stable grid. However, the difference is not big, as the number of EVs is increased, the total power demand is increased, which can results in more instability.

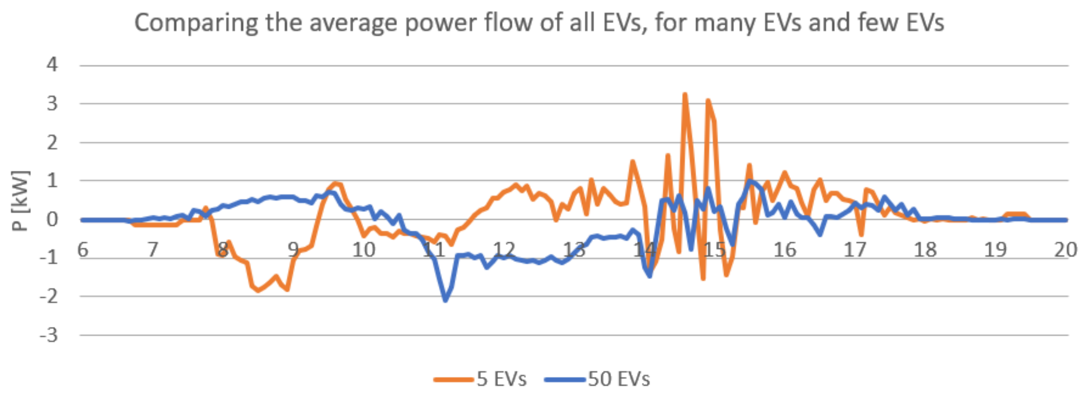

FIGURE 5.9: Comparing the average power flow of all EVs for simulations with on average 5 and 50 EVs per building

5.2.4 Charging speed

In this section, two scenarios with different charging speeds are compared. Scenario 1: the maximum (dis)charging speed is set at 7.2 kW, which is the charge rate of a level 2 charging pile according to (Office of Energy Efficiency & RE, 2017). Scenario 2: the maximum (dis)charging speed is increased by ten fold to 72 kW. As a result the charging rate is not a limiting factor anymore. Scenario 2 should result in a reduction in frequency deviation. Indeed, a higher charging speed the dampening effect of an EV should increase. Furthermore, in order to provide the dampening effect the load per EV will increase. Moreover, according to (Energy Element, 2013) the recharging time of an EV can be a barrier to EV adoption. So a higher charging rate can aid consumers' receptiveness to EVs and EV owners' receptiveness to smart charging.

The Figure 5.10 and Figure 5.11 show the TSO and DSO frequency deviation. Surprisingly, the results show that the total frequency deviation increased by 2% for faster charging. Moreover, the frequency deviation for the DSO network decreased by 12% and the frequency deviation for the TSO network increased by 7%. For the 7:45 AM to 17:45 PM time interval these values increase by 15%, decrease by 22% and increase by 27% for the frequency deviation of the total system, the DSO network and the TSO network, respectively. The higher charging speed brings stability to the TSO grid, however, it destabilizes the TSO grid.

In Figure 5.12 the total SOC of all EVs is shown for both scenarios. It can be seen that the total SOC develops differently over time. For scenario 1 the total SOC decreases

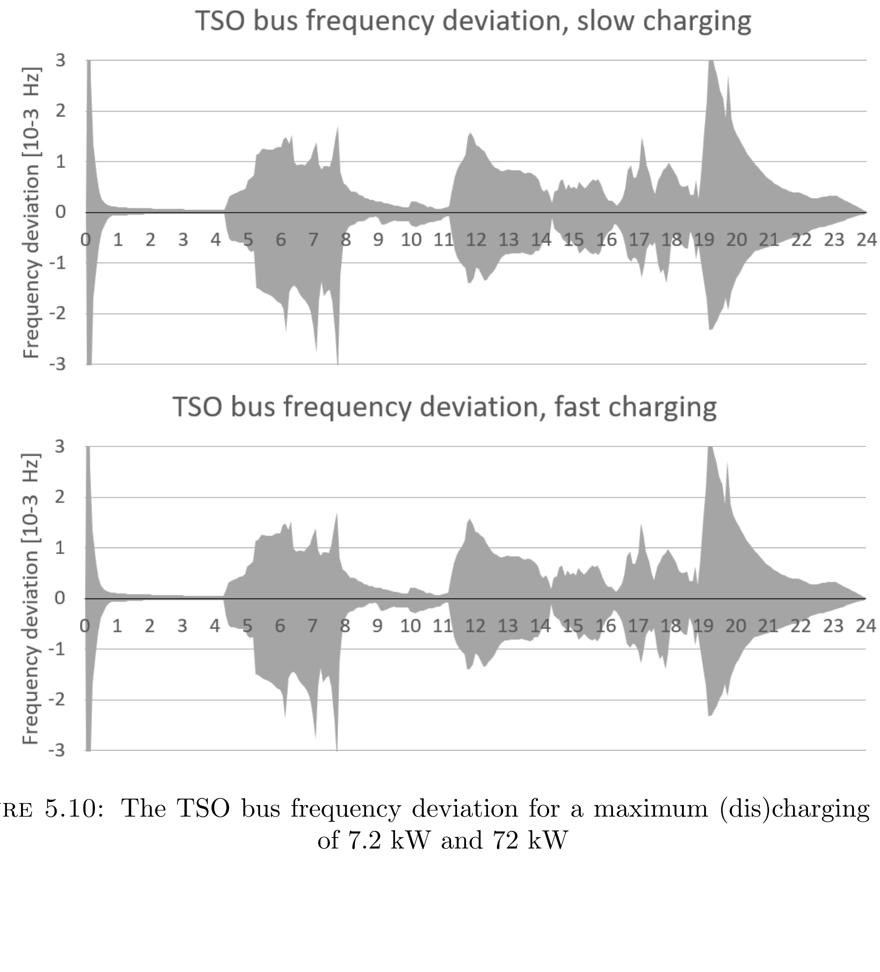

Figure 5.10: The TSO bus frequency deviation for a maximum (dis)charging speed of 7.2 kW and 72 kW

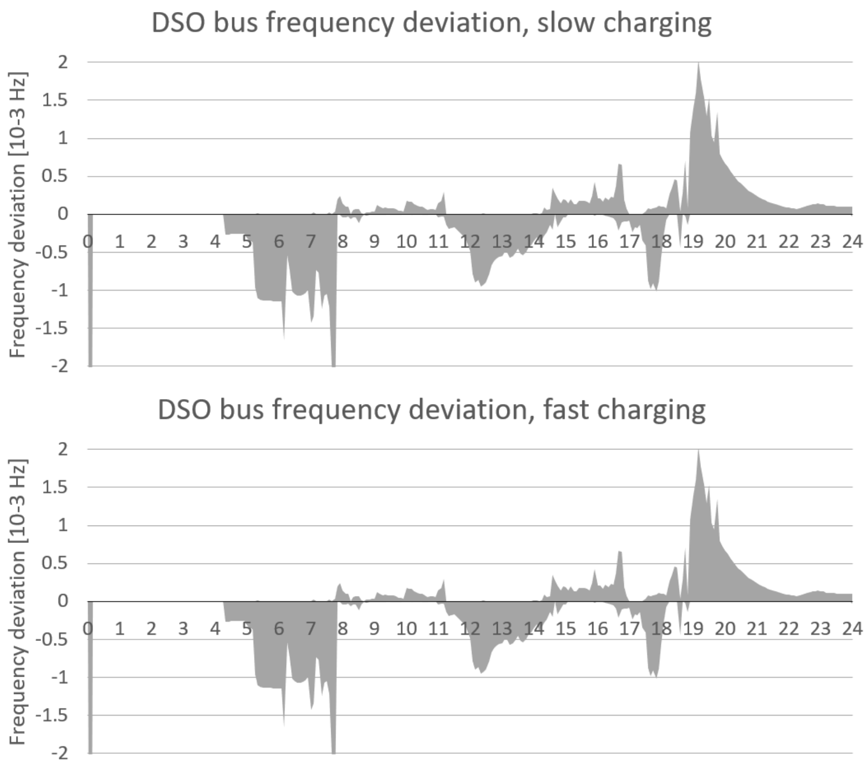

FIGURE 5.11: The DSO bus frequency deviation for a maximum (dis)charging speed of 7.2 kW and 72 kW

gradually over time and close to the departure time it increases again. While scenario 2 has two peaks in SOC, one right after the arrival of most EVs and one right before the departure of most EVs, the SOC remains relatively constant between the peaks. EVs should departure with at least their desired SOC and EVs departure at different times around 17:00, which explains the peaks before the departure time for both scenarios. In Figure 5.13 the total power flow of all EVs is shown for both scenarios. The power flow for scenario 1 is much smaller than scenario 2, since the charging is limited by its slower charging speed. In fact, the total G2V power load increased by 120% and the total V2G power load increased by 49% for a charging speed of 72 kW. The total power generation decreased by 6%.

It can be concluded that a faster charging speed for smart charging EVS does not necessarily result in more benefits to the power grid than a slower charging speed. It is possible that for the faster charging speed the simulation study parameters are not accurate. Moreover, the more a battery is used, the more it degrades. There is a cost function such that the EV's battery is only used when it is beneficial. However, for scenario 2 the batteries of EVs are used extensively without a clear benefit to the stability of the grid. It is also seen that the higher power flow of scenario 2 increases the stability of the DSO network, while the stability of the TSO network decreases. It is possible that due to the hierarchical nature of the model the increase in activity on the lower level has a negative effect on the stability of the upper TSO level.

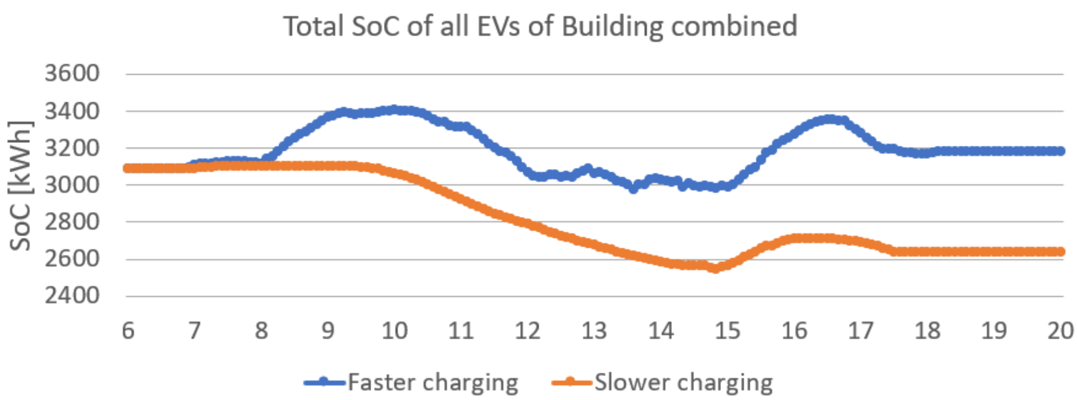

FIGURE 5.12: Comparing the total SOC of all EVs for simulations with a slow (7.2 kW) and fast (72 kW) maximum charging speed

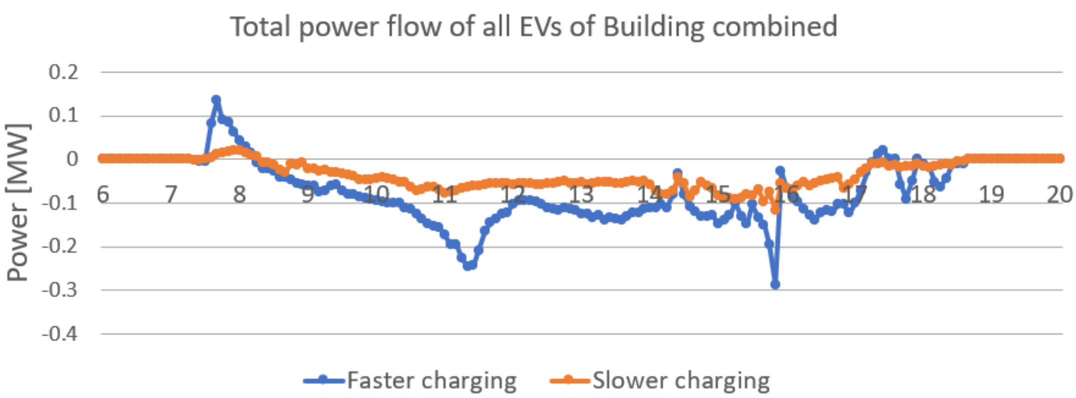

FIGURE 5.13: Comparing the total power flow of all EVs for simulations with a slow (7.2 kW) and fast (72 kW) maximum charging speed

5.2.5 The departure state of charge

For subsection 5.2.4 the average desired departure SOC of EVs is lower than the average arrival SOC. This is because they all use the survey results as input. However, in the survey it was asked how much participants want their battery to be charged at least when they leave work. Thus, the desired departure SOC of EV owners will very likely be higher than the values collected by the survey. In this section the desired departure state of charge is varied. For all scenario's the desired state of charge is normally distributed with a standard deviation of 10%. For scenario 1 the mean is 50%, for scenario 2 it is 70% and for scenario 3 it is 100%. With an increase of departure SOC it can be expected that; firstly, the total power load from G2V will increase. Secondly, the total V2G power load will decrease. Thirdly, the stabilizing benefits to the grid will decrease. Lastly, the power generated will increase.

	Total frequency deviation	TSO frequency deviation	DSO frequency deviation
Scenario 1	100%	100%	100%
Scenario 2	103%	103%	101%
Scenario 3	115%	114%	119%

	Total G2V power load	Total V2G power load	Power generation
Scenario 1	100%	100%	100%
Scenario 2	121%	49%	102%
Scenario 3	198%	4%	108%

TABLE 5.1: Tables that provide an overview of simulation results which can be used to compare the three scenarios

Table 5.1 gives the relevant simulation results where scenario 1 is the base case. From Table 5.1 it can be seen that the frequency deviation increases when the desired departure SOC increases. Furthermore, it shows that the total G2V load increases and the total V2G load decreases. Finally, it shows that the power generation increases, in order to provide the EVs with their desired SOC. In figure 5.14 it is shown that the average SOC of all the EVs approaches to the desired departure SOC over time. Thus, the simulation results are as expected. When the desired departure SOC is lowered, smart charging becomes beneficial to the stability of the grid.

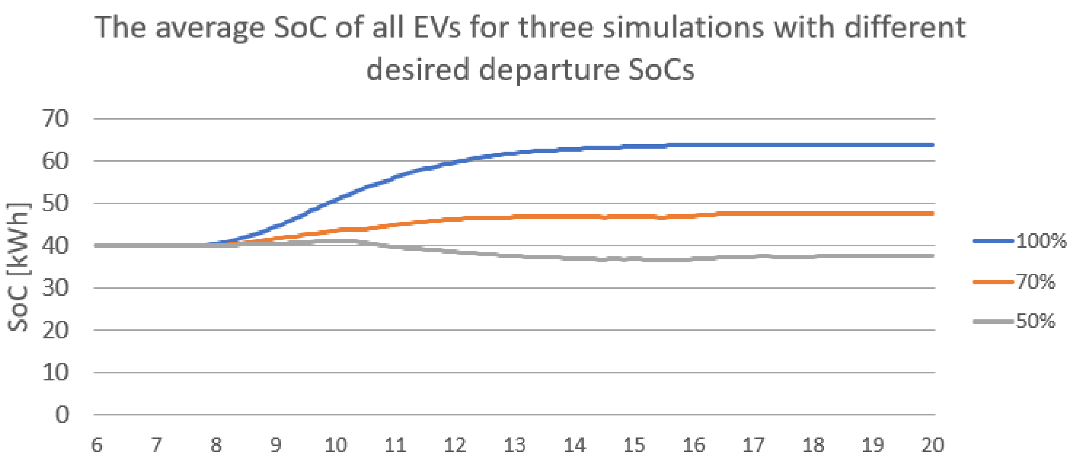

FIGURE 5.14: Comparing the average SOC of all EVs for three simulations with a different desired state of charge

5.2.6 Conclusion

In this chapter research questions 4 and 5 are addressed: 'How does the willingness to follow smart charging affect the stability of the power grid?' 'What other factors influence the success of smart charging?' The dynamical V2G framework with hierarchical interactions between TSO, DSO, Buildings and EVs was implemented into Yalmip, by using MATLAB, and it was optimized with Gurobi. The V2G MPC model is very flexible and can easily be extended, *e.g.*, by introducing smart homes to the system. The simulation results were discussed in this chapter.

First, it was shown that the increase of the willingness to smart charge significantly increases the regulative capacity for the grid, because for the scenarios, where 0% and 100% of EVs have smart charging mode ON, the total frequency deviation during which EVs are smart charging is reduced by 33%. Second, increasing the number of EVs for smart parking lots has a stabilizing effect. However, the power demand from EVs also increases, which also has a destabilizing effect on the grid. Third, a faster charging speed does not clearly provide stabilizing benefits to the grid. Due to the hierarchical nature of the grid the faster charging speed stabilizes the DSO grid, but destabilizes the TSO grid. The total power load for EVs also increases, which intensifies the battery degradation for the EVs. The current simulation study parameters might have to be adjusted to discourage this further. Lastly, An increase of the desired departure SOC results in a decrease of regulative capacity for the grid, an increase in G2V load, a reduction in V2G load and an increase in power generation. Indeed, EVs have to be charged, as its primary use is transportation, for which electricity is consumed. However, for smart charging it is preferable to minimize the desired departure charge.

Chapter 6

Vehicle-to-Grid Integration with High Wind Penetration

Smart charging aids in stabilizing the grid. Furthermore, the integration of RESs into the energy system can be aided by smart EV charging. The V2G MPC model developed in Chapter 4 can be applied for optimal frequency control in deterministic systems, in which power generation and loads are both known beforehand. However, for uncertain power generation a different approach is required. In this chapter the V2G framework is extended to include uncertain high wind power penetration. A largely similar approach as (Badings et al., 2019a) is used to integrate wind power generation into the V2G framework. In this extended model two ancillary services are considered: reserve power deployment and demand-side flexibility. Ancillary services compensate for the uncertain power generation by RESs. In this chapter it will be shown that wind power generation causes instability in the power system. Furthermore, in (Badings et al., 2019a) demand-side flexibility was proposed as an alternative form of short-term operating reserve, with potential long term benefits ,*e.g.*, less environmental impact (Hao, Lin, Kowli, Barooah, & Meyn, 2014) and lower cost (Lymperopoulos, Qureshi, Nghiem, Khatir, & Jones, 2015) than traditional reserve. We will show that the smart charging of EVs can significantly contribute to the demand-side flexibility method of compensating for uncertain power generation.

In section 6.1 the extension of the V2G framework will be proposed. As most of the framework was introduced in (Badings et al., 2019a) the discussion of the model will be limited and will mostly address its extension with V2G. In section 6.2 the simulation results of three scenarios are presented. The chapter is concluded in section 6.3.

6.1 framework/model

In this section the V2G model that was proposed in Chapter 4 is extended with uncertain wind power generation. Also, reserve power deployment and demand-side flexibility is integrated in order to compensate for the uncertain nature of wind power generation.

6.1.1 Wind-integrated TSO dynamics

Wind generation is typically connected to the sub-transmission grid, or to the distribution network (Stock, Sala, Berizzi, & Hofmann, 2018). In this thesis wind power generation is limited to one wind farm, in one location, connected to the TSO network. The model can easily be extended to include more wind farms.

We define $\mathcal{F} = \{1, \ldots, n_w\}$ as the set of windfarms. Let the power generated be denoted by the vector $P_w(t) \in \mathbb{R}^{n_w}$. It is assumed that P_w is a realization of an unknown stochastic process defined on some probability space. Wind farms are connected to TSO nodes through incidence matrix $\Upsilon \in \mathbb{R}^{n_t \times n_w}$, with entries

$$v_{l,n} = \begin{cases} 1, & \text{if wind farm } n \text{ is attached to TSO node} l, \\ 0, & \text{otherwise.} \end{cases} \tag{6.1}$$

A separate variable for the forecast value of the wind power is denoted by $P_w^f(t) \in \mathbb{R}^{n_w}$. The error between the two is denoted by

$$\Delta P_w(t) = P_w(t) - P_w^f(t) \tag{6.2}$$

For the scheduling process only the wind forecast value, $P_w^f(t)$, is available. The TSO dynamics in 4.4 and the TSO balance constraint in 4.7 are extended such that

$$x_{tso_f}(t+h) = f_{tso}\big(x_{tso}(t), P_g(t), P_w^f(t), P_{ld}(t), P_{bl}(t)\big) \tag{6.3}$$

$$\mathbf{1}_{n_t}^T\big(\Pi P_g(t+qh) - \Upsilon P_w^f(t+qh) - P_{ld}(t+qh)\big) = 0 \tag{6.4}$$

where the forecast wind power, $\Upsilon P_w^f(t+qh)$, is inserted. The TSO state variable is renamed to x_{tso_f}, to indicate that it is the expected trajectory.

When the wind power forecast is perfect, $\Delta P_w(t) = 0$, no intervention is needed to compensate for any wind cast error. However, if $\Delta P_w(t) \neq 0$, intervention is required to compensate for errors in the power dispatch. In this case, compensation by ancillary services is required.

6.1.2 Ancillary service deployment

Operators strive for the following general power balance, such that the stability is maximized and the frequency deviations minimized.

$$\sum_{i\in\mathcal{G}} P_{g_i}(t) + \sum_{f\in\mathcal{F}} P_{w_f}(t) = \sum_{i\in\mathcal{G}} P_{g_i}(t) + \sum_{f\in\mathcal{F}} \big(P^f_{w_f}(t) + \Delta P_{w_m}(t)\big) = \sum_{b\in\mathcal{B}} P_{BD_b}(t), \quad (6.5)$$

where $P_{GR}(k)$, $P_w(k)$ and $P_{BD}(k)$ are the power generation from generators, generation from wind power and power demand, respectively at time step t. If there is any wind power forecast error the balance is no longer satisfied. Ancillary service is needed.

6.1.2.1 Reserve scheduling

Common practice to restore the power balance is to deploy reserve power. Deviations from the predicted wind generation are compensated by adjusting the generator power output. We follow an approach similar to (Rostampour, Ter Haar, & Keviczky, 2018). The reserve power required is determined with the following equation

$$-\sum_{i\in\mathcal{G}} R_i(t) = \max\big(\sum_{f\in\mathcal{F}} \Delta P_{w_m}(t), 0\big) + \min\big(\sum_{f\in\mathcal{F}} \Delta P_{w_m}(t), 0\big) \quad (6.6)$$

Where $R \in \mathbb{R}^{n_g}$ is the reserve power dispatch. The generator output can either be increased or decreased, *i.e.*, up-spinning reserve R^{us} or down-spinning reserve R^{ds} is used. The reserve scheduling bounds, $R^{ds}(t)$ and $R^{us}(t)$, at each time step are

$$-R^{ds}(t) \leq R(t) \leq R^{us}(t). \quad (6.7)$$

The scheduled power should also satisfy the generation limits, *i.e.*,

$$P^{min}_{GR} \leq P_{GR}(t) + R(t) \leq P^{max}_{GR} \quad (6.8)$$

The reserve scheduling revers to the back-up plan that is made to schedule an appropriate buffer. While the actual reserve dispatch (R) is the actual power that is injected into the grid to compensate for the wind power error.

6.1.2.2 Demand-side Flexibility

Demand-side flexibility is the capability to shift the production of consumption of energy in time, while user requirements are still met, and without changing the total energy production or consumption (Roossien, 2012). An EV could provide flexibility by delaying charging for a period, but eventually still meeting the desired departure charge. The wind power error can be compensated by adjusting power demand. Similar to 6.6 the scheduled demand-side flexibility is defined as

$$-\sum_{n\in\mathcal{B}} S_n(t) = \max\big(\sum_{f\in\mathcal{F}} \Delta P_{w_m}(t), 0\big) + \min\big(\sum_{f\in\mathcal{F}} \Delta P_{w_m}(t), 0\big) \tag{6.9}$$

while the increased demand flexibility ($S^{dd}(t) > 0$) and decreased-demand flexibility ($S^{id}(t) > 0$) are determined at each time step

$$-S^{dd}(t) \leq S(k) \leq S^{id}(t) \tag{6.10}$$

In (Badings et al., 2019a) for the flexibility contribution of individual buildings two sources are considered: (1) building storage system and (2) building HVAC loads. We add a third source: (3) EVs. EVs can provide a flexibility dispatch when smart charging mode is ON. This yields the following bounds at time step t

$$-S^{dd}_{ev}(t) - S^{dd}_{stor}(t) - S^{dd}_{hvac}(t) \leq S(k) \leq S^{id}_{ev}(t) + S^{id}_{stor}(t) + S^{id}_{hvac}(t) \tag{6.11}$$

where $S^{dd}_{ev}(t)$, $S^{dd}_{stor}(t)$, $S^{dd}_{hvac}(t)$, $S^{id}_{ev}(t)$, $S^{id}_{stor}(t)$ and $S^{id}_{hvac}(t)$ are the increased- and decreased-demand flexibility using EVs, storage and HVAC loads, respectively. In this chapter, building energy storage is also integrated in the model. Which dynamics are given as

$$x^{n_b}_{stor}(t + qh + 1) = \zeta^{n_b} x^{n_b}_{stor}(k) + \eta^{n_b} P^{n_b}_{stor}(t + qh + 1) \tag{6.12}$$

where $x^{n_b}_{stor}$ is the storage SOC, h is the simulation time resolution, and ζ^{n_b} and η^{n_b} are efficiency coefficients of the storage unit. Physical limitations on the storage rate and SOC level are given as

$$x^{min}_{stor} \leq x^{n_b}_{stor} \leq x^{max}_{stor} \tag{6.13}$$

$$P^{min}_{stor} \leq P^{n_b}_{stor} \leq P^{max}_{stor} \tag{6.14}$$

6.1.2.3 Reserve and flexibility dispatch dynamics

Reserve and flexibility dispatch can be included in the TSO power balance as

$$\sum_{i\in\mathcal{G}} \big(P_{g_i}(t) + R_i(t)\big) + \sum_{f\in\mathcal{F}} \big(P^f_{w_f}(t) + \Delta P_{w_m}(t)\big) = \sum_{b\in\mathcal{B}} \big(P_{BD_b}(t) + S_{n_b}(t)\big), \tag{6.15}$$

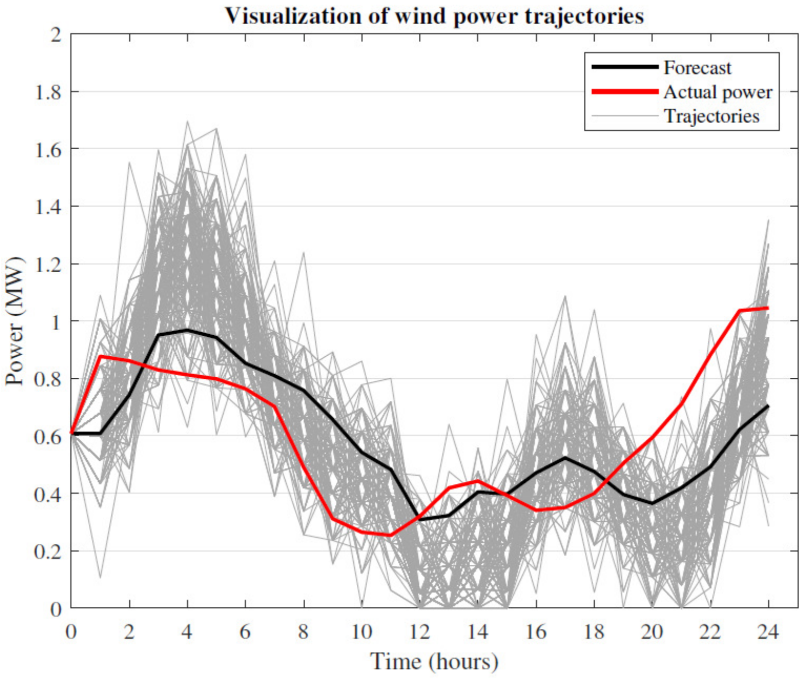

FIGURE 6.1: The forecast and actual wind power, and 300 wind power trajectories, generated by the Markov Chain-based wind power model (Badings et al., 2019a)

where the sum of the reserve and the flexibility dispatch compensate for the total wind power mismatch:

$$\sum_{i\in\mathcal{G}} R_i(t) - \sum_{n\in\mathcal{B}} S_n(t) = \max\Big(\sum_{f\in\mathcal{F}} \Delta P_{w_m}(t), 0\Big) + \min\Big(\sum_{f\in\mathcal{F}} \Delta P_{w_m}(t), 0\Big) \tag{6.16}$$

When equation 6.7 and 6.11 are taken into consideration we can give the following constraint to ensure compensation for wind power error is provided:

$$\begin{aligned} -\sum_{i\in\mathcal{G}} R_i^{us}(t) - \sum_{n\in\mathcal{B}} S_n^{dd}(t) \leq & \max\Big(\sum_{f\in\mathcal{F}} (P_{w_m}(t) - P_{w_m}^f(t)), 0\Big) + \\ & \min\Big(\sum_{f\in\mathcal{F}} (P_{w_m}(t) - P_{w_m}^f(t)), 0\Big) \leq \sum_{i\in\mathcal{G}} R_i^{ds}(t) - \sum_{n\in\mathcal{B}} S_n^{id}(t) \end{aligned} \tag{6.17}$$

6.1.3 Wind power model

For the wind power model only the power generated is considered, instead of considering the wind speed. The wind power model from (Rostampour, 2012) is considered. The model generates scenarios of the wind power and the corresponding error, while taking its temporal correlation into account. The wind power forecast, actual wind power and

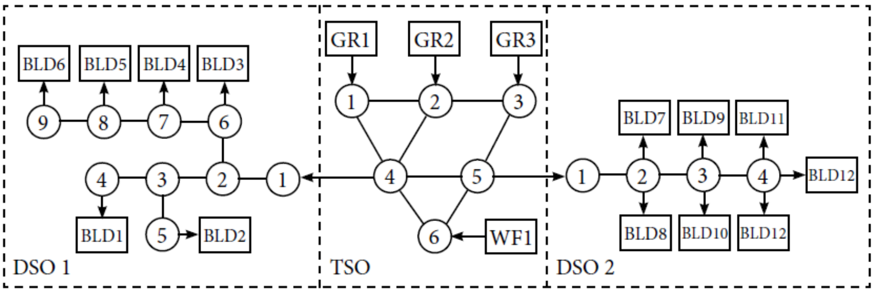

FIGURE 6.2: Network topology of the w-V2G MPC simulation, the grid structure, generators (GR), building (BLD) and wind farm (WF) are indicated.

error between the two were discretized, to construct a Markov Chain model capable of generating realistic wind power trajectories based on different error realizations, which is depicted in Figure 6.1. The model was successfully integrated into a power system in (Margellos et al., 2012). Furthermore, (Badings et al., 2019a) integrated the model in a w-BtG-MPC model. The formulation of the wind power model and the further integration can be found in (Rostampour, 2012) and (Badings et al., 2019a), respectively.

6.2 Simulation results

In this section the simulation results of three scenarios are discussed. The unique aspect of each scenario is as follows:

- Scenario 1: Simulation without wind power generation
- Scenario 2: Simulation with wind power generation, EVs are not used as flexibility dispatch
- Scenario 3: Simulation with wind power generation, EVs are part of the flexibility dispatch

The simulation parameters can be found in Appendix C. For each simulation the TSO, DSO, BLD, HVAC, storage and EV dynamics are included, its formulations can be found in Chapter 4 and section 6.1. For these scenarios every EV has smart charging mode ON. Furthermore, every EV has exactly the same capacity for these results, as it reduces the computational time significantly. If the capacity for every EV is varied, then EVs need individual constraints. Moreover, The EVs' and storages' (dis)charging speed bounds are increased to $P_{ev_i}^{min} = P_{stor}^{min} = -25$ kW and $P_{ev_i}^{max} = P_{stor}^{max} = 25$ kW. for each scenario the simulation time is 24 hours.

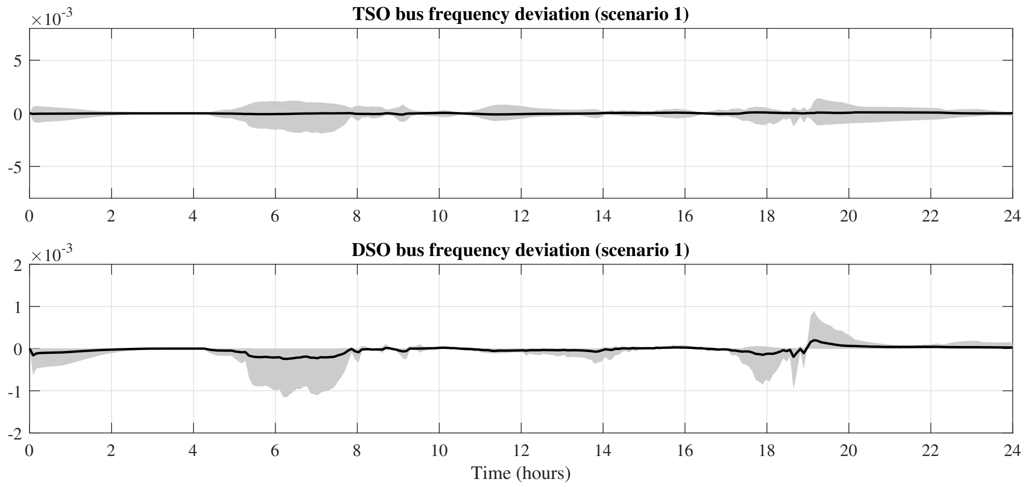

FIGURE 6.3: The TSO and DSO frequency deviation for scenario 1

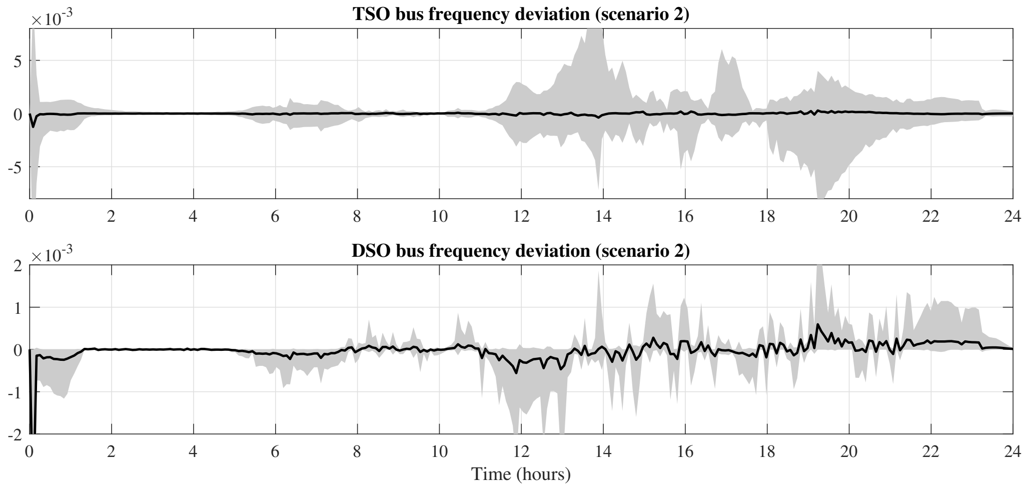

FIGURE 6.4: The TSO and DSO frequency deviation for scenario 2

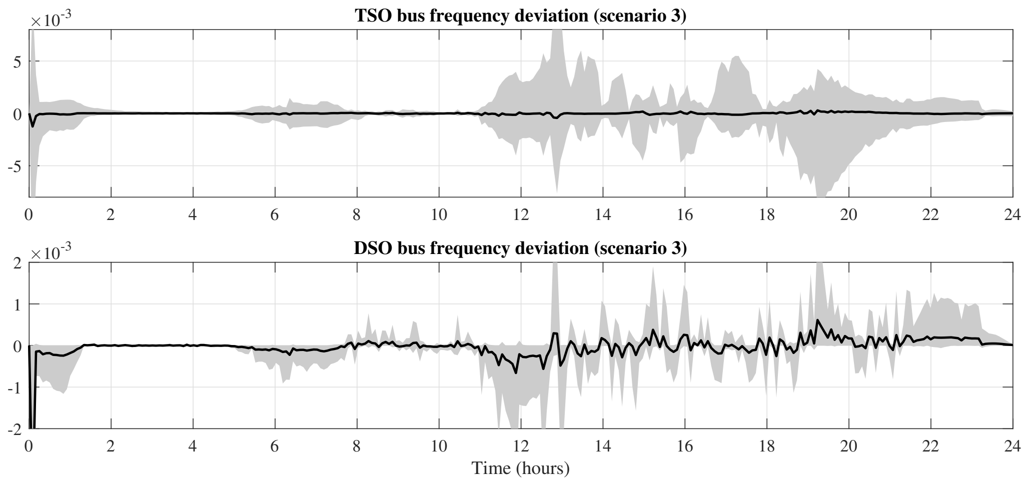

FIGURE 6.5: The TSO and DSO frequency deviation for scenario 3

For scenario 1; wind power generation is excluded. For scenario 2; wind power generation is enabled. Further, reserve and flexibility scheduling are both enabled, but smart charging EVs are excluded from flexibility scheduling. For scenario 3; EVs are included in the flexibility scheduling, and thus wind power generation is also enabled. The main purpose of the simulation of these scenarios is to show that: first, uncertain and uncontrolled wind power generation results in instability in the grid. Second, the smart charging of EVs can be used as flexibility dispatch to compensate for the error between the wind power prediction and the actual wind power load.

The frequency deviations for the TSO and DSO grid over time for all three scenarios are given in Figure 6.3, Figure 6.4 and Figure 6.5. It can be clearly seen that the grid is relatively stable for scenario 1. The introduction of energy storage units in the buildings provides an extra stabilizing factor, as storage was not included in the model of Chapter 5. The introduction of wind power in scenario 2 clearly increases the frequency deviation, in fact the total frequency deviation increases by 125%. This shows that even though reserve and flexibility dispatch are enabled the introduction of an uncontrollable form of energy production into a power system increases the instability of the system's grid. Furthermore, the frequency deviation for scenario 2 and 3 are mostly similar, as can be seen in Figure 6.4 and Figure 6.5. The total frequency deviation is increased by only 2% for scenario 3.

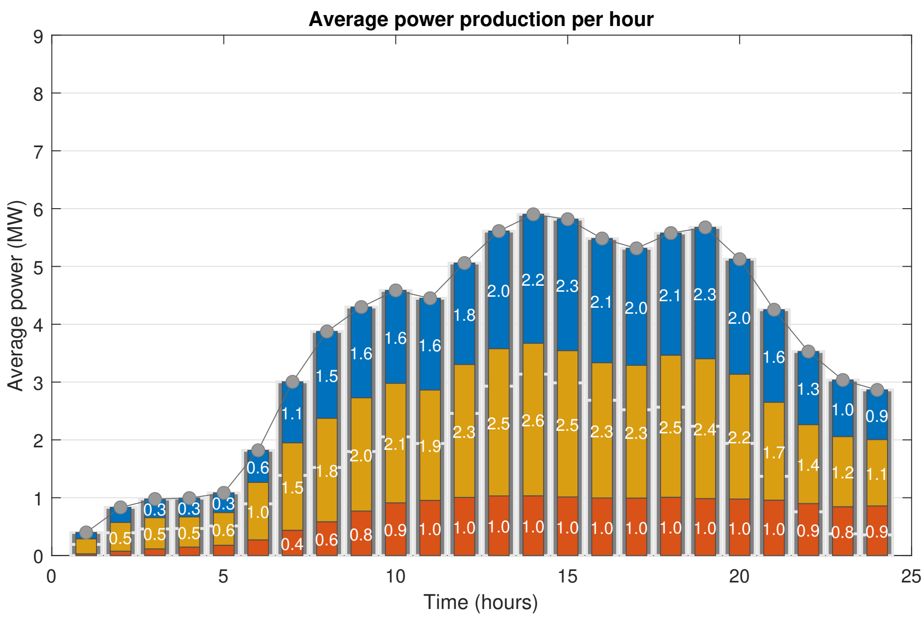

FIGURE 6.6: The total power generation for scenario 1

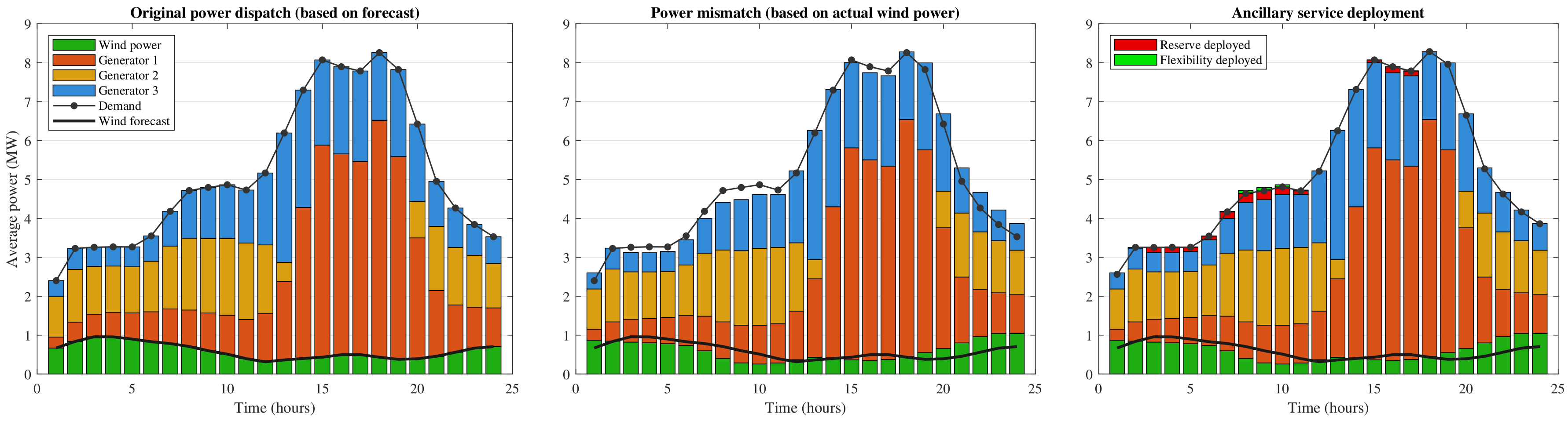

FIGURE 6.7: The original power dispatch, the power mismatch and the ancillary service deployment for scenario 2

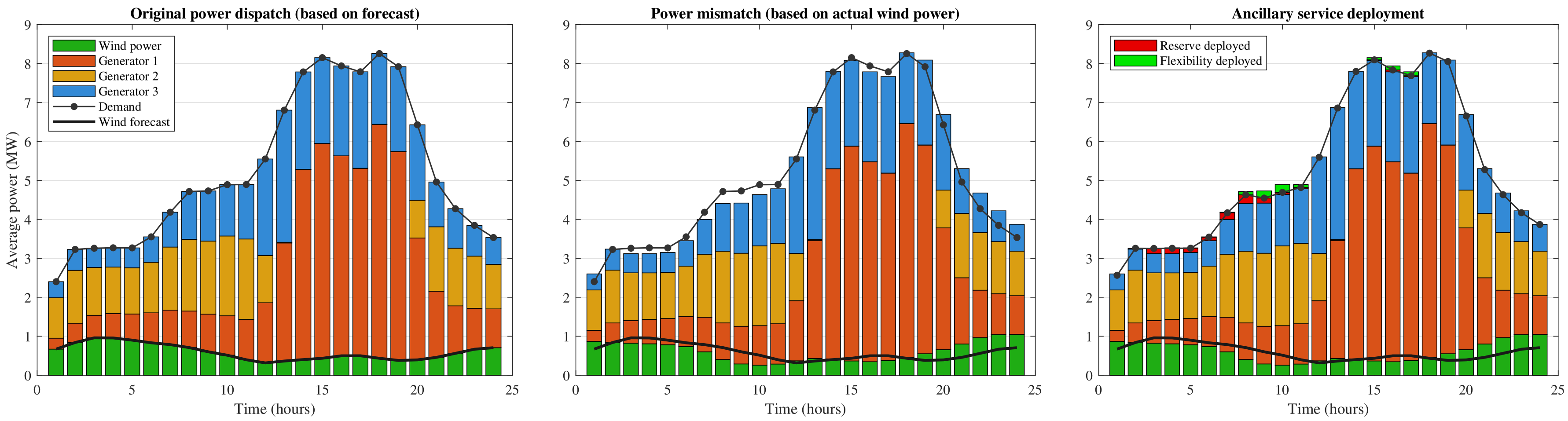

FIGURE 6.8: The original power dispatch, the power mismatch and the ancillary service deployment for scenario 3

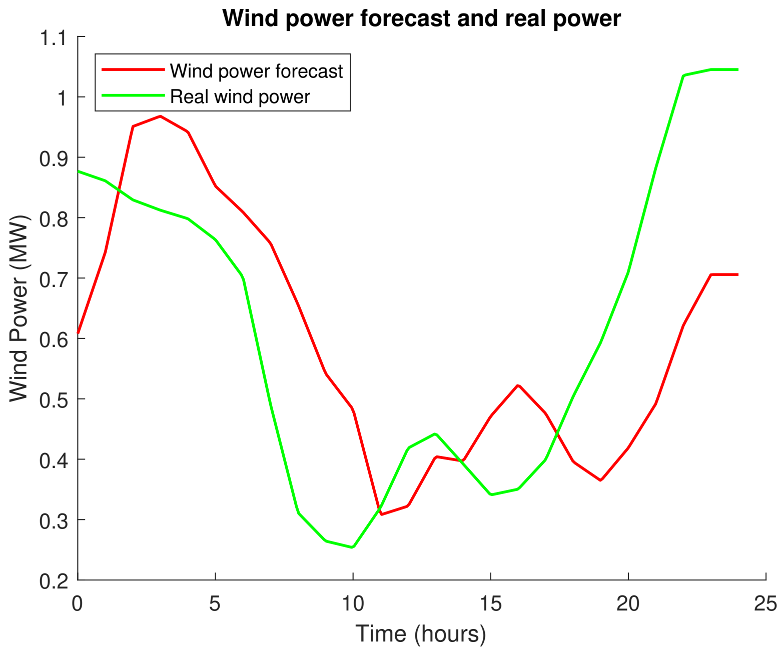

FIGURE 6.9: The wind power forecast and the real wind power for scenario 2 and 3

Now, we will look at the power production for all three scenarios. In Figure 6.6 the average power production per hour for scenario 1 is shown, where the three colours indicate generator 1, 2 and 3. Figure 6.9 shows the wind forecast and the actual wind power production for scenarios 2 and 3, which is the same for both scenarios, such that they can be compared. It shows that the forecast and real power have some similarities, but there is an wind power error during almost the entire simulation.

In figure 6.7 and Figure 6.8 the original power dispatch, the power mismatch and the ancillary service deployment for scenario 2 and 3 are shown, respectively. The original power dispatch is based on the wind power forecast and the power mismatch is based on the actual wind power. The power mismatch shows clearly the mismatch that is caused by the incorrect forecast of the wind power generated. This mismatch should be compensated by ancillary service deployment. This deployment can be be seen in the third figure. As the power generation for scenario 2 and 3 are identical there is no difference between the first two graphs of Figure 6.7 and Figure 6.8. However the third graph shows how reserve and flexibility dispatch are deployed to compensate for the power mismatch.

Furthermore, we look in detail to ancillary service scheduling and dispatch of scenario 2 and 3. In Appendix D Figures are presented that show the flexibility and reserve scheduling and dispatch for both scenarios. It indicates that the ancillary services have the capacity to deal with a significantly bigger wind error than the wind error in these simulations. Moreover, in Figure 6.10 and Figure 6.11, respectively. The figures give the total ancillary service dispatch per hour over time. When we compare both figures it becomes clear that the share of flexibility dispatch is higher for scenario 3 during the hours 8 through 17. Reserve dispatch is 47% and reserve dispatch is 53% of the total ancillary service dispatch for scenario 2. Reserve dispatch is 34% and reserve dispatch is 66% of the total ancillary service dispatch for scenario 3. The difference between these scenarios is the introduction of EV smart charging flexibility dispatch in scenario 3. Thus, the flexibility dispatch of EVs is used during the hours that EVs are available on the smart parking lot, instead of reserve dispatch.

Now, consider the Figures 6.12 and 6.13, which show the flexibility dispatch composition for scenarios 2 and 3, respectively. For Figure 6.12 EV flexibility dispatch is not included, while in Figure 6.13 it is. This shows the contribution of the smart charging of EVs to the compensating for the wind power error via demand-side flexibility. For scenario 2 storage is 45% and HVAC is 55% of the total flexibility dispatch. For scenario 3 storage is 32%, HVAC is 41% and EVs are 27% of the total flexibility dispatch. The EV deployment is limited by the arrival and departure time of the EVs. During the hours that EVs are available for smart charging the flexibility dispatch comes almost entirely from EVs.

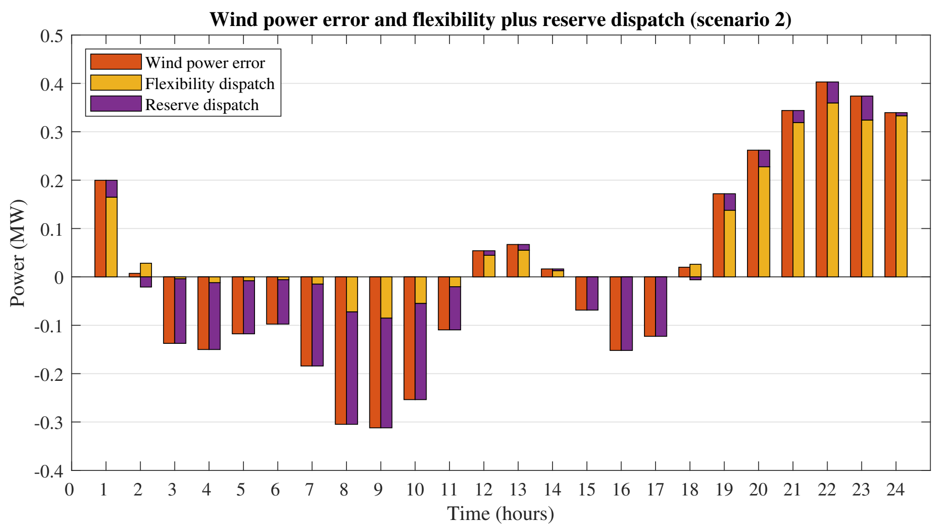

Figure 6.10: The wind power error and flexibility and reserve dispatch for scenario 2

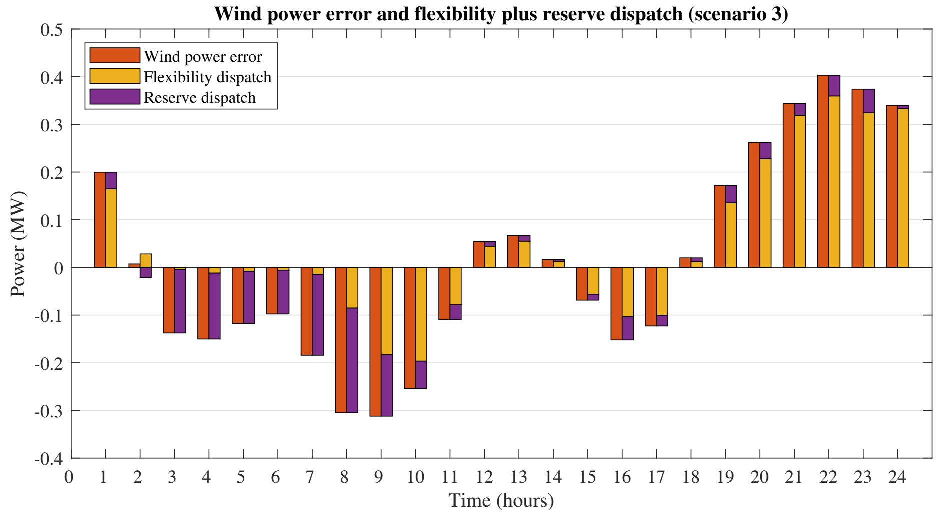

FIGURE 6.11: The wind power error and flexibility and reserve dispatch for scenario 3

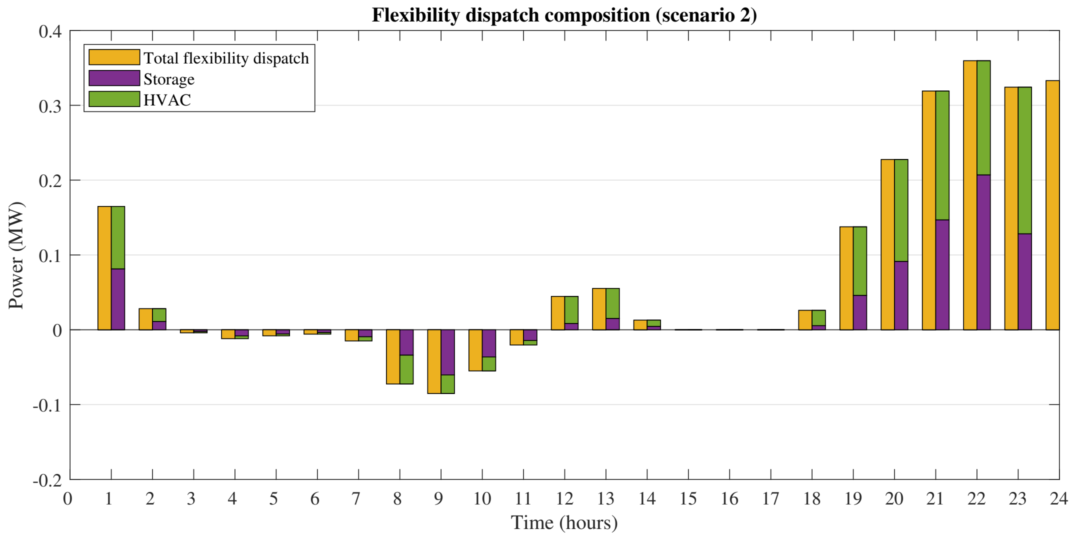

FIGURE 6.12: The composition of the flexibility dispatch for scenario 2

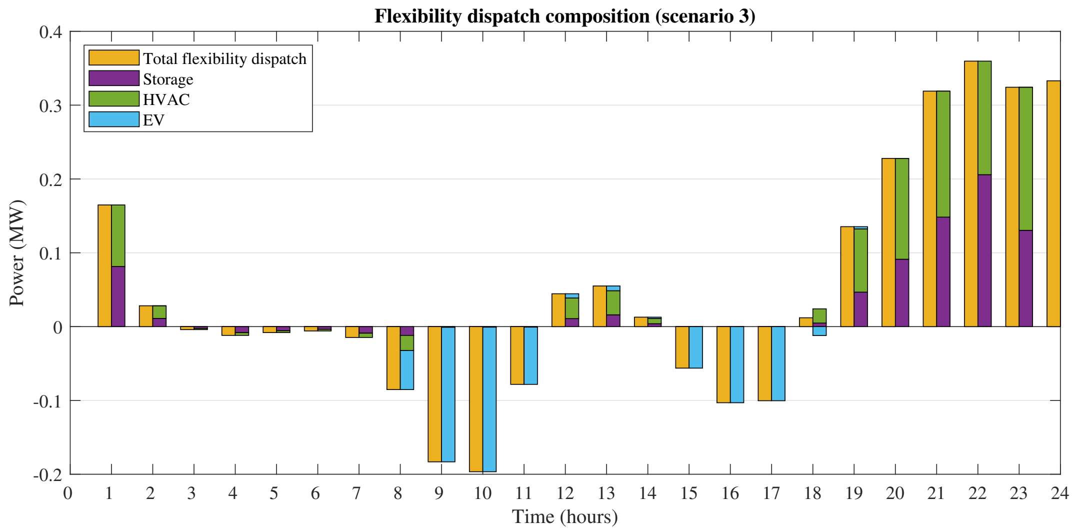

FIGURE 6.13: The composition of the flexibility dispatch for scenario 3

6.3 Conclusion

In this chapter the model for the integration of wind power generation was proposed, thus a W-V2G MPC model with social behavior was designed. Then, simulation results of this model were presented. It was shown that uncontrolled and hard to predict RESs have a destabilizing effect on the power grid. Moreover, in contrast to the traditional reserve scheduling method, flexibility scheduling can provide long-term benefits, *i.e.*, less environmental impact and lower cost. Furthermore, it was shown that the smart charging of EVs can contribute to the flexibility dispatch to compensate for the wind power error between the forecasted and the actual power load.

Chapter 7

Conclusion, Limitations and Further Work

7.1 Conclusion

This thesis has been undertaken in order to embed social behavioral factors in a smart charging framework, and to explore the social factor's role in this hierarchical smart charging framework. Some existing research work of EV owner's behavior is based around car adoption driving behavior, and attitudes towards EVs. However, it was found that social aspects are currently neglected in the field of smart charging. While, the participation of EV owners is essential. Hence, without many EVs participating in smart charging the concept will be unsuccessful. Similar to EV car adoption, we investigate the influence of the willingness of EV owners to smart charge. With this knowledge it becomes possible to propose policies to increase smart charging participation.

The main social factor is the willingness of an EV owner to follow a smart charging contract. This willingness is determined for a population of employed Dutch EV owners. It was found that EV owners are very willing to smart charge. The willingness to smart charge is positively correlated to the environmental self-identity and more weakly correlated to range anxiety. A financial incentive did not motivate survey participants to participate in smart charging.

Furthermore, a V2G-MPC model is proposed in which social behavior is embedded. The model is a holistic power system framework with an hierarchical integration of respectively, TSO, DSO and BLD with EV and HVAC. Later this model is expanded with wind power generation, for which the wind power prediction error can be compensated with reserve and flexibility scheduling. The smart charging of EVs can contribute to the flexibility dispatch. Due to the nature of MPC the model is very flexible and can be extended with relative ease. Granted that MPC models have to be mathematically accurate to provide good results and an expansion of the model will increase the computational time.

Moreover, it was found that increasing the willingness of EV owners to participate in smart charging, increases the beneficial effects of smart charging on the power grid. In other words, when more EVs are available for smart charging, then we have more regulative capacity for the grid. It was also shown that uncertain wind power generation has a destabilizing effect on the system. Lastly, it was shown that the smart charging of EVs can contribute to the penetration of renewable energy sources.

Concluding, as the penetration of RESs in energy production and the penetration of EVs in transportation increases, smart charging will become increasingly important. It provides a solution for the unstable nature of RESs, and it can provide a solution for the increase in peak power demand. The cooperation of EV owners is essential for the success of smart charging. In this thesis it was shown that EV owners are willing to participate in smart charging. Additionally, it was shown that environmental self-identity is possibly a more important motivational factor than financial incentives, indicating a behavior unique to EV owners.

7.2 Limitations & Furter work

The survey results used for this thesis was limited, as smart charging was only a small part of the survey. In order to establish a broader understanding of the social behavior of EV owners a more thorough survey can be done. Questions can be improved to further investigate the willingness of EV owners to smart charge and its relating measures.

The framework proposed in this thesis can be easily adjusted to different network and parameter settings, thus many different scenarios an be simulated. Furthermore, the framework can be easily extended. For example, smart homes, smart charging at the homes of EV owners, aggregators and solar power generation can be included in this model.

Moreover, the model for battery degradation was limited, as the depth of discharge and intermittent charging were not included in the model. In order to provide more accurate dynamics for battery degradation a model similar to (Koller, Borsche, Ulbig, & Andersson, 2013) can be integrated. Furthermore, the peak power demand was addressed as a problem for when the penetration of EVs in transportation increases and the smart charging model reduced the peak load. However, this dynamic was not specifically included in the model. The model can be further expanded with dynamics that reduce the peak load of EVs.

This thesis provides a starting point for further research on the social behavior of EV owners. As the results indicate a unique behavior that should be further investigated. Many studies exist on social factors related EV adoption. Further research on social factors related to smart charging should be done to create a good understanding. Then, policies and solutions can be proposed to aid in user receptiveness to smart charging.

Appendix A

Survey questions

In this appendix questions from the NewMotion customer survey are presented in order to give insight in how measures were determined. The results from these questions are discussed in chapter 4.

Q18:

To what degree do you recognize yourself in the following statements?

6. The range of my electric vehicle is sufficient for my everyday use.
   (totally disagree) 1 2 3 4 5 (totally agree)

Q19:

To what degree do you recognize yourself in the following statements?

3. "I see myself as a pro-environmental person."
   (totally disagree) 1 2 3 4 5 (totally agree)

4. "Acting environmentally-friendly is an important part of who I am"
   (totally disagree) 1 2 3 4 5 (totally agree)

Figure A.1: Questions that are used to determine range anxiety and environmental self-identity

Smart charging can offer a solution for the fluctuating supply of solar and wind energy by smoothing out peaks in supply and demand. For example with apps or software that enable delayed charging, slower charging and also with V2X technology. With V2X, electricity can be fed back into the public electricity grid, but also into private power grids like office buildings or private homes.

Using these sort of smart charging solutions might mean that the car does not immediately charge after plugging into the charge point or that charging may take longer.

Q37

Please indicate to what extent you are interested in using smart charging to maximize renewable energy use or to balance supply and demand of energy on the electricity grid. (1 (strongly disagree) to 5 (strongly agree))

- I'm willing to use it
- I'm willing to use it when I will gain from it financially

Figure A.2: Question on smart charging willingness

Q38:

When you arrive at work, how full is the battery of your EV usually?

- (0-100%)
- I don't know

Q39:

How much do you want your battery to be charged at least when you leave work? (0-100%)

- (0-100%)
- I don't know

Figure A.3: Questions on arrival and departure charge

Q40:

Offices could use electricity from electric vehicles parked at the office at times when energy demand is high. This can reduce the strain on the grid during, which means a more sustainable way of using the available energy. A disadvantage of this technology is that the battery of the EV might degenerate more rapidly.

Could you indicate how willing you are to share the power of your EV battery with the power grid of your office? (scale: not at all – very much)

- I am willing to have the battery of my EV used to power offices.
- I am willing to have the battery of my EV used to power offices if gain from it financially.
- I am willing to have the battery of my EV used to power offices as long as I have enough power to commute home.

Figure A.4: Question on providing power to the office, answers are given on a 1 to 5 scale

Appendix B

Survey results extension

Here some additional results from the NewMotion survey are given. First, tables on car brands, car types and age ranges and smart charging willingness are presented. Then, figures on EVs used to power the office, range anxiety, ESI and the range of EVs are shown. Finally, the composition of the survey participants in terms of gender, age, chargepoint locations, home location and car adoption method are presented.

Car Brand	Frequency	Average SC willingness
Tesla	516	4.00
Nissan	117	3.86
Hyundai	160	3.89
Renault	72	4.04
Opel	68	3.79
Jaguar	60	3.48
Other	46	3.80
BMW	46	4.17
Volkswagen	65	3.82
Kia	13	3.46
Fiat	7	3.57
Mercedes	12	4.33
Citroën	5	4.20
Peugeot	3	3.33
Smart	3	4.00
Mitsubishi	2	5.00
Audi	2	3.00
Think	1	3.00
Zero	2	3.00
Volvo	1	5.00
Total	1201	3.92

Table B.1: The frequency and average willingness to smart charge of participants with an EV of the specified brand

Age	**Frequency**	**Willingness to SC**	**SD**
21-30	8	4.75	0.43
31-40	77	4.00	1.14
41-50	315	3.95	1.14
51-60	548	3.87	1.18
61-70	217	3.93	1.13
71 and older	31	3.97	1.31

TABLE B.2: The frequency of participants in age group, the willingness to smart charge per age group and its standard deviation

Car	**Number**	**Capacity [kWh]**	**Avg range [km]**	**Avg SC willingness**
Tesla Model S	245	85.0	369	3.91
Tesla Model 3	181	72.5	403	4.13
Nissan Leaf	111	36.0	202	3.83
Hyundai KONA Electric	97	64.0	399	3.78
Tesla Model X	88	86.8	362	3.95
Renault Zoe	64	52.0	201	4.06
Hyundai IONIQ Electric	63	38.3	201	4.06
Opel Ampera-E	63	58.0	329	3.78
Jaguar I-PACE	60	84.7	343	3.48
Other	46	60.7	360	3.80
BMW i3	44	37.9	191	4.16
Volkswagen e-Golf	33	32.0	202	3.64
Volkswagen e-Golf 2017	27	32.0	197	4.07
Fiat 500e	7	42.0	124	-
Mercedes B250e	7	28.0	146	-
Renault Kangoo Z.E.	7	31.0	113	-
Nissan e-NV200 Evalia	6	38.0	124	-
Mercedes B-class	5	28.0	154	-
Citroën C-Zero	5	14.5	88	-
Opel Ampera	5	58.0	231	-
Volkswagen e-up!	5	32.3	112	-
Kia Soul EV -39kWh	3	39.2	155	-
Kia Soul EV -64kWh	1	64.0	430	-
Peugeot ION	3	14.5	97	-
Smart Fortwo	3	16.7	113	-
Mitsubishi iMiEV	2	14.5	105	-
Tesla Roadster	2	53.0	300	-
Renault Fluence Z.E.	1	70.0	95	-
Think City	1	24.0	100	-
Volvo C30 EV	1	24.0	250	-

TABLE B.3: The frequency that participants own a car type, the battery capacity per car (EV Database, n.d.) and the average range given by survey participants

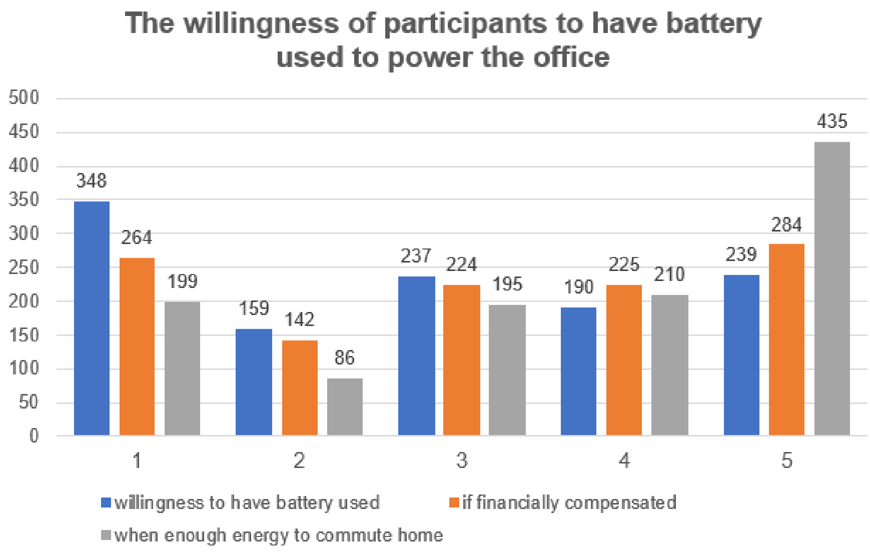

FIGURE B.1: Frequencies of answers on willingness to have battery used to power an office

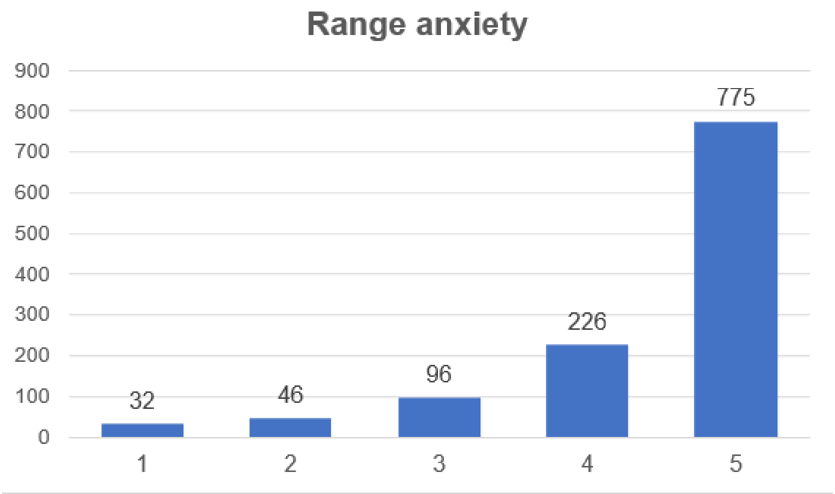

FIGURE B.2: Frequencies on whether a participant their EV has sufficient range

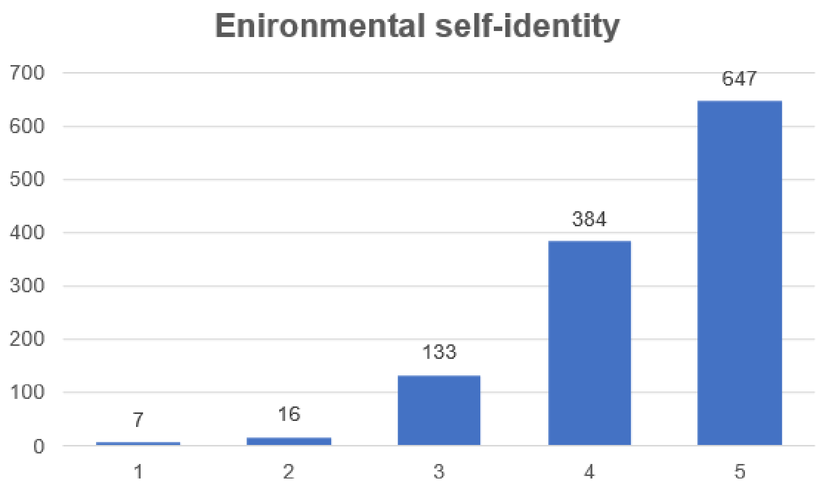

FIGURE B.3: Frequencies of answers on environmental self-identity questions combined

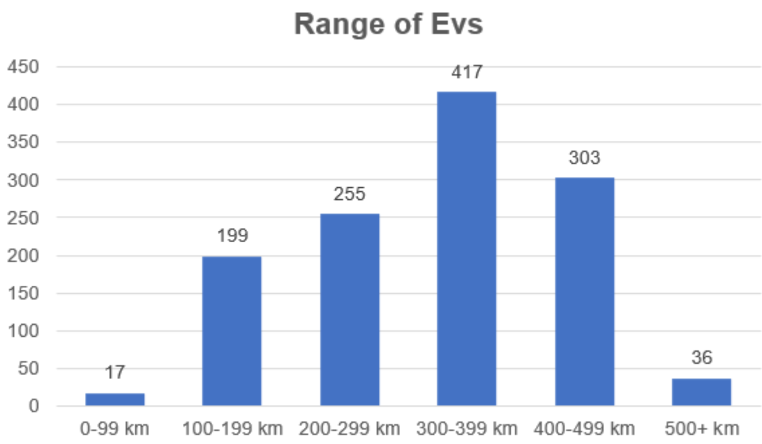

FIGURE B.4: Range of EVs in kms given by participants

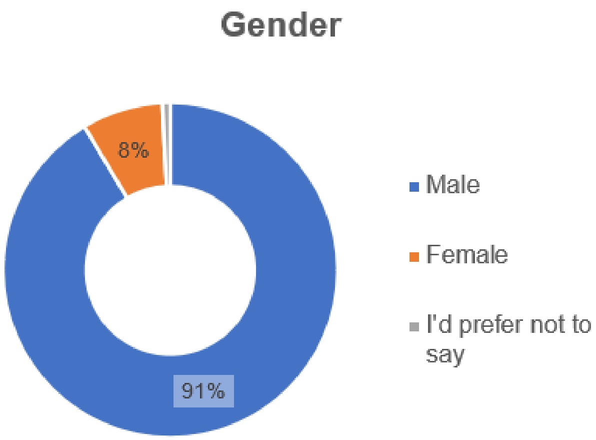

FIGURE B.5: Percentage of participants per gender

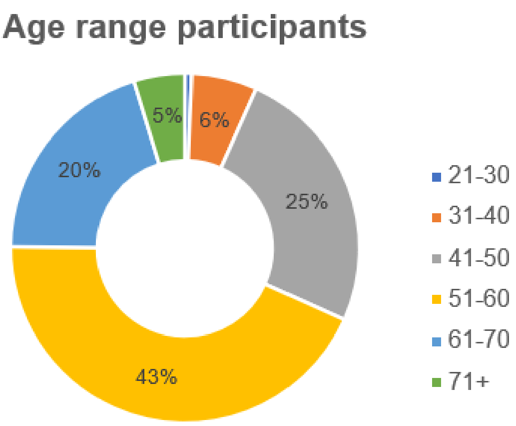

FIGURE B.6: Percentage of participants per age groups

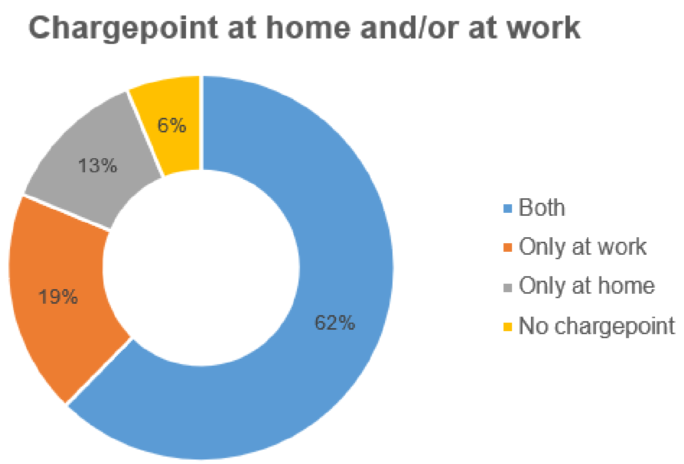

FIGURE B.7: Percentage of participants with a chargepoint at home, work, both or neither

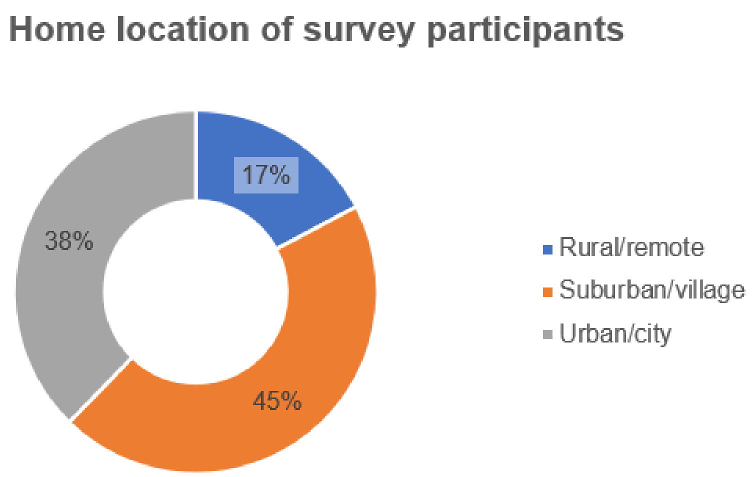

FIGURE B.8: Percentage of participants per home location area

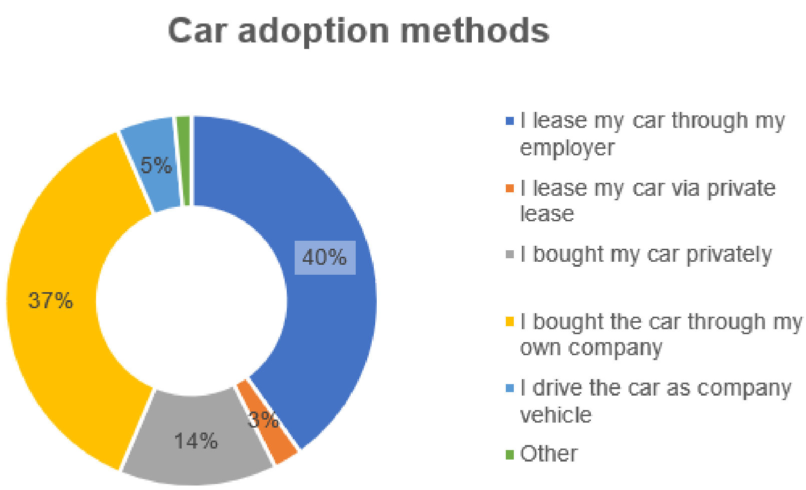

FIGURE B.9: Percentage of participants per car adoption type

Appendix C

Simulation study parameters

This appendix provides a full list of parameters used in the dynamics and constraints of the simulation studies in this thesis.

Parameter	Value	Units	Description of source
T_end	24	h	End time of simulation
T_p	3600	s	MPC receding horizon time
h	300	s	Simulation time resolution

Table C.1: Simulation time parameters

Parameter	Value	Units	Description of source
M	0.06	MW s^2	Inertia coefficient (Rodriguez, Rodríguez, & Payán, 2007)
D	4.50	MW s	Damping coefficient (Rodriguez et al., 2007)
$\hat{\mathrm{D}}$	0.00	MW s	Frequency sensitive load
P_{BL}	0.01	MW	Base load
P_{GR}^{min}	0	MW	Minimum power generation
P_{GR}^{max}	100	MW	Maximum power generation
$P_{GR}^{ramp,dw}$	-1	MW	Maximum generator ramp down
$P_{GR}^{ramp,up}$	1	MW	Maximum generator ramp up ’

Table C.2: TSO network parameters

Parameter	Value	Units	Description of source
M^i	0.06	MW s^{-2}	Inertia coefficient, interface (Rodriguez et al., 2007)
D^i	4.50	MW s^{-1}	Inertia coefficient, interface (Rodriguez et al., 2007)
$\hat{\mathrm{D}}^i$	0.00	MW s^{-1}	Frequency sensitive load
P_{BL}^i	0.01	MW	Base load

Table C.3: DSO network parameters

Parameter	Value	Units	Description of source
R_1	5.8	°C MW^{-1}	Outer wall resistance
R_2	11..6	°C MW^{-1}	Inner wall resistance
R_{win}	655	°C MW^{-1}	Window resistance
C_{zone}	21.1×10^3	MJ °C^{-1}	Zone thermal capacity
C_{wall}	11.3×10^2	MJ °C^{-1}	Wall thermal capacity
μ_{hvac}	3	-	HVAC coefficient of performance
T_{day}^{min}	21.5	°C	Minimum temperature during day
T_{day}^{max}	23	°C	Maximum temperature during day
T_{night}^{min}	21.5	°C	Minimum temperature during night
T_{night}^{max}	25	°C	Maximum temperature during night
t_{day}^{start}	8	h	Start time of day
t_{day}^{end}	20	h	End time of day
P_{hvac}^{min}	0	MW	Minimum HVAC power
P_{hvac}^{max}	1	MW	Maximum HVAC power
$P_{hvac}^{ramp,dw}$	-0.1	MW	Minimum HVAC ramp down
$P_{hvac}^{ramp,up}$	0.1	MW	Maximum HVAC ramp up

TABLE C.4: Building parameters, mostly adopted from (Taha et al., 2017)

Parameter	Value	Units	Description of source
$x_{ev_i}^{min}$	Differs per EV	kWh	The minimum SOC of an EV
$x_{ev_i}^{max}$	Differs per EV	kWh	The maximum SOC of an EV
$x_{ev_i}^{0}$	Differs per EV	kWh	The arrival SOC of an EV
P_{ev}^{min}	-10	kW	The maximum discharging rate, V2G (Office of Energy Efficiency & RE, 2017) (Renault, 2020)
P_{ev}^{max}	10	kW	The maximum charging rate, V2G (Office of Energy Efficiency & RE, 2017) (Renault, 2020)
T_{arr_i}	Normal distributed μ =08:30 σ =00:45	hh:mm	The arrival time of an EV
T_{dep_i}	Normal distributed μ =17:00 σ =00:45	hh:mm	The departure time of an EV
δ_{ev_i}	1	-	The state efficiency parameter
b_{ev_i}	1	-	The charging efficiency parameter

TABLE C.5: Electric vehicle parameters

Parameter	Value	Units	Description of source
x_s^{min}	10	kWh	Minimum buffer level
x_s^{max}	63	kWh	Maximum buffer level
x_s^{0}	25	kWh	Initial buffer level
P_{stor}^{min}	-25	kW	Minimum storage rate
P_{stor}^{max}	25	kW	Maximum storage rate
ζ	1	-	State efficiency parameter
η	1	-	Input efficiency parameter

TABLE C.6: Storage parameters for Chapter 6

Parameter	Value	Units	Description of source
q_{TSO}	10^3	$\$/MW^2$	Cost of TSO frequency deviation
q_{DSO}	10^3	$\$/MW^2$	Cost of DSO frequency deviation
q_{batdeg}	0.012	$\$/MW^2$	Cost of battery degradation (Koller et al., 2013)
q_{P_GR}	.05	$\$/MW^2$	Cost of generator production
q_{P_BLD}	.05	$\$/MW^2$	Cost of grid power

TABLE C.7: The cost parameters for *Chapter 5*

Parameter	Value	Units	Description of source
q_{TSO}	10^3	$\$/MW^2$	Cost of TSO frequency deviation
q_{DSO}	10^3	$\$/MW^2$	Cost of DSO frequency deviation
q_{batdeg}	0.012	$\$/MW^2$	Cost of battery degradation
q_{R_us}	10^3	$/MW	Up-spinning reserve cost
q_{R_ds}	10^3	$/MW	Down-spinning reserve cost
q_{S_BD}	10^3	$/MW	Cost of building flexibility

TABLE C.8: The cost parameters for *Chapter 6*

Appendix D

Simulation results extension

In this appendix some additional figures of the simulation results of Chapter 5 and Chapter 6 are presented. Firstly, the TSO and DSO frequency deviation for scenarios with averages of 5 and 50 EVs per building. Secondly, the TSO and DSO frequency deviation for scenarios with maximum (dis)charging speed of 7.2 kW and 72 kW, respectively. Lastly, the reserve scheduling and dispatch and the flexibility scheduling and dispatch are given for scenario 2 and scenario 3. For scenario 3 the smart charging of EVs is included in the demand-side flexibility composition for wind power errors. While for scenario 2 smart charging is not included, the flexibility scheduling only includes, storage and HVAC.

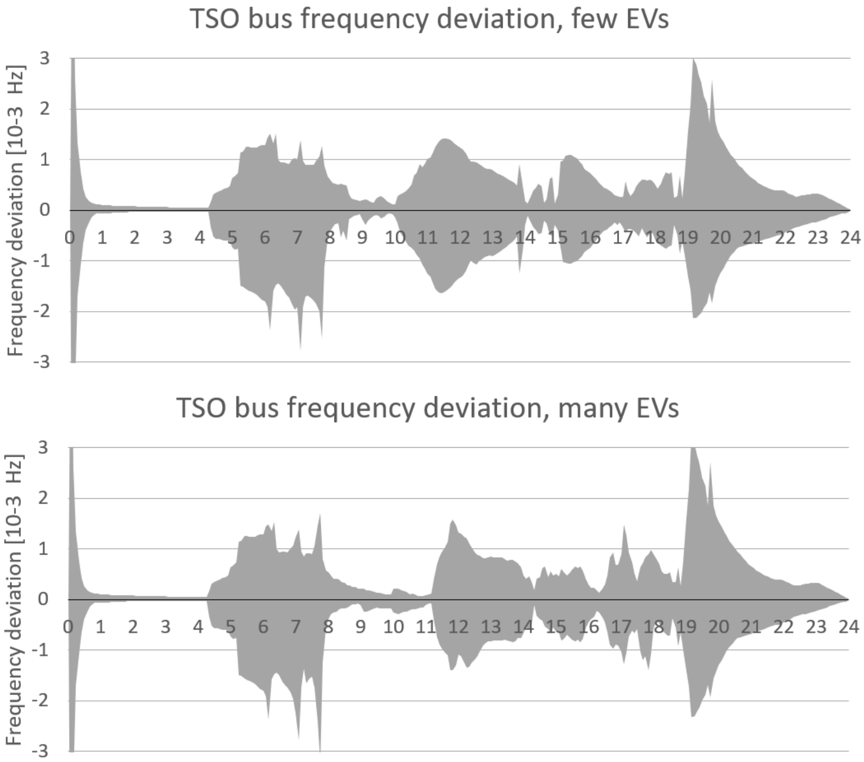

FIGURE D.1: The TSO bus frequency deviation for 5 and 50 EVs on average per building

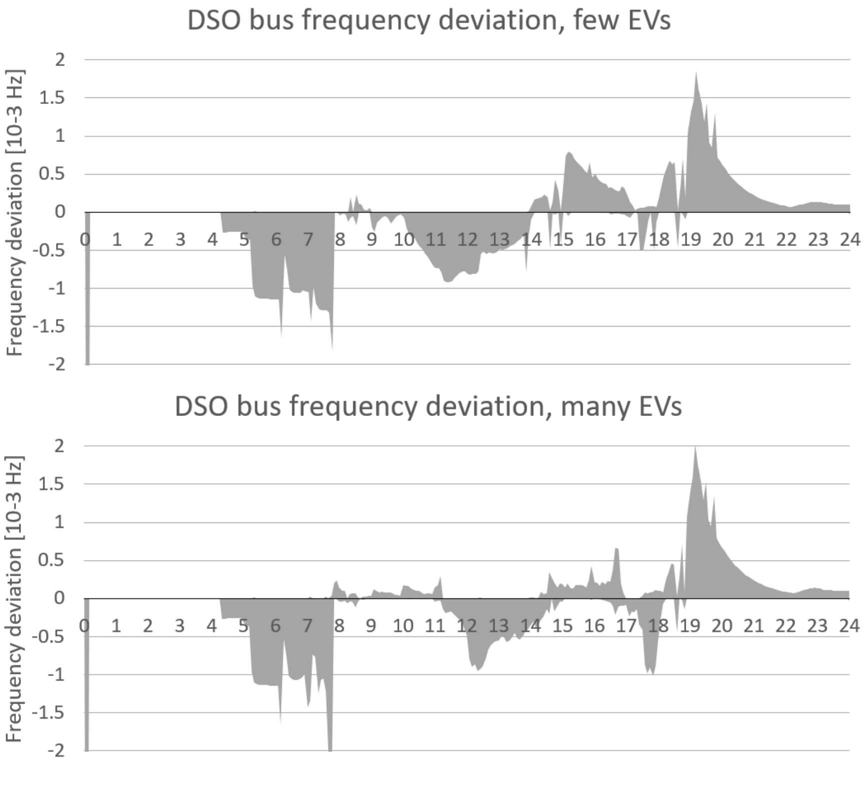

FIGURE D.2: The DSO bus frequency deviation for 5 and 50 EVs on average per building

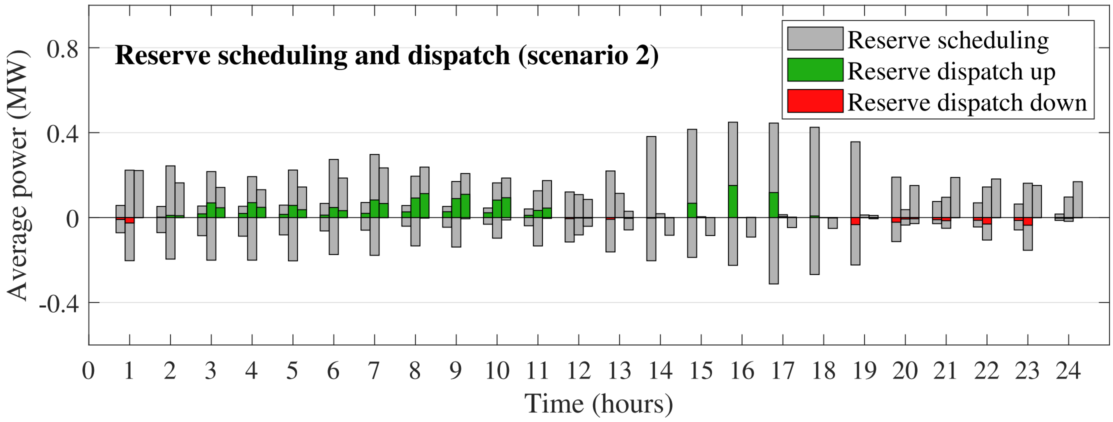

FIGURE D.3: The reserve scheduling and dispatch for scenario 2 from chapter 6

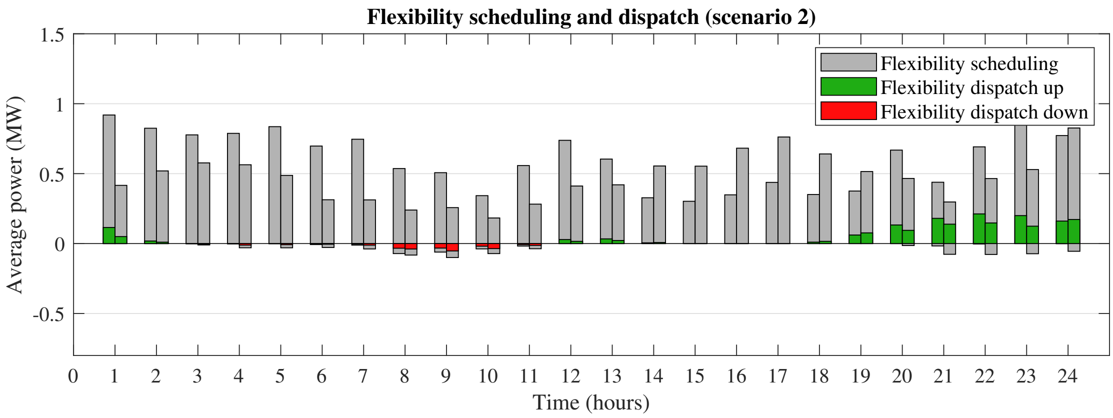

FIGURE D.4: The flexibility scheduling and dispatch for scenario 2 from chapter 6

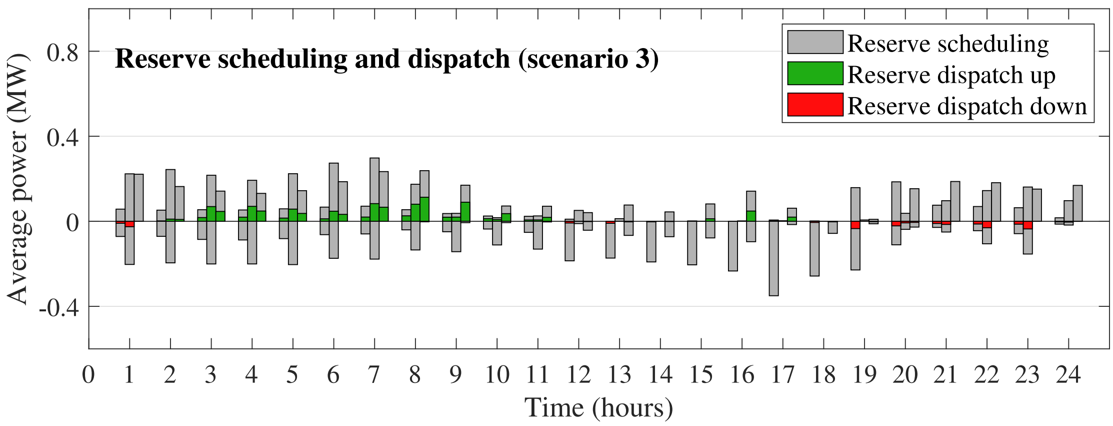

FIGURE D.5: The reserve scheduling and dispatch for scenario 3 from chapter 6

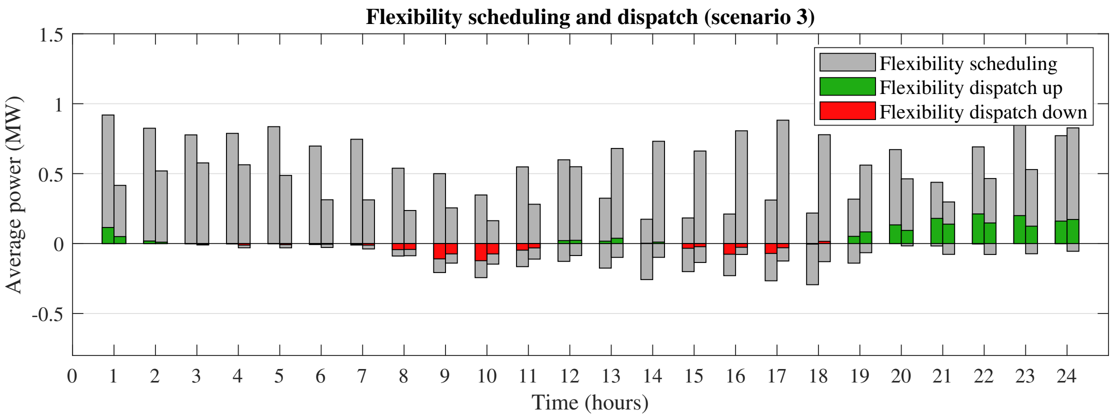

FIGURE D.6: The flexibility scheduling and dispatch for scenario 3 from chapter 6

References

Al-Alawi, B. M., & Bradley, T. H. (2013). Review of hybrid, plug-in hybrid, and electric vehicle market modeling studies. *Renewable and Sustainable Energy Reviews*, *21*, 190–203.

Amjad, S., Neelakrishnan, S., & Rudramoorthy, R. (2010). Review of design considerations and technological challenges for successful development and deployment of plug-in hybrid electric vehicles. *Renewable and Sustainable Energy Reviews*, *14*(3), 1104 - 1110. Retrieved from `http://www.sciencedirect.com/science/article/pii/S1364032109002639` doi: https://doi.org/10.1016/j.rser.2009.11.001

Ashkrof, P., de Almeida Correia, G. H., & van Arem, B. (2020). Analysis of the effect of charging needs on battery electric vehicle drivers' route choice behaviour: A case study in the netherlands. *Transportation Research Part D: Transport and Environment*, *78*, 102206.

Badings, T. S., Rostampour, V., & Scherpen, J. M. (2019a). *Buildings-to-grid integration for demand-side flexibility in power systems with uncertain generation* (Unpublished master's thesis).

Badings, T. S., Rostampour, V., & Scherpen, J. M. (2019b). Distributed building energy storage units for frequency control service in power systems. *IFAC-PapersOnLine*, *52*(4), 228–233.

Bessa, R. J., & Matos, M. A. (2012). Economic and technical management of an aggregation agent for electric vehicles: a literature survey. *European transactions on electrical power*, *22*(3), 334–350.

Bhandari, V., Sun, K., & Homans, F. (2018). The profitability of vehicle to grid for system participants-a case study from the electricity reliability council of texas. *Energy*, *153*, 278–286.

Bühler, F., Cocron, P., Neumann, I., Franke, T., & Krems, J. F. (2014). Is ev experience related to ev acceptance? results from a german field study. *Transportation Research Part F: traffic psychology and behaviour*, *25*, 34–49.

Camacho, E. F., & Alba, C. B. (2013). *Model predictive control*. Springer Science & Business Media.

Chen, R., Qian, X., Miao, L., & Ukkusuri, S. V. (2020). Optimal charging facility location and capacity for electric vehicles considering route choice and charging time equilibrium. *Computers & Operations Research*, *113*, 104776.

Darby, M. L., & Nikolaou, M. (2012). Mpc: Current practice and challenges. *Control Engineering Practice*, *20*(4), 328–342.

Dogger, J. D., Roossien, B., & Nieuwenhout, F. D. (2010). Characterization of li-ion batteries for intelligent management of distributed grid-connected storage. *IEEE Transactions on Energy Conversion*, *26*(1), 256–263.

Egbue, O., & Long, S. (2012). Barriers to widespread adoption of electric vehicles: An analysis of consumer attitudes and perceptions. *Energy policy*, *48*, 717–729.

Energy Element. (2013). Pathways to high penetration of electric vehicles–final report. *Element Energy Ltd, Ecolane And University Of Aberdeen For The Committee On Climate Change,, Cambridge*.

Ernst, D., Glavic, M., Capitanescu, F., & Wehenkel, L. (2008). Reinforcement learning versus model predictive control: a comparison on a power system problem. *IEEE Transactions on Systems, Man, and Cybernetics, Part B (Cybernetics)*, *39*(2), 517–529.

EV Database. (n.d.). *Ev database.* Retrieved from `https://ev-database.org/` (Accessed: 2020-03-20)

Faria, R., Marques, P., Moura, P., Freire, F., Delgado, J., & de Almeida, A. T. (2013). Impact of the electricity mix and use profile in the life-cycle assessment of electric vehicles. *Renewable and Sustainable Energy Reviews*, *24*, 271–287.

Fasugba, M. A., & Krein, P. T. (2011). Cost benefits and vehicle-to-grid regulation services of unidirectional charging of electric vehicles. , 827–834.

Folkestad, C. A., Hansen, N., Fagerholt, K., Andersson, H., & Pantuso, G. (2020). Optimal charging and repositioning of electric vehicles in a free-floating carsharing system. *Computers & Operations Research*, *113*, 104771.

Galus, M. D., Vayá, M. G., Krause, T., & Andersson, G. (2013). The role of electric vehicles in smart grids. *Wiley Interdisciplinary Reviews: Energy and Environment*, *2*(4), 384–400.

Garcia-Valle, R., & Lopes, J. A. P. (2012). *Electric vehicle integration into modern power networks.* Springer Science & Business Media.

García-Villalobos, J., Zamora, I., San Martín, J., Asensio, F., & Aperribay, V. (2014). Plug-in electric vehicles in electric distribution networks: A review of smart charging approaches. *Renewable and Sustainable Energy Reviews*, *38*, 717–731.

Green II, R. C., Wang, L., & Alam, M. (2011). The impact of plug-in hybrid electric vehicles on distribution networks: A review and outlook. *Renewable and sustainable energy reviews*, *15*(1), 544–553.

Hao, H., Lin, Y., Kowli, A. S., Barooah, P., & Meyn, S. (2014). Ancillary service to the grid through control of fans in commercial building hvac systems. *IEEE Transactions on smart grid*, *5*(4), 2066–2074.

Hildermeier, J., Kolokathis, C., Rosenow, J., Hogan, M., Wiese, C., & Jahn, A. (2019). Smart ev charging: A global review of promising practices. *World Electric Vehicle Journal*, *10*(4), 80.

Hong, J., Koo, Y., Jeong, G., & Lee, J. (2012). Ex-ante evaluation of profitability and government's subsidy policy on vehicle-to-grid system. *Energy Policy*, *42*, 95–104.

Ilic, M. D., Xie, L., & Joo, J.-Y. (2011). Efficient coordination of wind power and price-responsive demand—part i: Theoretical foundations. *IEEE Transactions on Power Systems*, *26*(4), 1875–1884.

Jensen, A. F., Cherchi, E., & Mabit, S. L. (2013). On the stability of preferences and attitudes before and after experiencing an electric vehicle. *Transportation Research Part D: Transport and Environment*, *25*, 24–32.

Jin, L., Kumar, R., & Elia, N. (2009). Model predictive control-based real-time power system protection schemes. *IEEE Transactions on Power Systems*, *25*(2), 988–998.

Karabasoglu, O., & Michalek, J. (2013). Influence of driving patterns on life cycle cost and emissions of hybrid and plug-in electric vehicle powertrains. *Energy policy*, *60*, 445–461.

Kempton, W., & Tomić, J. (2005a). Vehicle-to-grid power fundamentals: Calculating capacity and net revenue. *Journal of power sources*, *144*(1), 268–279.

Kempton, W., & Tomić, J. (2005b). Vehicle-to-grid power implementation: From stabilizing the grid to supporting large-scale renewable energy. *Journal of power sources*, *144*(1), 280–294.

Koller, M., Borsche, T., Ulbig, A., & Andersson, G. (2013). Defining a degradation cost function for optimal control of a battery energy storage system. In *2013 ieee grenoble conference* (pp. 1–6).

Kuang, Y., Chen, Y., Hu, M., & Yang, D. (2017). Influence analysis of driver behavior and building category on economic performance of electric vehicle to grid and building integration. *Applied Energy*, *207*, 427–437.

Lee, C.-H., & Wu, C.-H. (2016). A data driven approach to create an extensible ev driving data model. In *Proceedings of the the 3rd multidisciplinary international social networks conference on socialinformatics 2016, data science 2016* (pp. 1–6).

Lopes, J. A. P., Soares, F. J., & Almeida, P. M. R. (2010). Integration of electric vehicles in the electric power system. *Proceedings of the IEEE*, *99*(1), 168–183.

Lymperopoulos, I., Qureshi, F. A., Nghiem, T., Khatir, A. A., & Jones, C. N. (2015). Providing ancillary service with commercial buildings: The swiss perspective. *IFAC-PapersOnLine*, *48*(8), 6–13.

Ma, Y., Houghton, T., Cruden, A., & Infield, D. (2012). Modeling the benefits of vehicle-to-grid technology to a power system. *IEEE Transactions on power systems*, *27*(2), 1012–1020.

Margellos, K., Haring, T., Hokayem, P., Schubiger, M., Lygeros, J., & Andersson, G. (2012). A robust reserve scheduling technique for power systems with high wind penetration. In *International conference on probabilistic methods applied to power systems.*

Mukherjee, S. C., & Ryan, L. (2020). Factors influencing early battery electric vehicle adoption in ireland. *Renewable and Sustainable Energy Reviews*, *118*, 109504.

Mullan, J., Harries, D., Bräunl, T., & Whitely, S. (2012). The technical, economic and commercial viability of the vehicle-to-grid concept. *Energy Policy*, *48*, 394–406.

Mwasilu, F., Justo, J. J., Kim, E.-K., Do, T. D., & Jung, J.-W. (2014). Electric vehicles and smart grid interaction: A review on vehicle to grid and renewable energy sources integration. *Renewable and sustainable energy reviews*, *34*, 501–516.

Netherlands Enterprise Agency. (2020). *Statistics electric vehicles and charging in the netherlands.* Retrieved from https://www.rvo.nl/sites/default/files/2020/04/Statistics%20Electric%20Vehicles%20and%20Charging%20in%20The%20Netherlands%20up%20to%20and%20including%20March%202020.pdf (Accessed: 2020-04-28)

Niesten, E., & Alkemade, F. (2016). How is value created and captured in smart grids? a review of the literature and an analysis of pilot projects. *Renewable and Sustainable Energy Reviews*, *53*, 629–638.

Office of Energy Efficiency & RE. (2017). *Electric vehicle charging at home typically draws less than half the power of an electric furnace.* Retrieved from https://www.energy.gov/eere/vehicles/articles/fact-995-september-18-2017-electric-vehicle-charging-home-typically-draws (Accessed: 2020-05-22)

Pavlak, G. S., Henze, G. P., & Cushing, V. J. (2014). Optimizing commercial building participation in energy and ancillary service markets. *Energy and Buildings*, *81*, 115–126.

Peng, M., Liu, L., & Jiang, C. (2012). A review on the economic dispatch and risk management of the large-scale plug-in electric vehicles (phevs)-penetrated power systems. *Renewable and Sustainable Energy Reviews*, *16*(3), 1508–1515.

Peterson, S. B., Apt, J., & Whitacre, J. (2010). Lithium-ion battery cell degradation resulting from realistic vehicle and vehicle-to-grid utilization. *Journal of Power Sources*, *195*(8), 2385–2392.

Qin, S. J., & Badgwell, T. A. (2003). A survey of industrial model predictive control technology. *Control engineering practice*, *11*(7), 733–764.

Renault. (2020). *Calculate the charging time for your new zoe.* Retrieved from `https://www.renault.co.uk/electric-vehicles/zoe/battery.html` (Accessed: 2020-05-29)

Richardson, D. B. (2013). Electric vehicles and the electric grid: A review of modeling approaches, impacts, and renewable energy integration. *Renewable and Sustainable Energy Reviews*, *19*, 247–254.

Rodriguez, A. G., Rodríguez, A. G., & Payán, M. B. (2007). Estimating wind turbines mechanical constants. In *Proc. int. conf. renewable energies and power quality (icrepq'07)* (pp. 27–30).

Roossien, B. (2012). Mathematical quantification of near real-time flexibility for smart grids. *Energy research Centre of the Netherlands (ECN), http://www. flexines. org/publicaties/eindrapport/BIJLAGE14a. pdf (dostep 25.10. 2016)*.

Rostampour, V. (2012). Msc thesis. tractable reserve scheduling formulations for power systems with uncertain generation.

Rostampour, V., Ter Haar, O., & Keviczky, T. (2018). Distributed stochastic reserve scheduling in ac power systems with uncertain generation. *IEEE Transactions on Power Systems*, *34*(2), 1005–1020.

Schmidt, M., Staudt, P., & Weinhardt, C. (2020). Evaluating the importance and impact of user behavior on public destination charging of electric vehicles. *Applied Energy*, *258*, 114061.

Shalender, K., & Sharma, N. (2020). Using extended theory of planned behaviour (tpb) to predict adoption intention of electric vehicles in india. *Environment, Development and Sustainability*, 1–17.

Shen, Y., Fang, W., Ye, F., & Kadoch, M. (2020). Ev charging behavior analysis using hybrid intelligence for 5g smart grid. *Electronics*, *9*(1), 80.

Simon, D. (2017). *Fighter aircraft maneuver limiting using mpc: Theory and application* (Vol. 1881). Linköping University Electronic Press.

Sincovec, R., Erisman, A., Yip, E., & Epton, M. (1981). Analysis of descriptor systems using numerical algorithms. *IEEE Transactions on Automatic Control*, *26*(1), 139–147.

Sioshansi, R., & Denholm, P. (2009). Emissions impacts and benefits of plug-in hybrid electric vehicles and vehicle-to-grid services. *Environmental science & technology*, *43*(4), 1199–1204.

Sortomme, E., & El-Sharkawi, M. A. (2010). Optimal charging strategies for unidirectional vehicle-to-grid. *IEEE Transactions on Smart Grid*, *2*(1), 131–138.

Sovacool, B. K., & Hirsh, R. F. (2009). Beyond batteries: An examination of the benefits and barriers to plug-in hybrid electric vehicles (phevs) and a vehicle-to-grid (v2g) transition. *Energy Policy*, *37*(3), 1095–1103.

Sovacool, B. K., Noel, L., Axsen, J., & Kempton, W. (2018). The neglected social dimensions to a vehicle-to-grid (v2g) transition: a critical and systematic review. *Environmental Research Letters*, *13*(1), 013001.

Stock, D. S., Sala, F., Berizzi, A., & Hofmann, L. (2018). Optimal control of wind farms for coordinated tso-dso reactive power management. *Energies*, *11*(1), 173.

Taha, A. F., Gatsis, N., Dong, B., Pipri, A., & Li, Z. (2017). Buildings-to-grid integration framework. *IEEE Transactions on Smart Grid*, *10*(2), 1237–1249.

Tan, K. M., Ramachandaramurthy, V. K., & Yong, J. Y. (2016). Integration of electric vehicles in smart grid: A review on vehicle to grid technologies and optimization techniques. *Renewable and Sustainable Energy Reviews*, *53*, 720–732.

The Local. (2020). *How germany is preparing for the rise of the electric car.* Retrieved from `https://www.thelocal.de/20200110/germany-has-made-progress-with-e-cars-but-access-varies` (Accessed: 2020-05-15)

U.S. Department of Energy. (n.d.). Pev definition. Retrieved from `https://afdc.energy.gov/laws/9355` (Accessed: 2020-05-15)

Van Tilborgh, S. J. M., K. (2018). *Maximizing profits for an aggregator providing vehicle-to-grid and smart charging services in the dutch market* (Unpublished master's thesis).

Verbong, G., & Geels, F. (2007). The ongoing energy transition: lessons from a socio-technical, multi-level analysis of the dutch electricity system (1960–2004). *Energy policy*, *35*(2), 1025–1037.

Verma, A. K., Singh, B., & Shahani, D. (2011). Grid to vehicle and vehicle to grid energy transfer using single-phase bidirectional ac-dc converter and bidirectional dc-dc converter. In *2011 international conference on energy, automation and signal* (pp. 1–5).

Waldron, J., Rodrigues, L., Gillott, M., Naylor, S., & Shipman, R. (2019). Towards an electric revolution: a review on vehicle-to-grid, smart charging and user behaviour.

Wang, G., Makino, K., Harmandayan, A., & Wu, X. (2020). Eco-driving behaviors of electric vehicle users: A survey study. *Transportation Research Part D: Transport and Environment*, *78*, 102188.

Wang, X., Nie, Y., & Cheng, K.-W. E. (2019). Distribution system planning considering stochastic ev penetration and v2g behavior. *IEEE Transactions on Intelligent Transportation Systems*.

Wee, S., Coffman, M., & Allen, S. (2020). Ev driver characteristics: Evidence from hawaii. *Transport Policy*.

White, C. D., & Zhang, K. M. (2011). Using vehicle-to-grid technology for frequency regulation and peak-load reduction. *Journal of Power Sources*, *196*(8), 3972–3980.

Wieringa, R. (2010). Design science methodology: principles and practice. , 493–494.

Wu, Q., Nielsen, A. H., Ostergaard, J., Cha, S. T., Marra, F., Chen, Y., & Træholt, C. (2010). Driving pattern analysis for electric vehicle (ev) grid integration study. In *2010 ieee pes innovative smart grid technologies conference europe (isgt europe)* (pp. 1–6).

Yilmaz, M., & Krein, P. T. (2012). Review of the impact of vehicle-to-grid technologies on distribution systems and utility interfaces. *IEEE Transactions on power electronics*, *28*(12), 5673–5689.

Zhao, Z., Zhang, L., Yang, M., Chai, J., & Li, S. (2020). Pricing for private charging pile sharing considering ev consumers based on non-cooperative game model. *Journal of Cleaner Production*, 120039.

Zimmerman, R. D., Murillo-Sánchez, C. E., & Thomas, R. J. (2010). Matpower: Steady-state operations, planning, and analysis tools for power systems research and education. *IEEE Transactions on power systems*, *26*(1), 12–19.